AD_____

Award Number: DAMD17-02-1-0313

TITLE: Structural Basis for Bc12-Regulated Mitochondrion-Dependant Apoptosis

PRINCIPAL INVESTIGATOR: Francesca M. Marassi, Ph.D.

CONTRACTING ORGANIZATION: The Burnham Institute
La Jolla, CA 92037

REPORT DATE: April 2005

TYPE OF REPORT: Final

PREPARED FOR: U.S. Army Medical Research and Materiel Command
Fort Detrick, Maryland 21702-5012

REPORT DOCUMENTATION PAGE

Form Approved
OMB No. 074-0188

1. AGENCY USE ONLY	2. REPORT DATE	3. REPORT TYPE AND DATES COVERED
	April 2005	Final(15 Mar 2002 - 16 Mar 2005)

4. TITLE AND SUBTITLE
Structural Basis for Bc12-Regulated Mitochondrion-Dependant Apoptosis

5. FUNDING NUMBERS
DAMD17-02-1-0313

6. AUTHOR(S)

Francesca M. Marassi, Ph.D.

7. PERFORMING ORGANIZATION NAME(S) AND ADDRESS(ES)

The Burnham Institute
La Jolla, CA 92037

E-Mail: fmarassi@burnham.org

8. PERFORMING ORGANIZATION REPORT NUMBER

9. SPONSORING / MONITORING AGENCY NAME(S) AND ADDRESS(ES)
U.S. Army Medical Research and Materiel Command
Fort Detrick, Maryland 21702-5012

10. SPONSORING / MONITORING AGENCY REPORT NUMBER

11. SUPPLEMENTARY NOTES

12a. DISTRIBUTION / AVAILABILITY STATEMENT
Approved for Public Release; Distribution Unlimited

12b. DISTRIBUTION CODE

13. ABSTRACT (Maximum 200 Words)

The Bcl-2 family proteins are key regulators of programmed cell death, in health and major human diseases, including cancer. Their pro- or anti-apoptotic functions are regulated by subcellular location, as the proteins cycle between soluble and membrane-bound forms; by dimerization with other Bcl-2 family members; by binding to other non-homologous proteins; and by formation of membrane pores that are believed to regulate apoptosis by perturbing mitochondrial physiology. The solution structures of several Bcl-2 family proteins are very similar despite their antagonistic activities, however, the structures of the membrane-associated proteins are not known and may be key to their opposing functions. The goals of this project are: (1) to determine the structures of the membrane-associated Bcl-2 proteins; and (2) to determine their mechanism of apoptosis regulation. The research strategy combines NMR structure determination in lipid environments with biological assays carried out in parallel with structure determination.

14. SUBJECT TERMS
Structural biology; NMR; Bcl-2; cancer biology, ion channels

15. NUMBER OF PAGES
52

16. PRICE CODE

17. SECURITY CLASSIFICATION OF REPORT	18. SECURITY CLASSIFICATION OF THIS PAGE	19. SECURITY CLASSIFICATION OF ABSTRACT	20. LIMITATION OF ABSTRACT
Unclassified	Unclassified	Unclassified	Unlimited

TABLE OF CONTENTS

Reprints and Preprints:

Franzin CM, Choi J, Zhai D, Reed JC, Marassi FM (2004) **Structural studies of apoptosis and ion transport regulatory proteins in membranes**. *Magn Reson Chem* 42, 172-179.

Gong XM, Choi J, Franzin CM, Zhai D, Reed JC, Marassi FM (2004) **Conformation of membrane-associated proapoptotic tBid**. *J Biol Chem* 279, 28954-28960.

Thai K, Choi J, Franzin CM, Marassi FM (2005) **Bcl-XL as a fusion protein for the high-level expression of membrane-associated proteins**. *Protein Sci* 14, 948-955.

Gong XM, Choi J, Marassi FM (in press) **NMR of Membrane Proteins in Lipid Environments: the Bcl-2 family of apoptosis regulators**. In *Lipid Protein Interactions, Biophysics Monographs*, Gonzalez Ros JM, ed. (Berlin, Springer).

INTRODUCTION

The goal of this project was to determine the structures of the Bcl-2 family proteins in their membrane-associated forms. The Bcl-2 family proteins play major regulatory roles in programmed cell death, or apoptosis, and exert their activities through dimerization with other Bcl-2 family members, binding to non-homologous proteins, and the formation of membrane pores, believed to regulate apoptosis by perturbing mitochondrial physiology. Their functions are also regulated by subcellular location as the proteins cycle between soluble and membrane-bound forms. The soluble structures of several pro- and anti-apoptotic Bcl-2 family proteins are very similar, despite their antagonistic activities, however, the structures of their membrane-associated forms have not been previously examined, and may be important for understanding their opposing functions. Moreover, most of the previous structural and functional studies have focused on soluble truncated proteins, lacking the C-terminal 20-residue hydrophobic domain, which is present in many of the family members and is important for membrane targeting.

The support of this grant has enabled us to initiate a major research effort to determine the structures of membrane-bound and full-length Bcl-2 proteins. The results from these studies serve as a platform for additional structural and biological experiments aimed at examining the structural consequences of modifications (mutations, cleavage, phosphorylation, myristoylation) and interactions (with other Bcl-2 and non-homologous proteins), as we try to understand apoptosis regulation by the Bcl-2 family proteins.

We have focused our studies on Bcl-2 family members with opposing activities, namely, anti-apoptotic Bcl-xL, and pro-apoptotic Bid and Bim. These proteins share homology only in the BH3 domain, and Bid does not have a hydrophobic C domain. Our studies have led to the surprising but important discovery that both Bcl-XL and Bid associate with the membrane surface, without insertion of a hydrophobic helical hairpin which had been previously thought to mediate membrane association and pore formation. This suggests that mitochondrial membrane destabilization by some Bcl-2 family proteins may be similar to bacterial membrane destabilization by antibiotic polypeptides.

BODY

The research accomplishments associated with the tasks outlined in the original Statement of Work (SOW) are described below, and, in greater detail, in the manuscripts attached in the Appendix of this report [1-4].

Specific Aim 1.

(Task 1) Prepare milligrams of isotopically labeled full-length Bcl2 by expression in *E. coli*.

We have expressed and purified several recombinant members of the Bcl-2 family, Bcl-xL, Bid, Bim and several of their mutants and truncated forms. The proteins are expressed in *E. coli* as His-tagged proteins, or His-tagged TrpΔLE fusion proteins using pET vectors, or as GST fusion proteins using pGEX vectors [1,2,4]. Protein expression is obtained in minimal M9 media for isotopic labeling, as required for NMR.

This work also led us to develop a new plasmid vector for the expression of other membrane-associated proteins and hydrophobic peptides, which we named pBCL, and is based on fusion to the N-terminus of Bcl-XL [3]. This plasmid has been made available to the scientific community, and we have already shared it with other laboratories.

(Task 2) Prepare samples of Bcl2 in lipid bilayers and lipid micelles for solid-state and solution NMR.

We have prepared samples of Bcl-X_L, Bid, and Bim in lipid micelles and lipid bilayers for both solution and solid-state NMR structural studies.

We have developed new methods for NMR sample preparation and for rapid structure determination of membrane proteins in lipid bilayers [5-7], which are being applied to Bcl-2 proteins. These works are not directly associated with the tasks outlined in the SOW, however one of them [6] acknowledges the grant, because the ideas partially resulted from our experiments on Bcl-2 family proteins, funded by this grant.

(Task 3) Perform NMR experiments on Bcl2 proteins in lipid bilayers.

We have obtained NMR spectra of Bcl-X_L, Bid, tBid, and, more recently, Bim, in both lipid micelle and lipid bilayer environments. These spectra provide the first view of their conformations at membranes, and are being analyzed for structure determination [1,2,4].

The $^{1}H/^{15}N$ HSQC (heteronuclear single quantum correlation) NMR spectra from the purified proteins are well resolved with the appropriate number of backbone and side chain resonances, reflecting pure and homogenous preparations, and we have completely assigned the resonances in full-length Bcl-X_L in micelles [unpublished]. These spectra provide the basis for structure-activity-relationship studies with molecules that target Bcl-2 proteins.

John Reed, our collaborator on this grant (5% effort), has identified a peptide that binds pro-apoptotic Bax and Bid and modulates their activities [8]. We are carrying out solution chemical shit mapping NMR experiments to define the binding site of the peptide on Bid.

(Task 4) Determine the structures using orientation constraints.

We have measure several $^{1}H/^{15}N$ orientation restraints from samples of Bcl-XL and Bid in micelles oriented in stressed polyacrylamide gels, and lipid bilayers oriented on glass slides. We are using these restraints to determine the membrane bound structures.

Our studies on Bid and tBid, its activated product of caspase-8 cleavage, demonstrate that tBid associates with the membrane with its helices parallel to the membrane surface but without trans-membrane helix insertion. Thus the cytotoxic activity of tBid at mitochondria may be similar to that observed for antibiotic polypeptides, which bind to the surface of bacterial membranes as amphipathic helices and destabilize the bilayer structure promoting the leakage of cell contents [2]. Bcl-XL also appears to associate with the membrane surface rather than by inserting its helices across the lipid bilayer membrane [1,4].

Specific Aim 2.

(Task 1) Test the ion channel activities of mutant and wild-type Bcl2 proteins in lipid bilayers in vitro.

These measurements were intended to pursue the notion that Bcl-2 family proteins form ion-channels by inserting a helical hairpin in the mitochondrial membrane. However the structural studies supported by this grant [1,2,4], and the results of other laboratories [9], show that membrane penetration does not occur, and that the Bcl-2 proteins bind the membrane surface. Since it is difficult to reconcile this mode of membrane association with ion channel activity, we decided to shift our focus to cell-based and in-vitro functional assays of apoptosis.

(Task 2) Test the functions of wild-type and mutant Bcl2 proteins in cells.

The functional studies, carried out in parallel with the structural work, served the two purposes of (1) testing the functionality of the Bcl-2 samples that we prepare for structure determination, and (2) characterizing the biological functions of wild-type and mutant forms.

We have tested the ability of recombinant tBid to induce the release of mitochondrial proteins by incubating it with mitochondria isolated from HeLa cells, assaying the supernatant and pelleted fractions with antibodies to cytochrome-c and SMAC.

We also tested the ability of recombinant tBid and Bcl-XL to bind each other and to bind anti-apoptotic peptides. Recombinant tBid, used in the structural studies, is fully active in its ability to induce cytochrome-c and SMAC release from isolated mitochondria, and its capacity to bind anti-apoptotic Bcl-X_L through its BH3 domain is not disrupted by the M97L mutation introduced to facilitate protein expression [2].

KEY RESEARCH ACCOMPLISHMENTS

- We have expressed and purified milligram quantities of Bcl-2 family proteins (Bcl-XL, tBid, and Bim) that have been notoriously difficult to express and purify because of either poor solubility (full-length Bcl-XL) or toxicity (tBid and Bim) [2].
- We have determined the secondary structure and topology of Bcl-XL and tBid in membrane environments [1,2,4].
- We have confirmed the biological activity of recombinant tBid and Bcl-XL produced for NMR studies in bilayers [2].
- We have completely assigned the spectrum of full-length Bcl-XL, including its hydrophobic C-terminus, in lipid micelles, and have obtained orientation restraints for structure determination [unpublished].
- We have developed a new plasmid vector that is useful for the high-level expression of membrane-associated proteins and hydrophobic peptides. This vector, named pBCL, is based on fusion of a target protein to the N-terminus of Bcl-XL [3]. It has been made available to the scientific community, and we have already shared it with other laboratories.

REPORTABLE OUTCOMES

Development of a new Bcl-XL-based expression vector for membrane proteins.

- The new plasmid vector we developed for the high-level expression of membrane-associated proteins, and hydrophobic peptides, is described in reference [3], which is included in the appendix material. This vector, named pBCL, is based on fusion of a target protein to the N-terminus of Bcl-XL. It has been made available to the scientific community, and we have already shared it with other laboratories.

Publications directly related to the SOW of this award (entire grant period).

- Franzin CM, Choi J, Zhai D, Reed JC, Marassi FM (2004) Structural studies of apoptosis and ion transport regulatory proteins in membranes. Magn Reson Chem 42, 172-179.
- Gong XM, Choi J, Franzin CM, Zhai D, Reed JC, Marassi FM (2004) Conformation of membrane-associated proapoptotic tBid. J Biol Chem 279, 28954-28960.
- Thai K, Choi J, Franzin CM, Marassi FM (2005) Bcl-XL as a fusion protein for the high-level expression of membrane-associated proteins. Protein Sci 14, 948-955.
- Gong XM, Choi J, Marassi FM (in press) NMR of Membrane Proteins in Lipid Environments: the Bcl-2 family of apoptosis regulators. In Lipid Protein Interactions, Biophysics Monographs, Gonzalez Ros JM, ed. (Berlin, Springer).

Publications that acknowledge support of this award (entire grant period).

- Marassi FM, Opella SJ (2003) Simultaneous assignment and structure determination of a membrane protein from NMR orientational restraints. *Protein Sci* 12, 403-411.
- Franzin CM, Choi J, Zhai D, Reed JC, Marassi FM (2004) Structural studies of apoptosis and ion transport regulatory proteins in membranes. *Magn Reson Chem* 42, 172-179.
- Gong XM, Choi J, Franzin CM, Zhai D, Reed JC, Marassi FM (2004) Conformation of membrane-associated proapoptotic tBid. *J Biol Chem* 279, 28954-28960.
- Opella SJ, Marassi FM (2004) Structure determination of membrane proteins by NMR spectroscopy. *Chem Rev* 104, 3587-3606.
- Thai K, Choi J, Franzin CM, Marassi FM (2005) Bcl-XL as a fusion protein for the high-level expression of membrane-associated proteins. *Protein Sci* 14, 948-955.
- Gong XM, Choi J, Marassi FM (in press) NMR of Membrane Proteins in Lipid Environments: the Bcl-2 family of apoptosis regulators. In *Lipid Protein Interactions, Biophysics Monographs*, Gonzalez Ros JM, ed. (Berlin, Springer).

Meeting Abstracts that acknowledge support of this award (entire grant period).

- Crowell KJ, Franzin CM, Sahani K, Reed JC, and Marassi FM (2002). NMR structure determination of FXYD and Bcl2 family membrane proteins in lipid environments. 43rd Experimental Nuclear Magnetic Resonance Conference (Pacific Grove, CA) Abstr M/T P174.
- Crowell KJ, Franzin CM, Sahani K, Reed JC, and Marassi FM (2002). NMR Structural studies of membrane proteins in lipid environments. 46th Biophysical Society Meeting (San Francisco, CA.) Abstr 2280-Pos.
- Marassi FM, and Opella SJ (2002). Simultaneous resonance assignment and structure determination in the solid-state NMR spectrum of a membrane protein in lipid bilayers. *46th Biophysical Society Meeting* (San Francisco, CA.) Abstr 2279-Pos.
- Choi J, and Marassi FM (2003). Structural studies of the Bcl-2 family proteins in lipid environments. *California Breast Cancer Research Program Symposium* (San Diego, CA) Abstr BB-3.
- Marassi FM, Crowell KJ, Franzin CM, Koltay A, and Reed JC (2003). NMR of the FXYD and Bcl-2 family proteins in lipid bilayers and micelles. *Keystone Symposium: membrane proteins structure and mechanism* (Taos, NM) Abstr 416.
- Choi J, Gong X-M, Franzin CM, Zhai D, Reed JC, and Marassi FM (2004). Structural Studies of the Bcl-2 Family Proteins in Membrane Environments. *15th ISMAR-International Society for Magnetic Resonance* (Jacksonville, FL) Abstr C-52.
- Marassi FM (2004). Structural studies of apoptosis and ion transport regulatory proteins in membranes. *5th Biennial Structural Biology Symposium* (Tallahasse FL).
- Marassi FM (2004). Solid-state NMR Structure Determination of Membrane Peptides and Proteins. Gordon Conference: Chemistry and Biology of Peptides (Ventura, CA).
- Marassi FM, Choi J, Gong X-M, Zhai D, and Reed JC (2004). NMR Structures of membrane-bound Bcl-2 family proteins. *Keystone Symposium: Apoptosis in Biochemistry and Structural Biology* (Keystone, CO) Abstr 223.
- Marassi FM (2004). Structure Determination of Membrane-associated Cell Killers and Ion Transporters. 15th ISMAR-International Society for Magnetic Resonance (Jacksonville, FL).
- Choi J, Franzin CM, Gong X-M, Thai K, yu J, Zhai D, Reed JC, and Marassi FM (2005). Ion transport and apoptosis regulatory proteins in lipid environments: the FXYD and Bcl-2 family proteins. *Keystone Symposium: Frontiers of NMR in Molecular Biology IX* (Banff, Canada).
- Choi J, Franzin CM, Gong X-M, Thai K, yu J, Zhai D, Reed JC, and Marassi FM (2005). Structural studies of ion transport and apoptosis regulatory proteins in lipid environments: the FXYD and Bcl-2 family proteins. *49th Biophysical Society Meeting* (Long Beach, CA).

Funding obtained, based on work supported by this award.

R21 AI063563-01 (PI: Marassi) 03/15/05 - 0214/07

National Institutes of Health / NIAID

Bim structure and apoptosis: The goal is to determine the structure of Bim in its soluble form, and to begin structure determination in membrane environments.

R01 GM065374-01 (PI: Marassi) 04/01/05 - 03/31/09

National Institutes of Health / NIGMS

Structures of the Membrane-associated Bcl-2 Apoptotic Proteins: The goal is to continue our efforts to determine the structures of membrane-associated Bcl2 family proteins, and to understand the functional role of membrane-association in apoptosis.

List of personnel supported by this award (entire grant period).

Francesca M. MARASSI	principal investigator
John C. Reed	collaborating investigator
Komal Sahani	research assistant
Jungyuen Choi	research assistant
Xiao-Min Gong	postdoctoral fellow

CONCLUSIONS

Our work supported by this grant has enabled us to obtain the first membrane-bound structural data on the Bcl-2 protein family, using solid-state NMR in lipid bilayer samples [1,2]. The spectra provide the first structural view of Bcl-XL and Bid in membranes, and provide insights to their function in apoptosis regulation. We are currently working on NMR data analysis for three-dimensional structure determination, and have made additional progress in developing the methodology for NMR structure determination of membrane proteins in lipid bilayers [6]. In addition, in collaboration with John Reed, also at the Burnham Institute, we are carrying out NMR experiments to map the binding site of an apoptosis regulatory peptide on pro-apoptotic Bid. The work supported by this award and described in this report, enabled us to apply for funding from the National Institutes of Health (R01GM65374; R21AI063563) and the Department of Defense (BC044465) to extend the project to include other Bcl-2 proteins.

REFERENCES

1. Franzin CM, Choi J, Zhai D, Reed JC, and Marassi FM (2004). Structural studies of apoptosis and ion transport regulatory proteins in membranes. *Magn Reson Chem* 42, 172-179.
2. Gong XM, Choi J, Franzin CM, Zhai D, Reed JC, and Marassi FM (2004). Conformation of Membrane-associated Proapoptotic tBid. *J Biol Chem* 279, 28954-28960.
3. Thai K, Choi J, Franzin CM, and Marassi FM (2005). Bcl-XL as a fusion protein for the high-level expression of membrane-associated proteins. *Protein Sci* 14, 948-955.
4. Gong XM, Choi J, and Marassi FM (in press). NMR of Membrane Proteins in Lipid Environments: the Bcl-2 family of apoptosis regulators. In *Lipid Protein Interactions, Biophysics Monographs*, Gonzalez Ros JM, ed. (Berlin, Springer).
5. Marassi FM, and Crowell KJ (2003). Hydration-optimized oriented phospholipid bilayer samples for solid-state NMR structural studies of membrane proteins. *J Magn Reson* 161, 64-69.
6. Marassi FM, and Opella SJ (2003). Simultaneous assignment and structure determination of a membrane protein from NMR orientational restraints. *Protein Sci* 12, 403-411.
7. Mesleh MF, Lee S, Veglia G, Thiriot DS, Marassi FM, and Opella SJ (2003). Dipolar waves map the structure and topology of helices in membrane proteins. *J Am Chem Soc* 125, 8928-8935.
8. Guo B, Zhai D, Cabezas E, Welsh K, Nouraini S, Satterthwait AC, and Reed JC (2003). Humanin peptide suppresses apoptosis by interfering with Bax activation. *Nature* 423, 456-461.
9. Oh KJ, Barbuto S, Meyer N, Kim RS, Collier RJ, and Korsmeyer SJ (2004). Conformational changes in BID, a pro-apoptotic BCL-2 family member, upon membrane-binding: A site-directed spin labeling study. *J Biol Chem.*

APPENDIX

Reprints and preprints.

- Franzin CM, Choi J, Zhai D, Reed JC, Marassi FM (2004) Structural studies of apoptosis and ion transport regulatory proteins in membranes. *Magn Reson Chem* 42, 172-179.
- Gong XM, Choi J, Franzin CM, Zhai D, Reed JC, Marassi FM (2004) Conformation of membrane-associated proapoptotic tBid. *J Biol Chem* 279, 28954-28960.
- Thai K, Choi J, Franzin CM, Marassi FM (2005) Bcl-XL as a fusion protein for the high-level expression of membrane-associated proteins. *Protein Sci* 14, 948-955.
- Gong XM, Choi J, Marassi FM (in press) NMR of Membrane Proteins in Lipid Environments: the Bcl-2 family of apoptosis regulators. In *Lipid Protein Interactions, Biophysics Monographs*, Gonzalez Ros JM, ed. (Berlin, Springer).

MAGNETIC RESONANCE IN CHEMISTRY
Magn. Reson. Chem. 2004; **42**: 172–179
Published online in Wiley InterScience (www.interscience.wiley.com). DOI: 10.1002/mrc.1322

MRC

Structural studies of apoptosis and ion transport regulatory proteins in membranes

Carla M. Franzin, Jungyuen Choi, Dayong Zhai, John C. Reed and Francesca M. Marassi*

The Burnham Institute, 10901 North Torrey Pines Road, La Jolla, California 92037, USA

Received 30 May 2003; Revised 20 August 2003; Accepted 28 August 2003

Solid-state NMR spectroscopy is being used to determine the structures of membrane proteins involved in the regulation of apoptosis and ion transport. The Bcl-2 family includes pro- and anti-apoptotic proteins that play a major regulatory role in mitochondrion-dependent apoptosis or programmed cell death. The NMR data obtained for ^{15}N-labeled anti-apoptotic Bcl-xL in lipid bilayers are consistent with membrane association through insertion of the two central hydrophobic α-helices that are also required for channel formation and cytoprotective activity. The FXYD family proteins regulate ion flux across membranes, through interaction with the Na^+, K^+-ATPase, in tissues that perform fluid and solute transport or that are electrically excitable. We have expressed and purified three FXYD family members, Mat8 (mammary tumor protein), CHIF (channel-inducing factor) and PLM (phospholemman), for structure determination by NMR in lipids. The solid-state NMR spectra of Bcl-2 and FXYD proteins, in uniaxially oriented lipid bilayers, give the first view of their membrane-associated architectures. Copyright © 2004 John Wiley & Sons, Ltd.

KEYWORDS: NMR; Bcl-2; Bcl-xL; FXYD; Mat8; PLM; CHIF; apoptosis; membrane proteins; lipid bilayers

INTRODUCTION

NMR spectroscopy is ideally suited for the structure determination of membrane proteins in lipid environments. Solution NMR methods for structure determination can be utilized on samples consisting of proteins dissolved in lipid micelles, while solid-state NMR methods can be applied to samples of membrane proteins in planar lipid bilayers.[1,2] The latter approach is especially attractive because it enables structures to be determined in a native-like environment. Furthermore, since the lipid bilayers are oriented with respect to the applied magnetic field, the samples preserve the intrinsic directional character of membrane protein structure and function. For membrane proteins that can be expressed, isotopically labeled, and purified chromatographically, reconstitution in oriented lipid bilayers gives single-line spectra with line widths that rival those from single crystals[3] and with characteristic patterns that directly reflect protein structure and topology.[4–6] This direct relationship between spectrum and structure provides the basis for a method that permits the simultaneous sequential assignment of resonances and measurement of orientational restraints for backbone structure determination in the two-dimensional solid-state NMR ^{1}H/^{15}N PISEMA spectra from a limited set of uniformly and selectively ^{15}N-labeled samples.[7,8] Here we describe solid-state NMR structural studies of two families of membrane-associated proteins involved in the regulation of apoptosis, or programmed cell death, and ion transport. The spectra provide the first view of these protein structures in membranes, and also provide the starting point for three-dimensional structure determination which should give significant insights to their biological functions.

Bcl-2 family proteins

The Bcl-2 family includes both anti-apoptotic, or cytoprotective, proteins (Bcl-2, Bcl-xL) and pro-apoptotic, or death-promoting, proteins (Bid, Bax).[9–12] Imbalances in their relative expression levels or activities result in insufficient cell death, as in cancer and autoimmunity, or excessive cell death, as in Alzheimer's disease, stroke and AIDS. The Bcl-2 proteins exert their apoptotic activities through dimerization with other Bcl-2 family proteins, binding to other non-homologous proteins, and through the formation of ion channels or pores, that are believed to play an important role in apoptosis by perturbing mitochondrial physiology leading to the release of cytochrome *c*. Their function is also regulated by subcellular location, as they cycle between soluble and membrane-bound forms. For example, anti-apoptotic Bcl-xL is found predominantly in mitochondrial, endoplasmic reticulum, or nuclear membranes, and pro-apoptotic Bax is found in the cytosol when inactive, but is stimulated by death signals to insert in the mitochondrial outer

*Correspondence to: Francesca M. Marassi, The Burnham Institute, 10901 North Torrey Pines Road, La Jolla, California 92037, USA.
E-mail: fmarassi@burnham.org
Contract/grant sponsor: National Institutes of Health National Cancer Institute; Contract/grant numbers: R01CA82864; R01GM60554.
Contract/grant sponsor: Department of the Army Breast Cancer Research Program; Contract/grant numbers: DAMD17-00-1-0506; DAMD17-02-1-0313.
Contract/grant sponsor: California Breast Cancer Research Program; Contract/grant number: 8WB0100.

membrane, where it participates in cytochrome *c* release and mitochondrion-dependent apoptosis.

The Bcl-2 domains required for apoptotic activity and dimerization have been determined by deletional and mutational analyses, and corroborated by their solution structures, solved primarily by NMR spectroscopy.[13–23] The proteins are built in modules of up to four highly conserved Bcl-2 homology (BH) domains, of which the BH3 domain is highly conserved and essential for cell killing activity and for oligomerization with other family members [Fig. 1(A)]. Several family members also have a hydrophobic C-terminal domain, which is probably involved in membrane association. The solution structures are very similar [Fig. 1(B)], despite the lack of extensive sequence homology, and consist of two central and largely hydrophobic or α-helices, flanked on two sides by amphipathic helices and a large flexible loop which connects the first two helices. Notably, the structures also bear a striking similarity to those of the pore-forming domains of bacterial toxins, known to form ion channels in bacterial membranes [Fig. 1(C)], and indeed, several Bcl-2 proteins, including Bcl-xL, Bcl-2, Bax and Bid, form ion channels under conditions where bacterial toxins also form channels.[24–27] Solution NMR studies of anti-apoptotic Bcl-xL and pro-apoptotic Bax, in lipid micelles, indicate that the structures in membrane environments are very different.[20,28] The three-dimensional membrane-associated structures are not known, but may be key to the functional differences between pro- and anti-apoptotic members of the family. The expression and purification of several Bcl-2 family proteins have been described,[29–31] and here we present the first structural studies in lipid bilayer membranes.

FXYD family proteins

The FXYD family proteins are expressed abundantly in tissues that perform fluid and solute transport (breast/mammary gland, kidney, colon, pancreas, prostate, liver, lung and placenta), or that are electrically excitable (muscle, nervous system), where they function to regulate the flux of transmembrane ions, osmolytes and fluids.[32] The protein sequences are highly conserved through evolution, and are characterized by a 35-amino acid FXYD homology (FH) domain, which includes the transmembrane (TM) domain (Fig. 2). The short motif PFXYD (Pro, Phe, X, Tyr, Asp), preceding the transmembrane domain, is invariant in all known mammalian examples, and identical in other vertebrates, except for the proline. X is usually Tyr, but can also be Thr, Glu or His. In all these proteins, conserved basic residues flank the TM domain, the extracellular N-termini are acidic and the cytoplasmic C-termini are basic. PLM (phospholemman) is one of the best characterized members of this family, and the major substrate of hormone-stimulated phosphorylation by cAMP-dependent protein

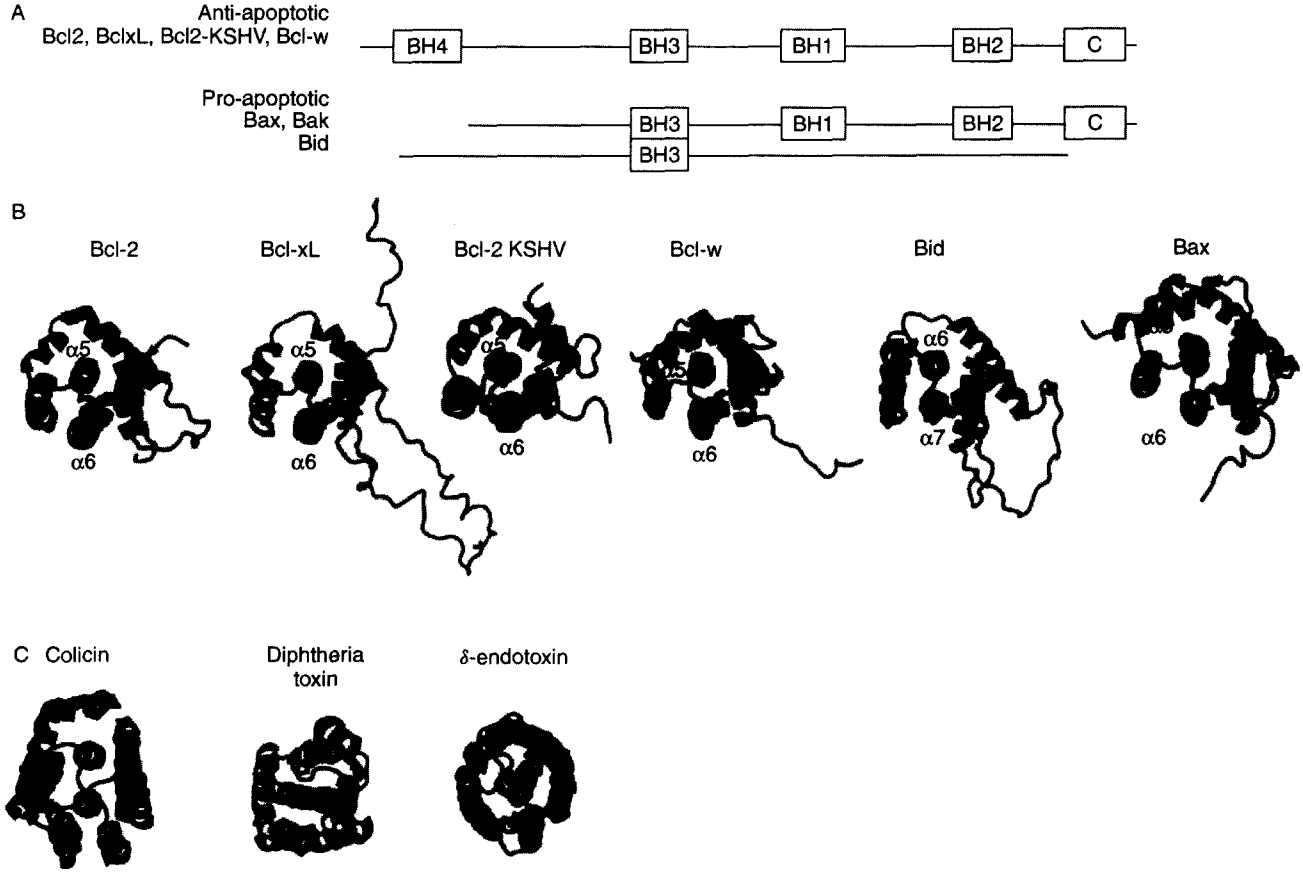

Figure 1. Conserved Bcl-2 homology (BH) domains (A) and solution structures (B) of the Bcl-2 protein super family.[13–23] The PDB file numbers of the structures are given in parentheses for Bcl-2 (1G5M), Bcl-xL (1LXL), Bax (1F16), Bid (2BID, 1DDB), KSHV-Bcl-2 (1K3K3) and Bcl-w (1O0L, 1MK3). The structures are highly homologous to those of (C) the channel-forming domains of the bacterial toxins, colicin (1COL), diphteria toxin (1DDT) and δ-endotoxin (1DLC).

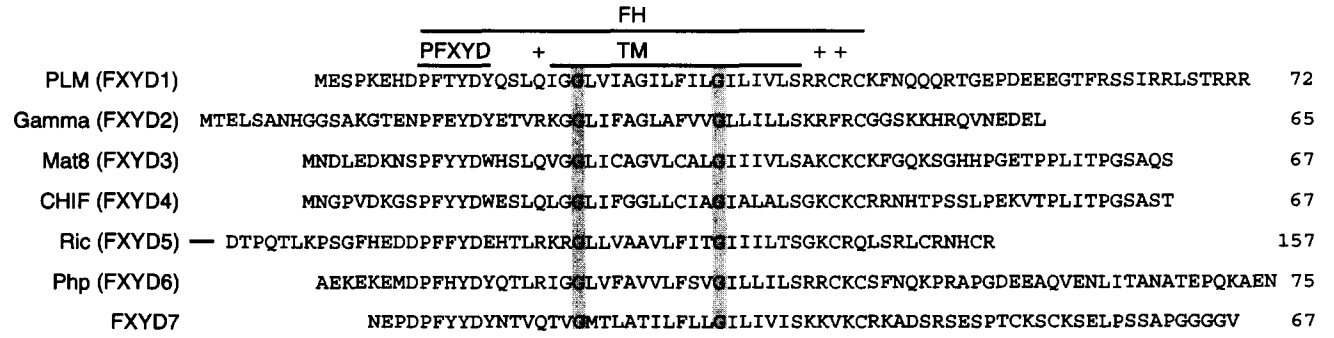

Figure 2. Amino acid sequences of the FXYD membrane proteins. The FXYD homology (FH) domain encompasses the FXYD consensus sequence and the transmembrane (TM) domain is flanked by conserved positively charged residues. Conserved Gly residues in the TM domain are highlighted in gray.

kinase A and C in the heart.[33] CHIF (channel-inducing factor) is upregulated by aldosterone and corticosteroids in mammalian kidney and intestinal tracks, where it regulates Na^+ and K^+ homeostasis.[34] Mat8 (mammary tumor protein 8 kDa) is expressed in breast, prostate, lung, stomach, and colon, and also in human breast tumors, breast tumor cell lines and prostate cancer cell lines, after malignant transformation by oncogenes.[35,36] Other FXYD proteins are also induced by oncogenic transformation. All three proteins, PLM, Mat8 and CHIF, induce ionic currents in *Xenopus* oocytes and PLM also forms ion channels in phospholipid bilayers.[35,37,38] The identification of several FXYD family members, including PLM and CHIF, as regulators of Na^+, K^+-ATPase, points to a mechanism for regulation of the pump that involves the expression of an auxiliary subunit.[39–42] Recently, we described the recombinant expression, purification and sample preparation in lipid micelles and bilayers for three members of the FXYD family: Mat8, PLM and CHIF.[43]

EXPERIMENTAL

Protein expression and purification

Cloning, protein expression in *E. coli* and protein purification, have been described for both Bcl-2 and FXYD family proteins.[29–31,43] For protein expression, transformed *E. coli* clones were grown on minimal M9 media [100 μg ml^{-1} ampicillin, 7.0 g l^{-1} Na_2HPO_4, 3.0 g l^{-1} KH_2PO_4, 0.5 g l^{-1} NaCl, 11 mg l^{-1} $CaCl_2$, 120 mg l^{-1} $MgSO_4$, 50 mg l^{-1} thiamine, 1% (v/v) LB, 10 g l^{-1} D-glucose, 1 g l^{-1} $(NH_4)_2SO_4$]. For uniformly ^{15}N-labeled proteins, $(^{15}NH_4)_2SO_4$ (Cambridge Isotope Laboratories, Andover, MA, USA) was supplied as the sole nitrogen source. The identity, purity and secondary structure folds of the proteins were characterized by N-terminal amino acid sequence analysis, MALDI/TOF mass spectrometry, CD spectroscopy and solution NMR spectroscopy.

The anti-apoptotic protein Bcl-xL was expressed in a pET vector, as a soluble protein lacking C-terminal residues 212–233, with a N-terminal $(His)_6$ tag. After Ni affinity purification, Bcl-xL was further purified by anion-exchange chromatography [HiPrep 16/10 Q FF (Amersham Biosciences, Piscataway, NJ USA); linear gradient of NaCl, in 50 mM sodium phosphate, pH 7.0], followed by size-exclusion chromatography [Sephacryl-100 (Amersham Biosciences) in 20 mM sodium phosphate, 150 mM NaCl, 1 mM EDTA, 1 mM NaN_3, pH 7].

The FXYD proteins PLM, CHIF and Mat8 were expressed in a pET vector as fusions with the His-Tag–TrpΔLE partner, which promotes the formation of inclusion bodies.[44] After Ni affinity purification, the fusion protein was reacted with CNBr to release intact FXYD, and the resulting mixture was purified first by size-exclusion chromatography [Sephacryl-100 (Amersham Biosciences) in 10 mM sodium phosphate, 4 mM SDS, 23 mM DTT, 1 mM EDTA, 1 mM NaN_3, pH 7.5] and then by preparative reversed-phase HPLC [Delta-Pak C4 column, 15 μm, 300 Å, 300 × 7.8 mm i.d. (Waters, Milford, MA, USA); linear gradient of acetonitrile in 9:1 water–acetonitrile containing 0.1% trifluoroacetic acid].

Solid-state NMR samples

Samples of Bcl-xL in lipid bilayers were prepared by mixing 2 mg of ^{15}N labeled Bcl-xL, dissolved in buffer (10% β-octylglucoside, 20 mM sodium phosphate, 150 mM NaCl, 1 mM EDTA, 1 mM NaN_3, pH 7.0), with 100 mg of lipid, DOPC (dioleoylphosphatidylcholine) and DOPG (dioleoylphosphatidylglycerol) in a molar ratio of 6:4, which had been sonicated to form unilamellar vesicles. After mixing, 5 ml of water were added, the mixture was quick-frozen in liquid nitrogen, allowed to thaw at room temperature and bath-sonicated for 30 s. Detergent was removed by dialyzing the preparation against two changes of 4 l of buffer, followed by two changes of 4 l of water, over 18 h. The reconstituted vesicles were concentrated by ultrafiltration and spread on the surface of 35 glass slides, excess water was evaporated at 42 °C and the slides were stacked.

Samples of CHIF and Mat8 in lipid bilayers were prepared by first dissolving 2 mg of ^{15}N-labeled protein in 0.5 ml of TFE with 50 μl of β-mercaptoethanol and then adding 100 mg of lipid, DOPC–DOPG (8:2 molar ratio), in 1 ml of $CHCl_3$. After spreading this solution on the surface of 35 glass slides, the solvents were removed under vacuum overnight and the slides were stacked. For both Bcl-xL and FXYDs, oriented lipid bilayers were formed by equilibrating the stacked slides (dimensions 11 × 20 × 0.06 mm) (Paul Marienfeld, Germany) for 24 h at 40 °C in a chamber containing a saturated solution of ammonium phosphate.

which provides an atmosphere of 93% relative humidity. The samples were wrapped in Parafilm and then sealed in thin polyethylene film prior to insertion in the NMR probe. Hydrogen-exchanged samples were prepared by exposing the stacked oriented bilayer samples to an atmosphere saturated with ^2H_2O. This was achieved by placing the sample in a closed chamber containing ^2H_2O and incubating at 40 °C for 24 h.

NMR spectroscopy

Solid-state NMR spectra were obtained at 23 °C on a Bruker (Billerica, MA, USA) AVANCE 500 spectrometer with a wide-bore 500/89 Magnex (Yarnton, UK) magnet, and on a Chemagnetics-Otsuka Electronics (Fort Collins, CO, USA) CMX400 spectrometer, with a wide-bore 400/89 Oxford Instruments (Abingdon, UK) magnet. The laboratory-built double-resonance ($^1H/^{15}N$ or $^1H/^{31}P$) probes had square r.f. coils wrapped directly around the samples. The ^{15}N spectra were obtained with single contact 1 ms CPMOIST[45,46] and the ^{31}P spectra with a single pulse. Both were acquired with continuous ^1H irradiation (r.f. field strength 63 kHz), in order to decouple the $^1H-^{15}N$ and $^1H-^{31}P$ dipolar interactions. The ^{15}N and ^{31}P chemical shifts were referenced to 0 ppm for liquid ammonia and phosphoric acid. The NMR data were processed using the programs NMRPipe[47] and FELIX (Accelerys, San Diego, CA, USA) on Linux/Dell (Round Rock, TX, USA) or Silicon Graphics (Mountain View, CA, USA) computer workstations.

RESULTS AND DISCUSSION

Anti-apoptotic Bcl-xL

The spectra in Figure 3 were obtained from samples of Bcl-xL in oriented [Fig. 3(A) and (C)] and unoriented [Fig. 3(B)] lipid bilayers. The spectra from unoriented samples are excellent indicators of protein dynamics, because motional averaging has pronounced effects on powder patterns. The spectrum from the unoriented sample of Bcl-xL, which spans the full range (60–220 ppm) of the amide ^{15}N chemical shift interaction, shows no evidence of motional averaging. The intensity near 35 ppm, also present in the spectrum from the oriented sample, is from the protein amino groups, which have a considerably narrower ^{15}N chemical shift anisotropy. In contrast, the spectrum obtained from oriented Bcl-xL [Fig. 3(A)] is very different, as it is separated into discernable resonances with distinctly increased intensity near 170 and 80 ppm. The dominant spectral features reflect a structural model where resonances near 170 ppm are from the membrane-inserted helices and resonances near 80 ppm are from helices resting on the membrane surface. The phospholipid phase and the degree of phospholipid bilayer alignment can be assessed with ^{31}P NMR spectroscopy of

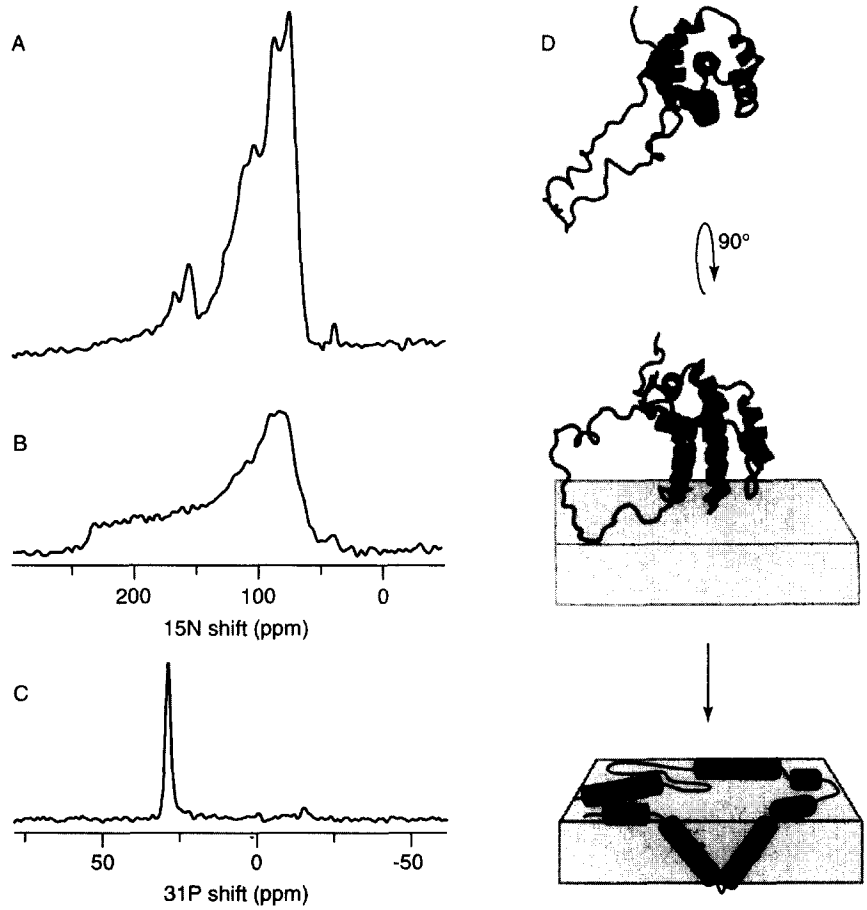

Figure 3. ^{31}P and ^{15}N chemical shift solid-state NMR spectra of uniformly ^{15}N-labeled Bcl-xL in oriented (A, C) and unoriented (B) lipid bilayers. The data support an umbrella model for membrane association of Bcl-2 family proteins (D), illustrated here for Bcl-xL (PDB file 1LXL)[14]

the lipid phosphate headgroup. The ^{31}P NMR spectrum obtained for oriented lipids with Bcl-xL has a single resonance near 30 ppm, which is characteristic of intact and highly oriented membranes in a bilayer arrangement [Fig. 3(C)]. The presence of a single peak demonstrates that the samples are highly oriented, as required for NMR structure determination. Thus, taken together, the ^{15}N and ^{31}P spectra provide evidence that Bcl-xL, an anti-apoptotic Bcl-2 family protein, inserts in membranes, and does so without disruption of the membrane integrity.

Like the pore-forming domain of bacterial colicin, Bcl-xL has two central hydrophobic helices, $\alpha5$ and $\alpha6$, that are long enough to span the membrane, and are required for both channel formation and cytoprotective activity.[48] We find that this structural similarity between the soluble forms of the two proteins appears to extend to their membrane associated structures. For colicin, insertion of the hydrophobic helical hairpin into the membrane is supported by planar bilayer experiments,[49] fluorescence energy transfer[50] and solid-state NMR.[51,52] Membrane association occurs when the colicin soluble helical bundle unfolds, exposing the hydrophobic helical hairpin which inserts in the membrane, while the rest of the protein forms a helical network on the membrane surface, adopting a so-called umbrella conformation.[50,53] The solid-state NMR data in Fig. 3(A) suggest that Bcl-xL associates with membranes in a similar fashion, as illustrated in Fig. 3(D), with the $\alpha5$–$\alpha6$ helical hairpin inserting in the membrane.

The two-dimensional $^{1}H/^{15}N$ PISEMA (Polarization Inversion with Spin Exchange at the Magic Angle)[54] spectra of oriented proteins display characteristic patterns of resonances that reflect helical wheel projections of protein residues, and that are sensitive to the tilt and rotation of helices in membranes [Fig. 4(C)].[4–6] These two-dimensional patterns serve as sensitive and visually accessible indices of membrane protein secondary structure and topology, but the positions of resonances in the corresponding one-dimensional projections can also provide good estimates of helix tilt [Fig. 4(B)]. Thus, in the spectrum from oriented Bcl-xL, the observation of ^{15}N chemical shifts near 170 ppm suggests that the membrane-inserting helices cross the lipid bilayer with a substantial angle. We determined this angle to be around 40°, by comparing the Bcl-xL spectrum [Fig. 4(B), black] with the spectra calculated for helices at varying degrees of tilt [Fig. 4(B), gray]. For helices with this tilt, the ^{15}N resonances are spread over a frequency range of about 60 ppm and, depending on helix rotation, they can be segregated into two major bands of equal intensity centered at 175 and 125 ppm. In the spectrum of oriented Bcl-xL, we determined the ratio of spectral intensities centered at 170 ppm (I_{170}) and 80 ppm (I_{80}) to be $I_{170}:I_{80} = 15:85$. This is consistent with a model for membrane association, where the $\alpha5$ and $\alpha6$ helices of Bcl-xL, which make up about 20% of the total protein, span the membrane with a tilt of 40°, adding to the spectral intensity at both 170 and 125 ppm, while the other helices rest on the membrane surface, adding to spectral intensity at 80 ppm. This is the umbrella model shown in Fig. 3(D).

The solid-state NMR samples of Bcl-xL in oriented lipid bilayers were prepared with the same Bcl-xL constructs and methods for sample preparation that were used for the ion-channel activity studies, which provided the initial evidence for membrane insertion by Bcl-xL. Nevertheless, we note that resonances at chemical shifts for transmembrane amide nitrogens simply imply amide NH bonds aligned with the bilayer normal, and demonstrating that these are indeed transmembrane domains requires the resolution and assignment of resonances in two- and three-dimensional spectra, followed by structure determination.

FXYD proteins

The solid-state NMR spectra of ^{15}N-labeled CHIF and Mat8 in lipid bilayers are shown in Fig. 5. The degree

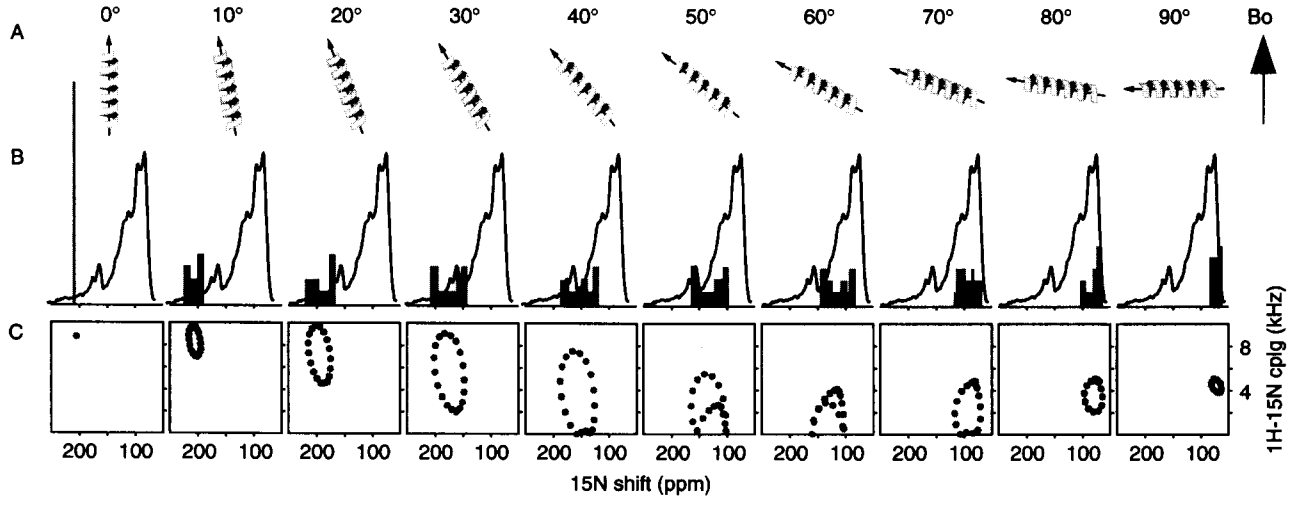

Figure 4. Experimental (black) and calculated (gray) solid-state NMR spectra for a 20-residue α-helix, with uniform dihedral angles ($\phi/\psi = -65/-40°$), at different helix tilts relative to the magnetic field direction and the membrane normal (A). The calculated one-dimensional spectra (gray) are superimposed with the spectrum from uniformly ^{15}N-labeled Bcl-xL in oriented lipid bilayers (black) (B). The two-dimensional $^{1}H/^{15}N$ PISEMA spectra trace out the characteristic resonance Pisa wheels from helices associated with membranes (C).

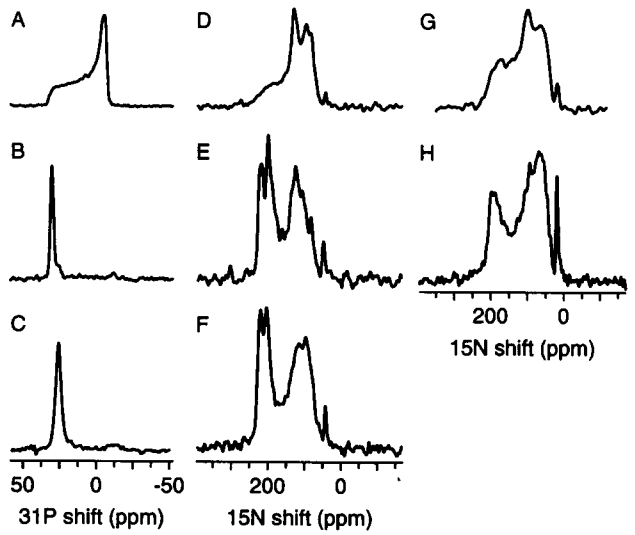

Figure 5. ^{31}P and ^{15}N chemical shift solid-state NMR spectra of uniformly ^{15}N-labeled CHIF (A–F) and Mat8 (G, H) in lipid bilayers. Spectra were obtained from unoriented lipid bilayer samples (A, D, G), from oriented lipid bilayer samples (B, E, H) and from hydration-optimized lipid bilayers containing CHIF (C, F).

of phospholipid bilayer alignment can be assessed with ^{31}P NMR spectroscopy of the lipid phosphate headgroup, as shown in Fig. 5(A) and (B). The ^{31}P NMR spectra obtained for the CHIF samples are characteristic of intact liquid-crystalline bilayers, in both unoriented [Fig. 5(A)] and oriented [Fig. 5(B)] samples. Moreover, the spectrum from the oriented sample has a single peak near 30 ppm, as expected for highly aligned bilayers with this lipid composition (DOPC–DOPG, 8:2 molar ratio). These spectra demonstrate that the samples are highly oriented.

The one-dimensional ^{15}N chemical shift spectra of CHIF [Fig. 5(D) and (E)] and Mat8 [Fig. 5(G) and (H)] provide a first view of the topology adopted by FXYD proteins in membranes. A preliminary analysis of the solid-state NMR data is possible since both CD and NMR spectroscopy in micelles show that the overall secondary structure of these proteins is α-helical.[43] Many membrane proteins in lipid bilayers are largely immobile on the NMR time-scales, and their resonances are therefore not motionally averaged but have frequencies that reflect the orientation of their respective sites relative to the direction of the magnetic field. In our samples, the lipid bilayer plane is perpendicular to the magnetic field direction, and therefore each resonance frequency reflects the orientation of its corresponding protein site relative to the membrane.

In the spectra of CHIF and Mat8 in oriented bilayers [Fig. 5(E) and (H)], the resonance intensity near 200 ppm arises from backbone amide sites in the FXYD transmembrane helix that have their NH bonds nearly perpendicular to the plane of the membrane, while the intensity near 80 ppm is from sites in the N- and C-termini, with NH bonds nearly parallel to the membrane surface. The rather narrow dispersion of ^{15}N resonances centered around 200 ppm suggests that the transmembrane helix crosses the lipid bilayer membrane with a very small tilt angle. The spectrum of CHIF, in particular, has significant resolution with identifiable peaks at frequencies throughout the range of the ^{15}N amide chemical shift, and is strikingly different from that obtained from unoriented bilayers, which provides no resolution [Fig. 5(D)]. The peak near 35 ppm results from the amino groups of the lysine side-chains and the N-terminus.

For both CHIF and Mat8 in unoriented bilayers, most of the backbone sites are structured and immobile on the timescale of the ^{15}N chemical shift interaction (10 kHz), and contribute to the characteristic amide powder patterns between about 220 and 60 ppm [Fig. 5(D) and (G)]. Some of the backbone sites, probably near the N- and C-termini, are mobile, and give rise to the resonance band centered near 120 ppm. Therefore, while certain resonances near 120 ppm in the spectrum of oriented CHIF may reflect specific orientations of their corresponding sites, some others arise from mobile backbone sites.

Recently, we described the preparation of oriented, hydration-optimized lipid bilayer samples, for NMR structure determination of membrane proteins.[55] The samples consist of planar phospholipid bilayers, containing membrane proteins, that are oriented on single pairs of glass slides, and that have significantly reduced water content. The hydration-optimized samples overcome some of the difficulties associated with multi-dimensional, high-resolution, solid-state NMR spectroscopy of membrane proteins. They have greater stability over the course of multi-dimensional NMR experiments, they have lower sample conductance for greater r.f. power efficiency and allow greater r.f. coil filling factors to be obtained for improved experimental sensitivity. Sample preparation was illustrated for the FXYD membrane protein CHIF; in going from fully hydrated to hydration-optimized conditions, samples of CHIF in bilayers retained a high degree of alignment, as evidenced from the ^{31}P NMR spectrum [Fig. 5(C)], and also retained the protein structural features, as reflected in the ^{15}N spectrum [Fig. 5(F)].

Hydrogen exchange experiments are useful for identifying hydrogen-bonded residues, and can also provide evidence of transmembrane helices. When the CHIF sample was exposed to deuterated water, the amide hydrogens in the transmembrane helix did not exchange whereas those in the rest of the protein underwent hydrogen exchange, and their resonances disappeared from the spectrum [Fig. 6(C)]. Thus, the spectra in Fig. 6 provide evidence for a tight hydrogen bonding network in the transmembrane helix of CHIF.

CONCLUSIONS

The Bcl-2 family proteins act as powerful promoters or repressors of programmed cell death. These proteins cycle between soluble forms with globular structures determined primarily by NMR, and membrane-bound forms, that probably perturb mitochondrial physiology leading to the release of cytochrome *c* in mitochondrion-dependent apoptosis, and whose structures have not yet been determined. The ^{15}N solid-state NMR spectra of the anti-apoptotic family member Bcl-xL in oriented lipid bilayers are consistent with a model for membrane association where the protein inserts its central hydrophobic helices in the membrane, while the

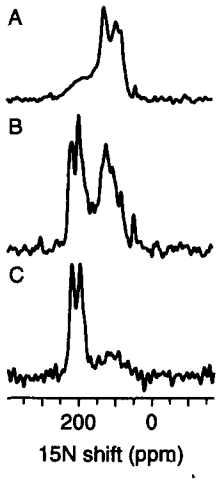

Figure 6. ^{15}N chemical shift solid-state NMR spectra of uniformly ^{15}N-labeled CHIF in unoriented (A) and oriented (B, C) lipid bilayers. Resonances near 200 ppm are from residues in the transmembrane helix that are resistant to hydrogen exchange, and are visible in the spectra obtained both after hydration with H_2O (A, B) and after hydration with ^2H_2O (C).

remaining helices fold up to rest on the membrane surface. This is similar to the umbrella model proposed for membrane association of the structurally homologous channel-forming bacterial colicins. The ^{31}P NMR spectra obtained from the oriented lipids in the sample demonstrate that membrane association of Bcl-xL maintains the lipid bilayer membranes intact, and highly oriented samples can be prepared for structural studies.

The FXYD membrane proteins regulate ion, osmolyte and fluid homeostasis in a variety of tissues, and are emerging as auxiliary tissue-specific and physiological state-specific subunits of the Na^+, K^+-ATPase. The cloning, expression and purification of the recombinant FXYD family members PLM, CHIF and Mat8 enable NMR structural studies to be performed in membrane environments, since the proteins can be isotopically labeled, and obtained in quantities that are suitable for NMR structure determination. The ^{15}N solid-state NMR spectra from oriented lipid bilayer samples provide a first view of the topological features of their transmembrane and terminal domains. The ability to produce milligram quantities of pure FXYD proteins lays the foundation for functional studies that, together with structure determination, can provide important structure–activity correlations. For example, the reconstitution of Na^+, K^+-ATPase activity in the presence of FXYD proteins would be an important step in understanding the mechanism of pump regulation, while the incorporation of FXYD proteins in lipid bilayers would enable ion channel activities to be characterized by measuring specific ionic currents.

Acknowledgments

This research was supported by grants from the National Institutes of Health National Cancer Institute (R01CA82864 to F.M.M. and R01GM60554 to J.C.R.), the Department of the Army Breast Cancer Research Program (DAMD17-00-1-0506 and DAMD17-02-1-0313 to F.M.M.), and the California Breast Cancer Research Program (8WB0110 to F.M.M.). It utilized the Burnham Institute NMR Facility supported by a grant from the National Institutes of Health (P30CA30199), and the Biomedical Technology Resources for Solid-state NMR of Proteins at the University of California San Diego, supported by a grant from the National Institutes of Health (P41EB002031).

REFERENCES

1. Marassi FM. *Concepts Magn. Reson.* 2002; **14**: 212.
2. Opella SJ, Ma C, Marassi FM. *Methods Enzymol.* 2001; **339**: 285.
3. Marassi FM, Ramamoorthy A, Opella SJ. *Proc. Natl. Acad. Sci. USA* 1997; **94**: 8551.
4. Marassi FM. *Biophys. J.* 2001; **80**: 994.
5. Marassi FM, Opella SJ. *J. Magn. Reson.* 2000; **144**: 150.
6. Wang J, Denny J, Tian C, Kim S, Mo Y, Kovacs F, Song Z, Nishimura K, Gan Z, Fu R, Quine JR, Cross TA. *J. Magn. Reson.* 2000; **144**: 162.
7. Marassi FM, Opella SJ. *J. Biomol. NMR* 2002; **23**: 239.
8. Marassi FM, Opella SJ. *Protein Sci.* 2003; **12**: 403.
9. Reed JC. *Nature (London)* 1997; **387**: 773.
10. Gross A, McDonnell JM, Korsmeyer SJ. *Genes Dev.* 1999; **13**: 1899.
11. Vander Heiden MG, Thompson CB. *Nat. Cell Biol.* 1999; **1**: E209.
12. Adams JM, Cory S. *Trends Biochem. Sci.* 2001; **26**: 61.
13. Fesik SW. *Cell* 2000; **103**: 273.
14. Muchmore SW, Sattler M, Liang H, Meadows RP, Harlan JE, Yoon HS, Nettesheim D, Chang BS, Thompson CB, Wong SL, Ng SL, Fesik SW. *Nature (London)* 1996; **381**: 335.
15. Aritomi M, Kunishima N, Inohara N, Ishibashi Y, Ohta S, Morikawa K. *J. Biol. Chem.* 1997; **272**: 27 886.
16. Petros AM, Medek A, Nettesheim DG, Kim DH, Yoon HS, Swift K, Matayoshi ED, Oltersdorf T, Fesik SW. *Proc. Natl. Acad. Sci. USA* 2001; **98**: 3012.
17. Sattler M, Liang H, Nettesheim D, Meadows RP, Harlan JE, Eberstadt M, Yoon HS, Shuker SB, Chang BS, Minn AJ, Thompson CB, Fesik SW. *Science* 1997; **275**: 983.
18. Chou JJ, Li H, Salvesen GS, Yuan J, Wagner G. *Cell* 1999; **96**: 615.
19. McDonnell JM, Fushman D, Milliman CL, Korsmeyer SJ, Cowburn D. *Cell* 1999; **96**: 625.
20. Suzuki M, Youle RJ, Tjandra N. *Cell* 2000; **103**: 645.
21. Huang Q, Petros AM, Virgin HW, Fesik SW, Olejniczak ET. *Proc. Natl. Acad. Sci. USA* 2002; **99**: 3428.
22. Denisov AY, Madiraju MS, Chen G, Khadir A, Beauparlant P, Attardo G, Shore GC, Gehring K. *J. Biol. Chem.* 2003; **278**: 21 124.
23. Hinds MG, Lackmann M, Skea GL, Harrison PJ, Huang DC, Day CL. *EMBO J.* 2003; **22**: 1497.
24. Schendel SL, Reed JC. *Methods Enzymol.* 2000; **322**: 274.
25. Minn AJ, Velez P, Schendel SL, Liang H, Muchmore SW, Fesik SW, Fill M, Thompson CB. *Nature (London)* 1997; **385**: 353.
26. Antonsson B, Montessuit S, Lauper S, Eskes R, Martinou JC. *Biochem. J.* 2000; **345**: (Pt 2): 271.
27. Schlesinger PH, Gross A, Yin XM, Yamamoto K, Saito M, Waksman G, Korsmeyer SJ. *Proc. Natl. Acad. Sci. USA* 1997; **94**: 11 357.
28. Losonczi JA, Olejniczak ET, Betz SF, Harlan JE, Mack J, Fesik SW. *Biochemistry* 2000; **39**: 11 024.
29. Zha H, Aime-Sempe C, Sato T, Reed JC. *J. Biol. Chem.* 1996; **271**: 7440.
30. Zha H, Fisk HA, Yaffe MP, Mahajan N, Herman B, Reed JC. *Mol. Cell. Biol.* 1996; **16**: 6494.
31. Schendel SL, Xie Z, Montal MO, Matsuyama S, Montal M, Reed JC. *Proc. Natl. Acad. Sci. USA* 1997; **94**: 5113.
32. Sweadner KJ, Rael E. *Genomics* 2000; **68**: 41.
33. Palmer CJ, Scott BT, Jones LR. *J. Biol. Chem.* 1991; **266**: 11 126.
34. Attali B, Guillemare E, Lesage F, Honore E, Romey G, Lazdunski M, Barhanin J. *Nature (London)* 1993; **365**: 850.
35. Morrison BW, Moorman JR, Kowdley GC, Kobayashi YM, Jones LR, Leder P. *J. Biol. Chem.* 1995; **270**: 2176.
36. Vaarala MH, Porvari K, Kyllonen A, Vihko P. *Lab. Invest.* 2000; **80**: 1259.
37. Moorman JR, Palmer CJ, John JE, 3rd, Durieux ME, Jones LR. *J. Biol. Chem.* 1992; **267**: 14 551.

38. Attali B, Latter H, Rachamim N, Garty H. *Proc. Natl. Acad. Sci. USA* 1995; **92**: 6092.
39. Arystarkhova E, Donnet C, Asinovski NK, Sweadner KJ. *J. Biol. Chem.* 2002; **277**: 10 162.
40. Beguin P, Crambert G, Guennoun S, Garty H, Horisberger JD, Geering K. *EMBO J.* 2001; **20**: 3993.
41. Beguin P, Crambert G, Monnet-Tschudi F, Uldry M, Horisberger JD, Garty H, Geering K. *EMBO J.* 2002; **21**: 3264.
42. Crambert G, Fuzesi M, Garty H, Karlish S, Geering K. *Proc. Nat. Acad. Sci. USA* 2002; **99**: 11 476.
43. Crowell KJ, Franzin CM, Koltay A, Lee S, Lucchese AM, Snyder BC, Marassi FM. *Biochim. Biophys. Acta* 2003; **1645**: 15.
44. Staley JP, Kim PS. *Protein Sci.* 1994; **3**: 1822.
45. Pines A, Gibby MG, Waugh JS. *J. Chem. Phys.* 1973; **59**: 569.
46. Levitt MH, Suter D, Ernst RR. *J. Chem. Phys.* 1986; **84**: 4243.
47. Delaglio F, Grzesiek S, Vuister GW, Zhu G, Pfeifer J, Bax A. *J. Biomol. NMR* 1995; **6**: 277.
48. Matsuyama S, Schendel SL, Xie Z, Reed JC. *J. Biol. Chem.* 1998; **273**: 30 995.
49. Kienker PK, Qiu X, Slatin SL, Finkelstein A, Jakes KS. *J. Membr. Biol.* 1997; **157**: 27.
50. Lindeberg M, Zakharov SD, Cramer WA. *J. Mol. Biol.* 2000; **295**: 679.
51. Kim Y, Valentine K, Opella SJ, Schendel SL, Cramer WA. *Protein Sci.* 1998; **7**: 342.
52. Kumashiro K, Schmidt-Rohr K, Murphy OJ, Ouellette KL, Cramer WA, Thompson LK. *J. Am. Chem. Soc.* 1998; **120**: 5043.
53. Elkins P, Bunker A, Cramer WA, Stauffacher CV. *Structure* 1997; **5**: 443.
54. Wu CH, Ramamoorthy A, Opella SJ. *J. Magn. Reson. A* 1994; **109**: 270.
55. Marassi FM, Crowell KJ. *J. Magn. Reson.* 2003; **161**: 64.

THE JOURNAL OF BIOLOGICAL CHEMISTRY
Vol. 279, No. 28, Issue of July 9, pp. 28954–28960, 2004
Printed in U.S.A.

Conformation of Membrane-associated Proapoptotic tBid*

Received for publication, March 30, 2004, and in revised form, April 26, 2004
Published, JBC Papers in Press, April 28, 2004, DOI 10.1074/jbc.M403490200

Xiao-Min Gong, Jungyuen Choi, Carla M. Franzin, Dayong Zhai, John C. Reed, and Francesca M. Marassi‡

From The Burnham Institute, La Jolla, California 92037

The proapoptotic Bcl-2 family protein Bid is cleaved by caspase-8 to release the C-terminal fragment tBid, which translocates to the outer mitochondrial membrane and induces massive cytochrome *c* release and cell death. In this study, we have characterized the conformation of tBid in lipid membrane environments, using NMR and CD spectroscopy with lipid micelle and lipid bilayer samples. In micelles, tBid adopts a unique helical conformation, and the solution NMR $^{1}H/^{15}N$ HSQC spectra have a single well resolved resonance for each of the protein amide sites. In lipid bilayers, tBid associates with the membrane with its helices parallel to the membrane surface and without trans-membrane helix insertion, and the solid-state NMR $^{1}H/^{15}N$ polarization inversion with spin exchange at the magic angle spectrum has all of the amide resonances centered at ^{15}N chemical shift (70–90 ppm) and ^{1}H-^{15}N dipolar coupling (0–5 kHz) frequencies associated with NH bonds parallel to the bilayer surface, with no intensity at frequencies associated with NH bonds in trans-membrane helices. Thus, the cytotoxic activity of tBid at mitochondria may be similar to that observed for antibiotic polypeptides, which bind to the surface of bacterial membranes as amphipathic helices and destabilize the bilayer structure, promoting the leakage of cell contents.

Programmed cell death is initiated when death signals activate the caspases, a family of otherwise dormant cysteine proteases. External stress stimuli trigger the ligation of cell surface death receptors, thereby activating the upstream initiator caspases, which in turn process and activate the downstream cell death executioner caspases (1). In addition, caspases can be activated when stress or developmental cues within the cell induce the release of cytotoxic proteins from mitochondria. This intrinsic mitochondrial pathway for cell death is regulated by the relative ratios of the pro- and antiapoptotic members of the Bcl-2 protein family (2).

Bcl-2 family proteins exert their apoptotic activities through binding with other Bcl-2 family members or other nonhomologous proteins and through the formation of ion-conducting pores that are thought to influence cell fate by regulating mitochondrial physiology. Their functions are also regulated by subcellular location, since they cycle between soluble and membrane-bound forms. The proteins share sequence homology in four evolutionarily conserved domains (BH1–BH4), of which the BH3 domain is highly conserved and essential for both cell killing and oligomerization among Bcl-2 family members. The antiapoptotic family members have all four domains, whereas all of the proapoptotic members lack BH4, and some only have BH3. These BH3-only proteins are activated by upstream death signals, which trigger their transcriptional induction or post-translational modification, providing a key link between the extrinsic death receptor and intrinsic mitochondrial pathways to cell death (3).

One of these BH3-only Bcl-2 family members, Bid, is a 195-residue cytosolic protein that lacks the hydrophobic C-terminal domain often found in other Bcl-2 family members and connects the extrinsic and intrinsic cell death pathways (4). The major mechanism for Bid activation involves its cleavage by caspase-8, after engagement of the Fas or TNFR1 cell surface receptors (5–7). Caspase-8 cleavage of Bid releases the 15-kDa C-terminal fragment tBid, which translocates to the outer mitochondrial membrane, where it induces massive cytochrome *c* release and cell death. tBid has a 10-fold greater binding affinity for its antagonist Bcl-X_L and is 100-fold more efficient in inducing cytochrome-c release from mitochondria than its full-length precursor. Upon translocation from the cytosol to mitochondria, tBid can interact with proapoptotic Bax and Bak to promote mitochondrial apoptosis (8, 9), or it can interact with antiapoptotic Bcl-2 and Bcl-X_L and, thus, be sequestered from the cell and held in check (10). Cell-free studies have shown that Bid and Bax are sufficient to form large openings in reconstituted lipid vesicles (11). In addition, tBid can promote the alteration of membrane curvature in artificial lipid bilayers (12), and it can associate directly with mitochondria, inducing a remodeling of mitochondrial structure. tBid-induced mitochondrial remodeling is characterized by the reorganization of inner membrane cristae to form a highly interconnected common intermembrane space and is accompanied by redistribution of the cytochrome *c* stores from individual cristae to the intermembrane space (13), which may account for the rapid and complete release of mitochondrial cytochrome *c* that is observed in the presence of tBid.

The Bid BH3 domain, while essential for binding to other Bcl-2 family members, is not required for either translocation to the outer mitochondrial membrane and mitochondrial remodeling or complete cytochrome *c* release. The specific targeting of tBid to the outer mitochondrial membrane is mediated by the abundant mitochondrial lipid cardiolipin (14, 15), whose metabolism further regulates cytochrome *c* release and mitochondrion-dependent apoptosis in a Bcl-2- and caspase-independent manner (16).

* This research was supported by Department of the Army Breast Cancer Research Program Grants DAMD17-00-1-0506 and DAMD17-02-1-0313 (to F. M. M.), California Breast Cancer Research Program Grant 8WB0110 (to F. M. M.), and National Institutes of Health Grant R01GM60554 (to J. C. R.). The NMR studies utilized the Burnham Institute NMR Facility, supported by National Institutes of Health Grant P30CA30199 and the Biomedical Technology Resources for Solid-State NMR of Proteins at the University of California San Diego, supported by National Institutes of Health Grant P41EB002031. The costs of publication of this article were defrayed in part by the payment of page charges. This article must therefore be hereby marked "*advertisement*" in accordance with 18 U.S.C. Section 1734 solely to indicate this fact.

‡ To whom correspondence should be addressed: The Burnham Institute, 10901 N. Torrey Pines Rd., La Jolla, CA 92037. Tel.: 858-713-6282; Fax: 858-713-6268; E-mail: fmarassi@burnham.org.

These lines of evidence suggest that Bid induces cell death through two separate mechanisms, a BH3-dependent mechanism that involves binding to other multidomain Bcl-2 family members and a BH3-independent mechanism that involves direct association and interaction with the outer mitochondrial membrane.

The structure of full-length Bid in solution consists of eight α-helices arranged with two central somewhat more hydrophobic helices forming the core of the molecule (17, 18). The third helix, which contains the BH3 domain, is connected to the first two helices by a long flexible loop, which includes the caspase-8 cleavage site, Asp^{60} (Fig. 1). Despite the lack of sequence homology, the structure of Bid is strikingly similar to those of other anti- and proapoptotic multidomain Bcl-2 family proteins (19–22), and it is also similar to the structure of the pore-forming domains of bacterial toxins. Indeed, like the toxins and other Bcl-2 family proteins, tBid also forms ion-conducting pores in lipid bilayers (23). The structural basis for Bcl-2 pore formation is not known, since the structures that have been determined are for the soluble forms of the proteins, but by analogy to the bacterial toxins, the Bcl-2 pores are thought to form by a rearrangement of their compactly folded helices upon contact with the mitochondrial membrane. One model proposes membrane insertion of the core hydrophobic helical hairpin with the other helices folding up to rest on the membrane surface, whereas an alternative model envisions the helices rearranging to bind the membrane surface without insertion (24, 25).

In this study, we have examined the conformation and topology of tBid in lipid membrane environments, using solution NMR and CD experiments with micelle samples and solid-state NMR experiments with lipid bilayer samples. In the absence of lipids, tBid is soluble and retains a largely helical conformation, but many of the $^1H/^{15}N$ resonances are missing from the solution NMR heteronuclear single quantum coherence (HSQC)[1] spectrum, suggesting that tBid aggregates, adopts multiple conformations, or undergoes dynamic averaging on the NMR time scale. In micelles, tBid adopts a unique helical conformation, reflected in the HSQC spectrum, where each of the 130 amide sites gives rise to a single well resolved resonance. The solid-state NMR polarization inversion with spin exchange at the magic angle (PISEMA) spectrum of tBid in lipid bilayers demonstrates that it binds the membrane with its helices parallel to the membrane surface and without transmembrane helix insertion. This suggests that the BH3-independent cytotoxic activity of tBid may be similar to that observed for antibiotic polypeptides that bind to the surface of bacterial membranes as amphipathic helices and destabilize the bilayer structure, promoting the leakage of cell contents.

MATERIALS AND METHODS

Protein Expression—The gene encoding human tBid was obtained by PCR amplification of the 405-base pair segment corresponding to amino acids 60–195 of full-length human Bid (accession number P55957). The gene was cloned into the pMMHa vector, which directs the expression of proteins fused to the C terminus of the His_9-TrpΔLE polypeptide (26). The plasmid was transformed in *Escherichia coli* C41(DE3), a mutant strain that was selected for the expression of insoluble or toxic proteins (27). tBid was expressed as an insoluble protein, with the His_9-TrpΔLE polypeptide fused to its N terminus. To enable CNBr (cyanogen bromide) cleavage of tBid from the TrpΔLE fusion partner, the Met residues (Met^{97}, Met^{142}, Met^{148}, and Met^{194}) in the tBid sequence were changed to Leu. The His_9-TrpΔLE-tBid fusion protein was purified from the inclusion body fraction of the lysate by nickel affinity chromatography (His·Bind Resin (Novagen, Madison, WI) in 6 M guanidine HCl, 20 mM Tris-Cl, pH 8.0, 500 mM NaCl, 500 mM imidazole). After dialysis against water, the fusion protein was dissolved in 0.1 N HCl and then cleaved from the TrpΔLE fusion partner by reaction with a 10-fold molar excess of CNBr (28). tBid was purified by reverse-phase high pressure liquid chromatography (Delta-Pak C4 (Waters, Milford, MA) in 50% water, 50% acetonitrile, 0.1% trifluoroacetic acid). The methods for inclusion bodies isolation and fusion protein purification were as described (26, 29). Cell cultures were in M9 minimal medium as described (29). For the production of uniformly ^{15}N-labeled proteins, $(^{15}NH_4)_2SO_4$ was supplied as the sole nitrogen source. For selectively labeled protein, individual ^{15}N-labeled and nonlabeled amino acids were provided. All isotopes were from Cambridge Isotope Laboratories (Andover, MA).

Mitochondrial Release Assays—HeLa cells were harvested and then washed and suspended in HM buffer (10 mM HEPES, pH 7.4, 250 mM mannitol, 10 mM KCl, 5 mM $MgCl_2$, 1 mM EGTA, 1 mM phenylmethylsulfonyl fluoride, and complete protease inhibitor mixture (Roche Applied Science)). Cells were homogenized with 50 strokes of a Teflon homogenizer with a B-type pestle and centrifuged twice at 600 × *g* for 5 min at 4 °C. The supernatant was centrifuged at 10,000 × *g* for 10 min at 4 °C, and the resulting pellet, containing mitochondria, was washed twice in HM buffer and then suspended in HM buffer at a concentration of 1 mg/ml. Isolated HeLa mitochondria (10 μl) were incubated with HM buffer (50 μl) containing increasing amounts of tBid at 30 °C for 1 h. The samples were centrifuged at 10,000 × *g* for 10 min, and the pellet and supernatant fractions were each resolved by SDS-PAGE and analyzed by immunoblotting using cytochrome *c* and second mitochondria-derived activator of caspases (SMAC) antibodies.

Bcl-X_L Binding Assays—The expression of recombinant His-tagged Bcl-X_L(ΔC), without the C-terminal amino acids 212–233, was as described (30). For the binding assays, His_6-Bcl-X_L(ΔC) protein (15 μg) was incubated at 4 °C for 4 h with 10 μl of Ni^{2+}-NTA resin (Novagen, Madison, WI) in phosphate-buffered saline buffer (10 mM sodium phosphate, 150 mM sodium chloride, pH 7.2), and then the resin was washed three times, tBid (15 μg) was added, and the mixture was further incubated for 4 h. The resin was washed three times with phosphate-buffered saline, and then the bound proteins were eluted with 500 mM imidazole. The samples were resolved by SDS-PAGE stained with Coomassie Blue. As a control, tBid was incubated with the resin in the absence of Bcl-X_L.

CD Spectroscopy—The samples were identical to those used for solution NMR experiments but contained 40 μM tBid. The samples were transferred to a quartz cuvette (0.1-mm path length), and far-UV CD spectra were recorded at 25 °C on a model 62A-DS CD spectrometer (Aviv, Lakewood, NJ) equipped with a temperature controller. A 5-s time constant and a 1-nm bandwidth were used during data acquisition over a wavelength range of 180–260 nm. For each sample, three spectra were recorded, averaged, and referenced by subtracting the average of three spectra obtained using the buffer alone. The spectra were analyzed for protein secondary structure with the k2d program (available on the World Wide Web at www.embl-heidelberg.de/~andrade/k2d/) (31).

Solution NMR—The sample of tBid without lipids contained 0.7–1 mM ^{15}N-labeled tBid, in 50 mM sodium phosphate, pH 5. In the absence of lipids, tBid is not soluble in the millimolar concentrations required for NMR at pH values greater than 5. The samples of tBid in micelles contained 1 mM ^{15}N-labeled tBid in 20 mM sodium phosphate, pH 7, with 500 mM SDS (Cambridge, Andover, MA) or 100 mM 1-palmitoyl-2-hydroxy-*sn*-glycero-3-[phospho-*rac*-(1-glycerol)] (LPPG); Avanti, Alabaster, AL).

Solution NMR experiments were performed on a Bruker AVANCE 600 spectrometer (Billerica, MA) with a 600/54 Magnex magnet (Yarnton, UK), equipped with a triple-resonance 5-mm probe with three-axis field gradients. The two-dimensional $^1H/^{15}N$ HSQC (32) spectra were obtained at 40 °C. The ^{15}N and ^1H chemical shifts were referenced to 0 ppm for liquid ammonia and tetramethylsilane, respectively. The NMR data were processed using NMR Pipe and rendered in NMR Draw (33) on a Dell Precision 330 MT Linux work station (Round Rock, TX).

Solid-state NMR—The lipids, 1,2-dioleoyl-*sn*-glycero-3-phosphocholine (DOPC) and 1,2-dioleoyl-*sn*-glycero-3-[phospho-*rac*-(1-glycerol)] (DOPG) were from Avanti (Alabaster, AL). Samples of tBid in lipid bilayers were prepared by mixing 5 mg of ^{15}N-labeled tBid in water with 100 mg of lipids (DOPC/DOPG, 6:4 molar ratio) that had been sonicated in water to form unilamellar vesicles. The protein and lipid vesicle

[1] The abbreviations used are: HSQC, heteronuclear single quantum coherence; PISEMA, polarization inversion with spin exchange at the magic angle; SMAC, second mitochondria-derived activator of caspases; NTA, nitrilotriacetic acid; DOPC, 1,2-dioleoyl-*sn*-glycero-3-phosphocholine; DOPG, 1,2-dioleoyl-*sn*-glycero-3-[phospho-*rac*-(1-glycerol)]; LPPG,

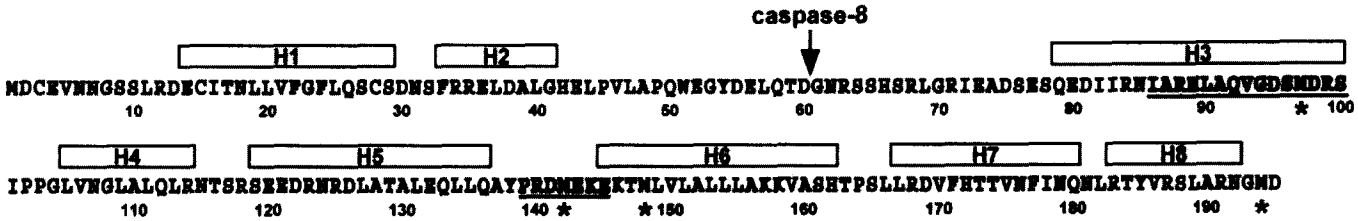

FIG. 1. **Amino acid sequence of human Bid (accession number P55957).** The eight helices (H1–H8) are those determined in the solution NMR structure of full-length human Bid (Protein Data Bank number 2BID) (17). The central core helices are H6 and H7. The BH3 domain in H3 and the putative lipid binding motif before H6 are in *boldface type* and *underlined*. The *arrow* marks the caspase-8 cleavage site at Asp^{60}, and the sequences of both wild-type and recombinant tBid start at Gly^{61}. The *asterisks* mark the four Met residues that were mutated to Leu in recombinant tBid.

surface of 15 glass slides (11 × 11 × 0.06 mm; Marienfeld, Germany). After allowing excess water to evaporate at 40 °C, the slides were stacked and equilibrated for 12 h at 40 °C and 93% relative humidity, in order to form oriented lipid bilayers. The samples were wrapped in parafilm and then sealed in thin polyethylene film prior to insertion in the NMR probe. Hydrogen-exchanged samples were prepared by exposing the stacked oriented bilayer samples to an atmosphere saturated with D_2O.

Solid-state NMR experiments were performed on a Bruker AVANCE 500 spectrometer (Billerica, MA) with a 500/89 AS Magnex magnet (Yarnton, UK). The home-built $^1H/^{15}N$ double resonance probe had a square radiofrequency coil (11 × 11 × 3 mm) wrapped directly around the samples. The one-dimensional ^{15}N chemical shift spectra were obtained with single contact cross-polarization with mismatch-optimized IS polarization transfer (34, 35). The two-dimensional spectra that correlate ^{15}N chemical shift with ^1H-^{15}N dipolar coupling were obtained with PISEMA (36). The spectra were obtained with a cross-polarization contact time of 1 ms, a ^1H 90° pulse width of 5 μs, and continuous ^1H decoupling of 63-kHz radio frequency field strength. The two-dimensional data were acquired with 512 accumulated transients and 256 complex data points, for each of 64 real t1 values incremented by 32.7 μs. The recycle delay was 6 s. The ^{15}N chemical shifts were referenced to 0 ppm for liquid ammonia. The data were processed using NMR Pipe and rendered in NMR Draw (33) on a Dell Precision 330 MT Linux work station (Round Rock, TX).

Calculation of Solid-state NMR Spectra—Two-dimensional $^1H/^{15}N$ PISEMA spectra were calculated on a Linux Dell computer as described previously (37). The ^{15}N chemical shift and ^1H-^{15}N dipolar coupling frequencies were calculated for various orientations of an 18-residue α-helix, with 3.6 residues per turn and uniform backbone dihedral angles for all residues ($\phi = -57°$; $\psi = -47°$). The principal values and molecular orientation of the ^{15}N chemical shift tensor (σ_{11} = 64 ppm; σ_{22} = 77 ppm; σ_{33} = 217 ppm; angle (σ_{11}NH) = 17°) and the NH bond distance (1.07 Å) provided the input for the spectrum calculation at each helix orientation.

RESULTS

Protein Expression and Biological Activity—Full-length Bid can be expressed at high levels, in *E. coli*, as a soluble protein, but tBid overexpression is toxic for bacterial cells. To produce milligram quantities of ^{15}N-labeled tBid for NMR studies, we used the pMMHa fusion protein vector that directs high level protein expression as inclusion bodies, and we transformed the plasmid in *E. coli* C41(DE3) cells, selected for the expression of insoluble and toxic proteins (27). tBid was separated from the fusion partner by means of CNBr cleavage at the engineered N-terminal Met residue (26). This method yields ~10 mg of purified ^{15}N-labeled tBid from 1 liter of culture. To avoid cleavage within the tBid segment, the four Met residues in the tBid amino acid sequence were mutated to Leu (Fig. 1, *asterisks*), and therefore, it was important to demonstrate that the recombinant protein retained its biological activity.

We tested the ability of recombinant tBid to induce the release of mitochondrial proteins by incubating it with mitochondria isolated from HeLa cells, assaying the supernatant and pelleted fractions with antibodies to cytochrome *c* and SMAC. Fig. 2*A* demonstrates that, in both cases, tBid is fully active, in a dose-dependent manner and at levels similar to

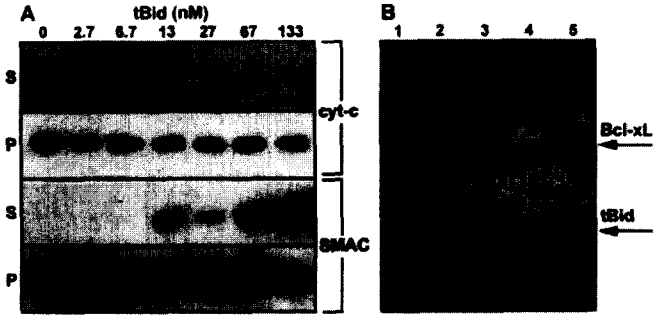

FIG. 2. **Recombinant tBid induces the release of cytochrome-c and SMAC from isolated mitochondria and binds to Bcl-X_L *in vitro*.** *A*, isolated HeLa mitochondria (10 μl, 1 mg/ml) were incubated with increasing amounts (0–133 nM in 50 μl) of tBid. The supernatant (*S*) and pellet (*P*) fractions were separated by centrifugation, resolved on SDS-PAGE, and analyzed by Western blotting with either cytochrome *c* (*top*) or SMAC (*bottom*) antibody. In *B*, Ni^{2+}-NTA resin (10 μl) was incubated first with His-Bcl-X_L(ΔC) (15 μg) and then with tBid (15 μg). The Ni^{2+}-NTA-bound protein was eluted with 500 mM imidazole, and the samples were resolved by SDS-PAGE and stained with Coomassie Blue (*lane 5*). In the control experiment, tBid was directly incubated with the resin without preincubation with Bcl-X_L(ΔC) (*lane 4*). Individual Bcl-X_L(ΔC) monomers (24 kDa) are resolved in *lane 2*, and individual tBid monomers (15 kDa) are resolved in *lane 3*. Molecular weight markers are shown in *lane 1*.

tested the ability of recombinant tBid to bind Bcl-X_L, since this interaction requires the BH3 domain, and recombinant tBid contains the mutation M97L in this segment. When recombinant tBid, which does not have a His tag, was incubated with Ni^{2+}-NTA without Bcl-X_L, it did not bind the resin, as evidenced by the absence of tBid in the imidazole elution (Fig. 2*B*, *lane 4*). However, when tBid was incubated with Ni^{2+}-NTA that had been previously incubated with His-tagged Bcl-X_L, it also bound to the resin and eluted with Bcl-X_L in imidazole (Fig. 2*B*, *lane 5*).

Thus, we conclude that recombinant tBid, isolated from inclusion bodies, is fully active in its ability to induce cytochrome *c* and SMAC release from isolated mitochondria and that its capacity to bind antiapoptotic Bcl-X_L through its BH3 domain is not disrupted by the M97L mutation. The pMMHa vector may be generally useful for the high level expression of other proapoptotic proteins that are difficult to express because of their cytotoxic properties. The use of chemical cleavage eliminates the difficulties, poor specificity, and enzyme inactivation, often encountered with protease treatment of insoluble proteins, and in cases where Met mutation is not feasible, protein cleavage from the fusion partner can be obtained enzymatically by engineering specific protease cleavage sites for the commonly used enzymes thrombin, Fxa, enterokinase, and tobacco etch virus protease. Thrombin and tobacco etch virus retain activity in the presence of detergents, including low millimolar concentrations of SDS.

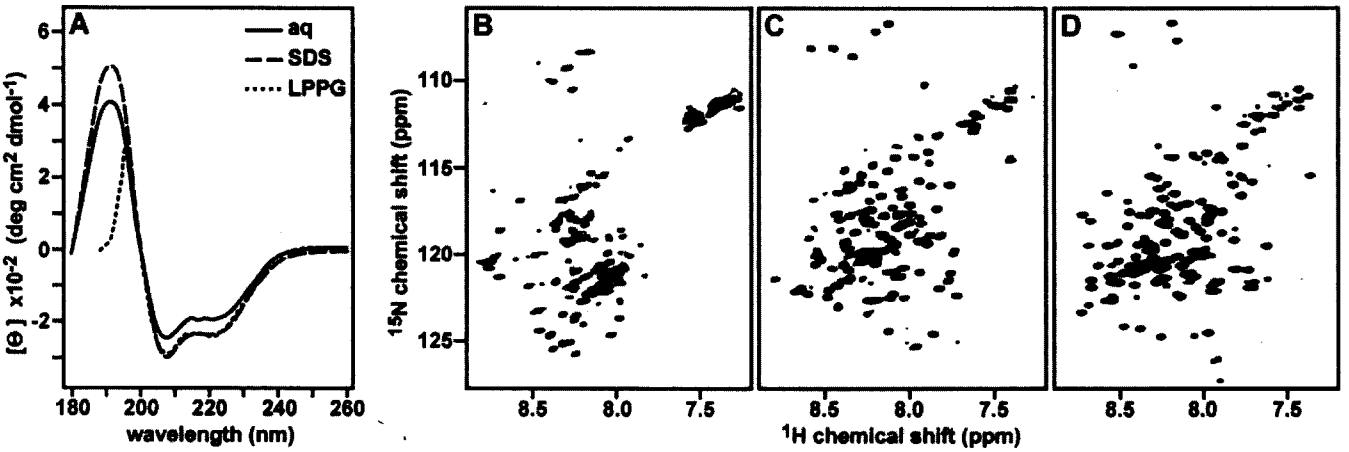

FIG. 3. **tBid adopts a helical fold in lipid micelles.** The CD spectra in *A* were obtained at 25 °C for tBid in aqueous solution (*solid line*), SDS micelles (*broken line*), or LPPG micelles (*dotted line*). The ^{1}H/^{15}N HSQC NMR spectra in *B–D* were obtained at 40 °C for uniformly ^{15}N-labeled tBid, in aqueous solution (*B*), SDS micelles (*C*), or LPPG micelles (*D*). Aqueous samples were in 20 mM sodium phosphate, pH 5; SDS micelle samples were in 20 mM sodium phosphate, pH 7, 500 mM SDS; and LPPG micelle samples were in 20 mM sodium phosphate, pH 7, 100 mM LPPG.

results in a C-terminal product, tBid, which targets mitochondria and induces apoptosis with strikingly enhanced activity (5–7). To characterize the conformation of tBid in lipid environments, we obtained its CD and solution NMR ^{1}H/^{15}N HSQC spectra in the absence or in the presence of lipid micelles (Fig. 3). The HSQC spectra of proteins are the starting point for additional multidimensional NMR experiments that lead to structure determination. In these spectra, each ^{15}N-labeled protein site gives rise to a single peak, characterized by ^{1}H and ^{15}N chemical shift frequencies that reflect the local environment. In addition, the peak line widths and line shapes and their dispersion in the ^{1}H and ^{15}N frequency dimensions reflect protein conformation and aggregation state.

In the absence of lipids, the CD spectrum of tBid displays minima at 202 and 222 nm, characteristic of predominantly helical proteins (Fig. 3*A*, *solid line*). The helical content estimated from the CD spectrum is ~65%, which is similar to the 67% helical content determined from the three-dimensional structure of Bid (17) for the 135 C-terminal amino acids that correspond to tBid. However, whereas tBid retains its helical conformation even when it is separated from the 60-residue N-terminal fragment, many of the resonances in its ^{1}H/^{15}N HSQC spectrum cannot be detected (Fig. 3*B*), suggesting that the protein aggregates in solution, adopts multiple conformations, or undergoes dynamic conformational exchange on the NMR time scale. tBid has very limited solubility at pH values greater than 5, and the addition of KCl up to 200 mM did not improve the appearance of the HSQC spectrum, whereas KCl concentrations above 200 mM yielded a gel. This behavior is consistent with the dramatic changes in the physical properties of the protein that accompany caspase-8 cleavage. Bid has a theoretical pI of 5.3 and a net charge of −7, but caspase-8 cleavage and removal of the 60 N-terminal amino acids shift these parameters to the opposite end of their spectrum, and tBid has a pI of 9.3 and a net charge of +2. In addition, the removal of helix-1 and helix-2 following caspase-8 cleavage exposes hydrophobic residues in the BH3 domain in helix-3 and in the central core helices, helix-6 and helix-7 (17, 18, 23).

When tBid associates with lipid micelles, its HSQC spectrum changes dramatically, and single, well defined ^{1}H/^{15}N resonances are observed for each ^{15}N-labeled NH site in the protein, indicating that tBid adopts a unique conformation in this environment (Fig. 3, *C* and *D*). Micelles provide suitable membrane mimetic samples for solution NMR studies of membrane proteins because their small size affords rapid and effectively isotropic reorientation of the protein and because their amphipathic nature simulates that of membranes. The principle goal of micelle sample preparation is to reduce the effective rotational correlation time of the protein so that resonances will have the narrowest achievable line widths while providing an environment that maintains the protein fold.

Several lipids are available for protein solubilization, and we tested both SDS (Fig. 3*C*) and LPPG (Fig. 3*D*) for their ability to yield high quality HSQC spectra of tBid for structure determination. Both gave excellent spectra where most of the 130 tBid amide resonances could be resolved. Both SDS and LPPG are negatively charged, but they differ substantially in the lengths of their hydrocarbon chains (C12 for SDS; C16 for LPPG) and their polar headgroups (sulfate for SDS; phosphatidylglycerol for LPPG); thus, the differences in ^{1}H and ^{15}N chemical shifts between the two HSQC spectra most likely reflect the different lipid environments. The spectrum in LPPG has exceptionally well dispersed resonances with homogeneous intensities and line widths. LPPG was recently identified as a superior lipid for NMR studies of several membrane proteins (39) and is particularly interesting for this study because it is a close analog of cardiolipin and monolysocardiolipin, the major components of mitochondrial membranes that bind tBid (14).

In both the SDS and LPPG spectra, the limited chemical shift dispersion is typical of helical proteins in micelles, and this is confirmed by the corresponding CD spectra, which are dominated by minima at 202 and 222 nm, and thus show that tBid retains a predominantly helical fold in both types of micelles (Fig. 3*A*, *broken* and *dotted lines*). We estimated the helical content of tBid in lipid micelles to be ~65%, similar to that of tBid in the absence of lipids and to the value determined for the 135-residue C-terminal segment in the three-dimensional solution structure of Bid (17).

tBid in Lipid Bilayers—By analogy to the structurally homologous colicin and diphtheria bacterial toxins, the mechanism of pore formation by tBid has been thought to involve insertion through the membrane of the two central core helices, helix-6 and helix-7 (23, 25). To examine the conformation of tBid associated with membranes, we obtained one-dimensional ^{15}N chemical shift and two-dimensional ^{1}H/^{15}N PISEMA solid-state NMR spectra of ^{15}N-labeled tBid reconstituted in lipid bilayers (Fig. 4). In these samples, the lipid composition of 60% DOPC and 40% DOPG was chosen to mimic the highly negative

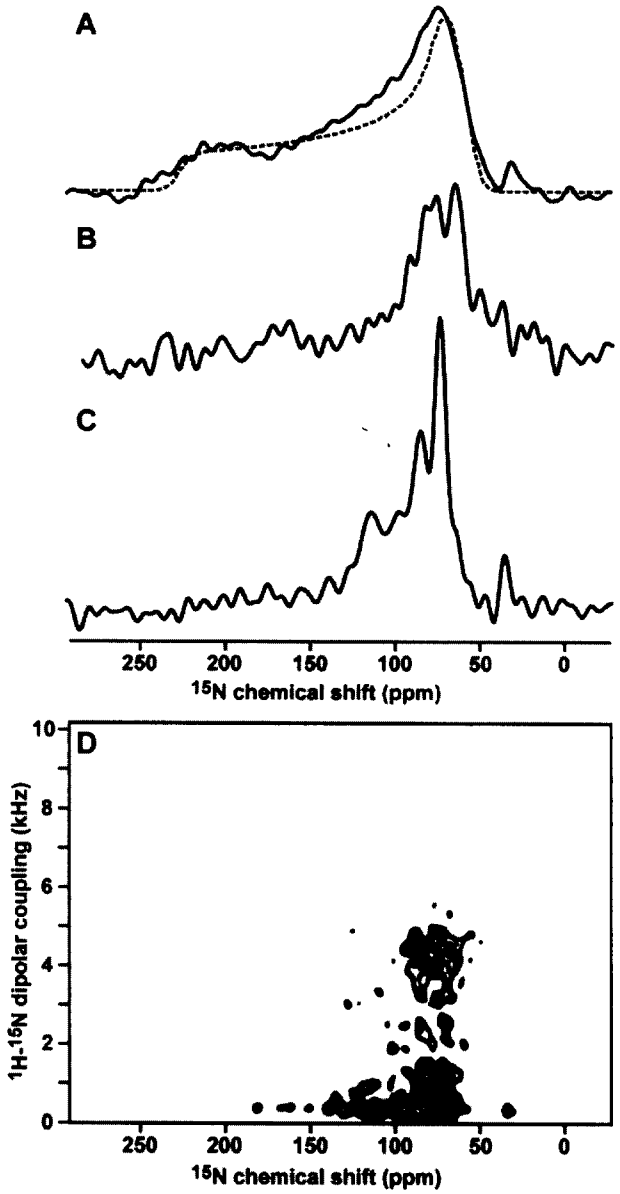

FIG. 4. **Solid-state NMR spectra of tBid in lipid bilayers show that tBid binds membranes with a unique fold and parallel orientation.** *A*, one-dimensional ^{15}N chemical shift spectrum of uniformly ^{15}N-labeled tBid in unoriented lipid bilayer vesicles (*solid line*) and powder pattern calculated for a rigid ^{15}N amide site (*dotted line*). *B*, one-dimensional ^{15}N spectrum of selectively ^{15}N-Lys-labeled tBid in oriented lipid bilayers. *C*, one-dimensional ^{15}N spectrum of uniformly ^{15}N-labeled tBid in oriented lipid bilayers. *D*, two-dimensional ^{1}H/^{15}N PISEMA spectrum of tBid in oriented lipid bilayers.

identical to that of the liposomes used for the measurement of the ion channel activities of Bid and tBid (23), and since the oriented lipid bilayers used in this study were obtained from liposomes prepared in the same way as for the channel studies, the NMR spectra obtained in this work represent the channel-active conformation of tBid.

When the lipid bilayers are oriented with their surface perpendicular to the magnetic field, the solid-state NMR spectra of the membrane-associated proteins trace out maps of their structure and orientation within the membrane and thus provide very useful structural information prior to complete structure determination. For example, helices give characteristic solid-state NMR spectra where the resonances from amide sites in the protein trace-out helical wheels that contain infor-

40, 41). Typically, trans-membrane helices have PISEMA spectra with ^{15}N chemical shifts between 150 and 200 ppm, and ^{1}H-^{15}N dipolar couplings between 2 and 10 kHz, whereas helices that bind parallel to the membrane surface have spectra with shifts between 70 and 100 ppm and couplings between 0 and 5 kHz. We refer to these as the trans-membrane and in-plane regions of the PISEMA spectrum, respectively.

The ^{15}N chemical shift spectrum of tBid in unoriented lipid bilayer vesicles is a powder pattern (Fig. 4*A*, *solid line*) that spans the full range (60–220 ppm) of the amide ^{15}N chemical shift interaction (Fig. 4*A*, *dotted line*). The absence of additional intensity at the isotropic resonance frequencies (100–130 ppm) demonstrates that the majority of amino acid sites are immobile on the time scale of the ^{15}N chemical shift interaction, although it is possible that some mobile unstructured residues cannot be observed by cross-polarization. The peak at 35 ppm is from the amino groups at the N terminus and side chains of the protein.

The spectrum of tBid in planar oriented lipid bilayers is very different (Fig. 4*C*). The amide resonances are centered at a frequency associated with NH bonds in helices parallel to the membrane surface (80 ppm), whereas no intensity is observed at frequencies associated with NH bonds in trans-membrane helices (200 ppm). The resonances near 120 ppm are unlikely to result from mobile sites, since little or no isotropic intensity is observed in the spectrum from unoriented bilayers; instead, they probably reflect specific orientations of their corresponding sites near the magic angle, which corresponds to 35.3° from the membrane surface. The NMR data show no evidence of conformational exchange on the millisecond to second time scale of the channel opening and closing events, excluding the possibility of transient insertion of tBid in the membrane. Therefore, we conclude that tBid binds strongly to the membrane surface, adopting a unique conformation and orientation in the presence of phospholipids.

Amide hydrogen exchange rates are useful for identifying residues that are involved in hydrogen bonding and that are exposed to water. The amide hydrogens in trans-membrane helices can have very slow exchange rates due to their strong hydrogen bonds in the low dielectric of the lipid bilayer environment, and their ^{15}N chemical shift NMR signals persist for days after exposure to D_2O (42). On the other hand, trans-membrane helices that are in contact with water because they participate in channel pore formation and other water-exposed helical regions of proteins have faster exchange rates, and their NMR signals disappear on the order of hours (43). To examine the amide hydrogen exchange rates for membrane-bound tBid, we obtained solid-state NMR spectra after exposing the oriented lipid bilayer sample to D_2O for 2, 5, and 7 h. The majority of resonances in the ^{15}N chemical shift spectrum of tBid disappeared within 7 h, indicating that the amide hydrogens exchange and, hence, are in contact with the lipid bilayer interstitial water.

The tBid amino acid sequence has four Lys residues (Lys^{144}, Lys^{146}, Lys^{157}, and Lys^{158}), all located in or near helix-6, one of the two helices thought to insert in the membrane and form the tBid ion-conducting pore. The spectrum of ^{15}N-Lys-labeled tBid in bilayers is notable because its amide resonances all have chemical shifts near 80 ppm, in the in-plane region of the spectrum, and this cannot be reconciled with membrane insertion (Fig. 4*B*). Since tBid maintains a helical fold in lipid micelles and it is reasonable to assume that the helix boundaries are not appreciably changed from those of full-length Bid, the solid-state NMR data demonstrate that helix-6 does not insert through the membrane but associates parallel to its

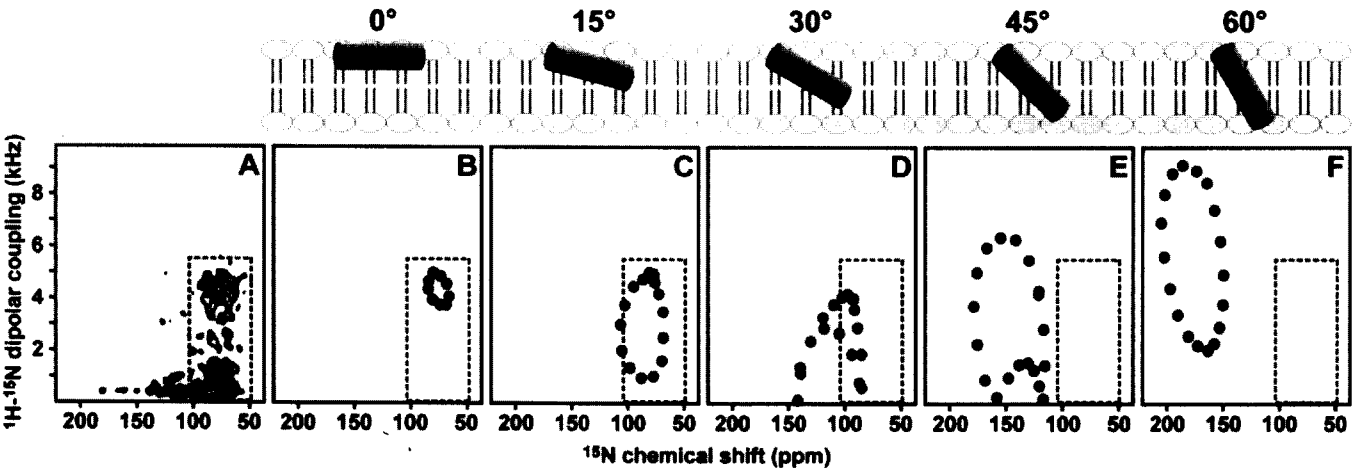

FIG. 5. **Two-dimensional solid-state NMR ^{1}H/^{15}N PISEMA spectrum of uniformly ^{15}N-labeleld tBid in oriented lipid bilayers.** The experimental spectrum (*A*) is compared with the theoretical spectra (*B–F*) calculated for an 18-residue α-helix, with uniform backbone dihedral angles ($\phi = -57°$; $\psi = -47°$) and different helix tilts (0–60°) relative to the membrane surface, as depicted in the *schematic diagrams above* the *spectra*. The 0° orientation is for a helix parallel to the membrane surface.

These findings are confirmed and refined with the two-dimensional ^{1}H/^{15}N PISEMA spectrum of tBid in bilayers (Fig. 4*D*). Each amide site in the protein contributes one correlation peak, characterized by ^{1}H-^{15}N dipolar coupling and ^{15}N chemical shift frequencies that reflect NH bond orientation relative to the membrane. For tBid, the circular wheel-like pattern of resonances in the spectral region bounded by 0–5 kHz and 70–90 ppm provides definitive evidence that tBid associates with the membrane as surface-bound helices without transmembrane insertion. The substantial peak overlap reflects a similar orientation of the tBid helices parallel to the membrane, and spectral resolution in this region requires three-dimensional correlation spectroscopy and selective isotopic labeling (45).

Since the NMR frequencies directly reflect the angles between individual bonds and the direction of the applied magnetic field, it is possible to calculate solid-state NMR spectra for specific models of proteins in oriented samples. For example, the spectra of helices have wheel-like patterns of resonances, called *Pisa Wheels*, that mirror helix tilt and rotation in the membrane (37, 40, 41), and a comparison of calculated and experimental spectra provides very useful structural information prior to complete structure determination. The spectra calculated for several orientations of an ideal 18-residue helix, with 3.6 residues per turn and identical backbone dihedral angles for all residues ($\phi, \psi = -57°, -47°$), are shown in Fig. 5 (*B–F*) and are compared with the experimental PISEMA spectrum obtained for tBid in oriented bilayers, in Fig. 5*A*. In each spectrum, the characteristic *Pisa Wheel* pattern reflects helix tilt, but only the spectra calculated for membrane surface helices, with tilts from 0 to 15°, have intensity in the region of the experimental spectrum of tBid (*inset box*), whereas trans-membrane helices with tilts ranging from 45 to 90° from the membrane surface, have *Pisa Wheels* in a completely unpopulated region of the experimental spectrum. Based on this comparative analysis, we estimate that the helices of tBid are nearly parallel to the lipid bilayer plane (0° orientation), with tilts of no more than 20° from the membrane surface.

DISCUSSION

The results of this study demonstrate that tBid adopts a unique helical fold in lipid environments and that it binds the membrane without insertion of its helices. Solid-state NMR studies of the antiapoptotic Bcl-2 family member, Bcl-X_L, also indicate that membrane insertion of the Bcl-X_L helices is limited [illegible] extended helical conformation in lipid micelles (46). Both tBid and Bcl-X_L form ion-conductive pores that are thought to play a role in apoptosis through their regulation of mitochondrial physiology (23, 25), and since the samples in both the solid-state NMR and ion channel activity studies of tBid were identical in their lipid composition and the manner of sample preparation (23), the membrane surface association of tBid, observed by solid-state NMR in this study, is very likely to represent the channel-active conformation of the protein.

Pore formation by the Bcl-2 family proteins has been thought to involve translocation of the central core helices through the membrane, and the helices of both Bid and Bcl-X_L are sufficiently long to span the lipid bilayer. However, their amphipathic character is also compatible with membrane surface association, in a manner that is reminiscent of the antimicrobial polypeptides, where binding of the polypeptide helices to the bacterial membrane surface is thought to transiently destabilize the membrane and change its morphology, inducing leakage of the cell contents, disruption of the electrical potential, and ultimately cell death (45, 47). It is notable that bacterial and mitochondrial membranes have very similar structures and surface charge and that tBid is both capable of altering bilayer curvature (12) and of remodeling the mitochondrial membrane (13), which would be sufficient to cause the release of mitochondrial cytotoxic molecules. The membrane surface association of tBid may also serve to display the BH3 domain on the mitochondrial membrane surface, making it accessible for binding by other Bcl-2 family members.

Although tBid does not insert in DOPC/DOPG lipid bilayers, we cannot exclude the possibility that trans-membrane insertion may be driven by the presence of natural mitochondrial lipids, such as cardiolipin and monolysocardiolipin. These lipids both bind tBid (14) and are concentrated at mitochondrial outer-inner membrane contact sites where tBid localizes; however, a recent EPR study using these lipids also found no evidence of tBid helix insertion through the membrane (44). It is also possible that trans-membrane insertion of tBid requires post-translational N-terminal myristoylation, since this has been shown to enhance Bid-induced cytochrome *c* release and apoptosis (48), and that the interactions with other Bcl-2 family proteins such as Bak and Bax or with other nonhomologous proteins such as the mitochondrial voltage dependent anion channel may promote insertion of the tBid helices through the mitochondrial membrane.

$^{1}H/^{15}N$ HSQC spectrum of Bid after the addition of caspase-8, testing the hypothesis that Bid activation is accompanied by a conformational change. They found that the structure of Bid is not changed by caspase-8 cleavage, since tBid remains associated with the N-terminal fragment, but proposed that dissociation occurs at lower physiological concentrations, through a conformational on-off equilibrium. In light of the lipid affinity of Bid and the data in Fig. 3 demonstrating that tBid is well-folded in lipid micelles independently of the N terminus, it is possible that lipids act as a third partner during caspase-8 cleavage of Bid. Thus, whereas in the absence of lipids the two cleavage fragments remain associated, the presence of lipids may enable dissociation by providing an environment where tBid can fold independently.

In this regard, it is interesting to note that the Bid amino acid sequence (^{141}PRDMEKE^{147}) at the beginning of helix-6 is similar to the conserved sequence (^{95}PDVEKE^{100}) that forms a short lipid recognition helix in the lipoprotein apolipophorin-III. In Bid, this sequence forms a short loop that is solvent-exposed and perpendicular to the axis of helix-6, whereas in apolipophorin-III it forms a short helix at one solvent-exposed end of the molecule that is perpendicular to the helix bundle (49). This short motif is conserved in the Bid sequences from various species, suggesting that it plays a role in the protein biological function, and given the documented lipid-binding activity of Bid (14), it may constitute a lipid recognition domain for Bid similar to that of apolipophorin-III. Thus, it is possible that the structure of tBid, destabilized by dissociation from the N-terminal fragment after caspase-8 cleavage, undergoes a conformational change whereby it opens about the flexible loops that connect its helical segments to an extended helical conformation, which binds to the membrane surface. This would be similar to the mechanism proposed for apolipophorin-III, which adopts a marginally stable helix bundle topology that allows for concerted opening of the bundle about hinged loops (49).

Acknowledgment—We thank Jinghua Yu for assistance with the NMR experiments.

REFERENCES

1. Denault, J. B., and Salvesen, G. S. (2002) *Chem. Rev.* **102,** 4489–4500
2. Green, D. R., and Reed, J. C. (1998) *Science* **281,** 1309–1312
3. Cory, S., and Adams, J. M. (2002) *Natl. Rev. Cancer* **2,** 647–656
4. Wang, K., Yin, X. M., Chao, D. T., Milliman, C. L., and Korsmeyer, S. J. (1996) *Genes Dev.* **10,** 2859–2869
5. Li, H., Zhu, H., Xu, C. J., and Yuan, J. (1998) *Cell* **94,** 491–501
6. Luo, X., Budihardjo, I., Zou, H., Slaughter, C., and Wang, X. (1998) *Cell* **94,** 481–490
7. Gross, A., Yin, X. M., Wang, K., Wei, M. C., Jockel, J., Milliman, C., Erdjument-Bromage, H., Tempst, P., and Korsmeyer, S. J. (1999) *J. Biol. Chem.* **274,** 1156–1163
8. Eskes, R., Desagher, S., Antonsson, B., and Martinou, J. C. (2000) *Mol. Cell. Biol.* **20,** 929–935
9. Korsmeyer, S. J., Wei, M. C., Saito, M., Weiler, S., Oh, K. J., and Schlesinger, P. H. (2000) *Cell Death Differ.* **7,** 1166–1173
10. Cheng, E. H., Wei, M. C., Weiler, S., Flavell, R. A., Mak, T. W., Lindsten, T., and Korsmeyer, S. J. (2001) *Mol. Cell* **8,** 705–711
11. Kuwana, T., Mackey, M. R., Perkins, G., Ellisman, M. H., Latterich, M., Schneiter, R., Green, D. R., and Newmeyer, D. D. (2002) *Cell* **111,** 331–342
12. Epand, R. F., Martinou, J. C., Fornallaz-Mulhauser, M., Hughes, D. W., and Epand, R. M. (2002) *J. Biol. Chem.* **277,** 32632–32639
13. Scorrano, L., Ashiya, M., Buttle, K., Weiler, S., Oakes, S. A., Mannella, C. A., and Korsmeyer, S. J. (2002) *Dev. Cell* **2,** 55–67
14. Degli Esposti, M., Cristea, I. M., Gaskell, S. J., Nakao, Y., and Dive, C. (2003) *Cell Death Differ.* **10,** 1300–1309
15. Lutter, M., Fang, M., Luo, X., Nishijima, M., Xie, X., and Wang, X. (2000) *Nat. Cell Biol.* **2,** 754–761
16. Ostrander, D. B., Sparagna, G. C., Amoscato, A. A., McMillin, J. B., and Dowhan, W. (2001) *J. Biol. Chem.* **276,** 38061–38067
17. Chou, J. J., Li, H., Salvesen, G. S., Yuan, J., and Wagner, G. (1999) *Cell* **96,** 615–624
18. McDonnell, J. M., Fushman, D., Milliman, C. L., Korsmeyer, S. J., and Cowburn, D. (1999) *Cell* **96,** 625–634
19. Fesik, S. W. (2000) *Cell* **103,** 273–282
20. Suzuki, M., Youle, R. J., and Tjandra, N. (2000) *Cell* **103,** 645–654
21. Denisov, A. Y., Madiraju, M. S., Chen, G., Khadir, A., Beauparlant, P., Attardo, G., Shore, G. C., and Gehring, K. (2003) *J. Biol. Chem.* **278,** 21124–21128
22. Hinds, M. G., Lackmann, M., Skea, G. L., Harrison, P. J., Huang, D. C., and Day, C. L. (2003) *EMBO J.* **22,** 1497–1507
23. Schendel, S. L., Azimov, R., Pawlowski, K., Godzik, A., Kagan, B. L., and Reed, J. C. (1999) *J. Biol. Chem.* **274,** 21932–21936
24. Cramer, W. A., Heymann, J. B., Schendel, S. L., Deriy, B. N., Cohen, F. S., Elkins, P. A., and Stauffacher, C. V. (1995) *Annu. Rev. Biophys. Biomol. Struct.* **24,** 611–641
25. Schendel, S. L., Montal, M., and Reed, J. C. (1998) *Cell Death Differ.* **5,** 372–380
26. Staley, J. P., and Kim, P. S. (1994) *Protein Sci.* **3,** 1822–1832
27. Miroux, B., and Walker, J. E. (1996) *J. Mol. Biol.* **260,** 289–298
28. Gross, E., and Witkop, B. (1961) *J. Am. Chem. Soc.* **83,** 1510–1511
29. Opella, S. J., Ma, C., and Marassi, F. M. (2001) *Methods Enzymol.* **339,** 285–313
30. Xie, Z., Schendel, S., Matsuyama, S., and Reed, J. C. (1998) *Biochemistry* **37,** 6410–6418
31. Andrade, M. A., Chacon, P., Merelo, J. J., and Moran, F. (1993) *Protein Eng.* **6,** 383–390
32. Mori, S., Abeygunawardana, C., Johnson, M. O., and Vanzijl, P. C. M. (1995) *J. Magn. Reson. B* **108,** 94–98
33. Delaglio, F., Grzesiek, S., Vuister, G. W., Zhu, G., Pfeifer, J., and Bax, A. (1995) *J. Biomol. NMR* **6,** 277–293
34. Pines, A., Gibby, M. G., and Waugh, J. S. (1973) *J. Chem. Phys.* **59,** 569–590
35. Levitt, M. H., Suter, D., and Ernst, R. R. (1986) *J. Chem. Phys.* **84,** 4243–4255
36. Wu, C. H., Ramamoorthy, A., and Opella, S. J. (1994) *J. Magn. Reson. A* **109,** 270–272
37. Marassi, F. M. (2001) *Biophys. J.* **80,** 994–1003
38. Guo, B., Zhai, D., Cabezas, E., Welsh, K., Nouraini, S., Satterthwait, A. C., and Reed, J. C. (2003) *Nature* **423,** 456–461
39. Krueger-Koplin, R. D., Sorgen, P. L., Krueger-Koplin, S. T., Rivera-Torres, I. O., Cahill, S. M., Hicks, D. B., Grinius, L., Krulwich, T. A., and Girvin, M. E. (2004) *J. Biomol. NMR* **28,** 43–57
40. Marassi, F. M., and Opella, S. J. (2000) *J. Magn. Reson.* **144,** 150–155
41. Wang, J., Denny, J., Tian, C., Kim, S., Mo, Y., Kovacs, F., Song, Z., Nishimura, K., Gan, Z., Fu, R., Quine, J. R., and Cross, T. A. (2000) *J. Magn. Reson.* **144,** 162–167
42. Franzin, C. M., Choi, J., Zhai, D., Reed, J. C., and Marassi, F. M. (2004) *Magn. Reson. Chem.* **42,** 172–179
43. Tian, C., Gao, P. F., Pinto, L. H., Lamb, R. A., and Cross, T. A. (2003) *Protein Sci.* **12,** 2597–2605
44. Oh, K. J., Barbuto, S., Meyer, N., and Korsmeyer, S. (2004) in *The 5th Biennial Structural Biology Symposium,* Tallahassee, FL
45. Marassi, F. M., Ma, C., Gesell, J. J., and Opella, S. J. (2000) *J. Magn. Reson.* **144,** 156–161
46. Losonczi, J. A., Olejniczak, E. T., Betz, S. F., Harlan, J. E., Mack, J., and Fesik, S. W. (2000) *Biochemistry* **39,** 11024–11033
47. Boman, H. G. (1995) *Annu. Rev. Immunol.* **13,** 61–92
48. Zha, J., Weiler, S., Oh, K. J., Wei, M. C., and Korsmeyer, S. J. (2000) *Science* **290,** 1761–1765
49. Wang, J., Sykes, B. D., and Ryan, R. O. (2002) *Proc. Natl. Acad. Sci. U. S. A.* **99,** 1188–1193

Bcl-XL as a fusion protein for the high-level expression of membrane-associated proteins

KHANG THAI, JUNGYUEN CHOI, CARLA M. FRANZIN, AND FRANCESCA M. MARASSI
The Burnham Institute, La Jolla, California 92037, USA

(RECEIVED November 19, 2004; FINAL REVISION December 22, 2004; ACCEPTED December 22, 2004)

Abstract

An *Escherichia coli* plasmid vector for the high-level expression of hydrophobic membrane proteins is described. The plasmid, pBCL, directs the expression of a target polypeptide fused to the C terminus of a mutant form of the anti-apoptotic Bcl-2 family protein, Bcl-XL, where the hydrophobic C terminus has been deleted, and Met residues have been mutated to Leu to facilitate CNBr cleavage after a single Met inserted at the beginning of the target sequence. Fusion protein expression is in inclusion bodies, simplifying the protein purification steps. Here we report the high-level production of PLM, a membrane protein that is a member of the FXYD family of tissue-specific and physiological-state–specific auxiliary subunits of the Na,K-ATPase, expressed abundantly in heart and skeletal muscle. We demonstrate that milligram quantities of pure, isotopically labeled protein can be obtained easily and in little time with this system.

Keywords: membrane protein expression; FXYD; PLM; Mat-8; CHIF; Bcl-XL; NMR; lipid

The most versatile and widely used method for obtaining recombinant proteins is by expression in *Escherichia coli*. The ability to express proteins in bacteria is particularly useful for NMR structure determination, because it allows milligram quantities of isotopically labeled proteins to be obtained relatively economically, and a variety of isotopic labeling schemes to be incorporated in the NMR experimental strategy.

Some polypeptides, however, are toxic to the bacterial hosts that express them. For example, some membrane proteins and peptides, including some of bacterial origin, congest the cell membranes when they are overexpressed, and act as toxic, antibacterial agents, regardless of their actual biological functions. For these difficult polypeptides, solid-phase synthesis is not a practical alternative, because it is typically limited to sequences shorter than 50 amino acids, and while this size limit can be extended through the use of chemical ligation methods (Dawson et al. 1994; Kochendoerfer 2001) that can also be applied to membrane proteins (Kochendoerfer et al. 1999, 2004), NMR studies still require bacterial expression of the polypeptide precursors for the practical introduction of various isotopic labels.

Several *E. coli* cell strains and expression strategies have been developed to address this problem (Miroux and Walker 1996; Rogl et al. 1998; Jones et al. 2000; Majerle et al. 2000; Opella et al. 2001; Sharon et al. 2002; Bannwarth and Schulz 2003; Booth 2003; Kiefer 2003; Lindhout et al. 2003; Smith and Walker 2003; Wiener 2004), and more recently, cell-free expression has been used to obtain milligram quantities of isotopically labeled membrane proteins (Klammt et al. 2004). Many strategies rely on the use of

Reprint requests to: Francesca M. Marassi, The Burnham Institute, 10901 North Torrey Pines Road, La Jolla, CA 92037, USA; e-mail: fmarassi@burnham.org; fax: (858) 713-6281.

Abbreviations: BCL, Bcl-XL mutant lacking the hydrophobic C terminus adapted as fusion partner; Bcl-2, B-cell leukemia/lymphoma 2; Bcl-XL, B-cell leukemia/lymphoma extra long; CHIF, corticosteroid-hormone-induced factor, FXYD4; CNBr, cyanogen bromide; CPMOIST, cross polarization with mismatch-optimized IS polarization transfer; DOPC, 1,2-dioleoyl-sn-glycero-3-phosphocholine; DOPG, 1,2-dioleoyl-sn-glycero-3-[phospho-rac-(1-glycerol)]; GdnHCl, guanidinium HCl; HPLC, high-performance liquid chromatography; HSQC, heteronuclear single quantum coherence; HSQC-NOESY, HSQC–nuclear overhauser effect spectroscopy; IPTG, isopropyl β-D-thiogalactopyranoside; KSI, ketosteroid isomerase; ER, endoplasmic reticulum; MALDI-TOF, matrix-assisted laser desorption ionization–time of flight; Mat-8, mammary tumor protein 8 kDa, FXYD3; NMR, nuclear magnetic resonance; PISEMA, polarization inversion with spin exchange at the magic angle; PLM, phospholemman, FXYD1; PAGE, polyacrylamide gel electrophoresis; pI, isoelectric point; SDS, sodium dodecyl sulfate; TLE, a portion of the Trp ΔLE 1413 polypeptide.

Article published online ahead of print. Article and publication date are at http://www.proteinscience.org/cgi/doi/10.1110/ps.041244305.

fusion protein tags to improve expression and facilitate purification, and many involve protein expression in inclusion bodies, to keep the hydrophobic polypeptide away from the bacterial membranes, and thus increase the level of expression. The formation of inclusion bodies also limits proteolytic degradation and simplifies protein purification, which can be further assisted by the incorporation of an engineered His tag for metal affinity chromatography.

The TLE (a portion of the Trp ΔLE 1413 polypeptide) (Miozzari and Yanofsky 1978; Kleid et al. 1981; Staley and Kim 1994), and KSI (Kuliopulos et al. 1994) fusion partners promote the accumulation of expressed proteins as inclusion bodies, and have been used to express several membrane peptides and proteins ranging in size from 20 to 200 amino acids (Opella et al. 2001; Opella and Marassi 2004). We have found TLE to be useful for the production of Mat-8 (mammary tumor protein 8 kDa, or FXYD3) and CHIF (corticosteroid-hormone–induced factor, or FXYD4), two 67-residue membrane proteins that belong to the FXYD family of tissue-specific and physiological-state–specific auxiliary subunits of the Na,K-ATPase, with yields of purified protein that range between 3 and 4 mg/L cell culture in M9 minimal medium (Crowell et al. 2003).

The FXYD proteins are widely expressed in mammalian tissues that specialize in fluid and solute transport or that are electrically excitable (Sweadner and Rael 2000; Crambert and Geering 2003), and we are using NMR spectroscopy to determine their structures in lipid micelles and bilayers environments. They are characterized by the short amino acid sequence Phe-X-Tyr-Asp (or FXYD, hence the name) before their single *trans*-membrane helix, which is conserved in all examples, and where X is usually Tyr, but can also be Thr, Glu, or His (Sweadner and Rael 2000). The ability to produce milligram quantities of pure FXYD proteins also facilitates functional studies that, together with structure determination, can provide important structure–activity correlations. Since Mat-8 and CHIF could be purified in sufficiently high quantities, we were able to obtain resonance assignments for their solution NMR spectra in micelles, as well as two-dimensional solid-state NMR spectra in lipid bilayers (Franzin et al. 2005). However, phospholemman (PLM, or FXYD1), a 72-residue FXYD family member that is the major substrate of hormone-stimulated phosphorylation by cAMP-dependent protein kinase A and C in heart and skeletal muscle, resists high-level expression with either the TLE or KSI fusion protein system, yielding amounts of purified material (0.5–1 mg/L cell culture) that are insufficient for NMR structural studies.

In the course of our separate studies with the apoptosis regulatory proteins of the Bcl-2 family (named after B-cell leukemia/lymphoma where they were first discovered), we have found that the anti-apoptotic protein Bcl-XL (B-cell leukemia/lymphoma extra long), which contains a hydrophobic C-terminal sequence of ~ 20 amino acids, can be overexpressed in *E. coli* and purified in high-yields. In nature, Bcl-XL localizes primarily to the outer mitochondrial and ER membranes, presumably through its hydrophobic C terminus, which is sufficiently long to span the lipid bilayer membrane (Adams and Cory 1998; Reed 1998), and while a deletion mutant of Bcl-XL, lacking the C-terminal sequence, can be expressed in bacteria as a soluble protein (Muchmore et al. 1996), the full-length protein accumulates as insoluble inclusion bodies. These observations prompted us to explore the usefulness of Bcl-XL as a fusion partner for the expression of hydrophobic polypeptides that, similar to PLM, are difficult to express and purify.

To test this possibility, we constructed a fusion protein expression plasmid (pBCL) where the hydrophobic C terminus of Bcl-XL was deleted to be replaced with a hydrophobic polypeptide gene of interest by insertion at an engineered cloning site. The plasmid utilizes a T7 expression system (Studier et al. 1990), and a single Met residue, inserted at the beginning of the target polypeptide sequence, enables its release from Bcl-XL by CNBr cleavage. Here we report the high-level production of PLM with this plasmid, and we demonstrate that milligram quantities of pure, isotopically labeled protein can be obtained easily and in little time.

Results and Discussion

The pBCL plasmid vector that we constructed directs the expression of a target polypeptide fused to the C terminus of BCL, a mutant form of Bcl-XL lacking the hydrophobic C-terminal domain of the wild-type protein. The configuration of pBCL is shown in Figure 1A, and the amino acid sequences of wild-type Bcl-XL, mature PLM and the two other FXYD proteins, Mat-8 and CHIF, are shown in Figure 1B.

We prepared and tested two mutant forms of Bcl-XL, BCL173 and BCL99, as fusion tags for the high-level expression of PLM and the other FXYD proteins. To obtain BCL173, the 173-residue 21.5-kDa fusion tag (Fig. 1B, solid underline), we deleted the C-terminal domain (residues 213–233) and the flexible loop (residues 44–84) of Bcl-XL, we changed the two remaining Met residues (Met159 and Met170) to Leu, and we introduced an AflII/XhoI cloning site (Leu-Lys) after Arg212 at the C-terminal end of the gene to facilitate the insertion of target polypeptide sequences. To obtain BCL99, the 99-residue 12.9-kDa tag (Fig. 1B, dashed underline), we further deleted residues 1–116, spanning the loop as well as helices 1–4 in the structure of the soluble form of Bcl-XL (Muchmore et al. 1996). Both fusion tags have an N-terminal $(His)_6$ sequence to allow protein purification by Ni-affinity chromatography.

Reaction with CNBr cleaves the expressed fusion protein after the single Met residue introduced at the start of the

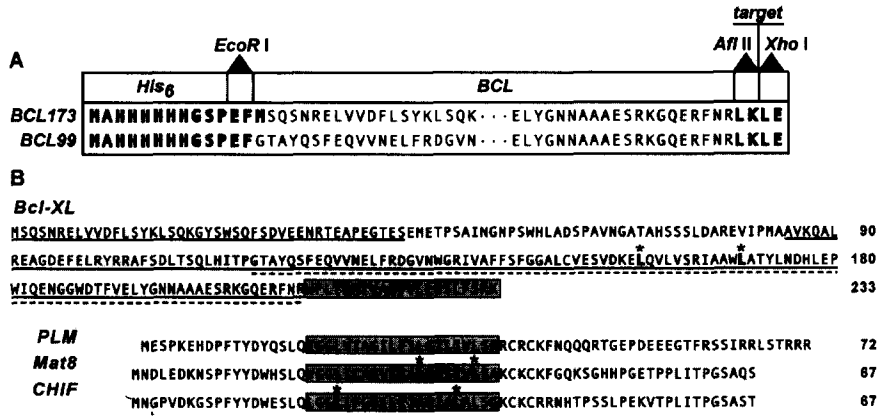

Figure 1. (*A*) Construction of the pBCL173 and pBCL99 fusion protein expression plasmids. The target sequence with N-terminal Met is inserted between the AflII and XhoI cloning sites. BCL173 has a cleavable Met after the His tag, while BCL99 does not. (*B*) Amino acid sequences of wild-type Bcl-XL and of the FXYD proteins, PLM (human), Mat-8 (human), and CHIF (rat), that were inserted in the pBCL plasmid vectors. Met residues that were changed to Leu are marked with asterisks. Both BCL173 and BCL99 lack the Bcl-XL hydrophobic C terminus (highlighted in the gray box), and BCL173 (solid-underline) also lacks the flexible loop of Bcl-XL while BCL99 (dashed underline) lacks the first 116 residues. The *trans*-membrane domains of PLM, Mat-8, and CHIF are highlighted in the gray boxes.

inserted target sequence, releasing the protein of interest intact. In cases where the target protein contains Met residues that cannot be mutated, separation from BCL can be obtained by introducing amino acid sequences specific for cleavage by other chemical means, such as hydroxylamine (Asn-Gly), or for cleavage by one of the commonly used proteases: thrombin, factor Xa, enterokinase, and tobacco etch virus protease. Chemical cleavage is an attractive option because it eliminates the difficulties—poor specificity and enzyme inactivation—often encountered with protease treatment of hydrophobic proteins in detergents.

The expression of PLM using pBCL173 and pBCL99, as well as the two other commonly used plasmids, pKSI and pTLE, is compared in Figure 2A by SDS-PAGE. For this study, each of the four plasmids containing the PLM gene insert were used to transform *E. coli* C41(DE3) cells, a mutant strain selected for the expression of insoluble and toxic proteins (Miroux and Walker 1996), and the positive clones were grown to a cell density of OD_{600} = 0.7 before induction with IPTG for 4 h. The total lysate from cells transformed with pBCL173-PLM, before induction with IPTG, is shown in the first lane of the gel, while IPTG induction of each of the four clones is shown in the following lanes. In all four cases, fusion protein overexpression is marked by the appearance of a distinct band at the calculated molecular weight of the corresponding fusion protein, albeit with different intensities (Fig. 2A, solid arrows). To obtain a quantitative estimate of protein expression, we compared the intensity of each fusion protein band to the intensity of the band from a 39-kDa protein that is expressed in the cells without IPTG induction (Fig. 2A, dashed arrow). In Figure 2A, the intensity of each band is reported as $\%I_{rel}$, the percentage relative to the intensity of the band at 39 kDa.

Induction of BCL173-PLM and BCL99-PLM both yield very strong bands at 29.8 kDa and 21.2 kDa, as expected from their calculated molecular weights. Both these bands have significantly greater intensity than those observed for the expression of KSI-PLM at 23.4 kDa or of TLE-PLM at 22.1 kDa, demonstrating the superior performance of pBCL for the expression of PLM. Similar expression levels were obtained for the other FXYD family proteins Mat-8 and CHIF in pBCL.

Upon overexpression, both full-length Bcl-XL and BCL-PLM accumulate as insoluble proteins and cannot be driven to the soluble cellular fraction by lowering the temperature of the cell culture to 15°C. This is demonstrated in Figure 2B, where the insoluble fraction of the cell lysate (lane P1) is highly enriched in BCL173-PLM (arrow), while the soluble fraction (lane S1) contains very little. In the initial steps of fusion protein isolation, the N-terminal His tag can be used for purification by Ni-affinity chromatography; however, in practice, we have found that the isolation of inclusion bodies already yields very pure protein (Fig. 2B, lane P2) and that the purity is not improved by Ni-affinity. Therefore, after isolating the inclusion bodies by centrifugation, we dissolved them in acidic GdnHCl and proceeded directly to CNBr cleavage. The cleavage reaction was monitored by SDS-PAGE and found to be virtually 100% complete, releasing two fragments corresponding to BCL and PLM, which could be separated chromatographically.

After CNBr cleavage, PLM was separated from the BCL fusion partner by using ion exchange chromatography, to exploit the large difference in isoelectric point (pI) between

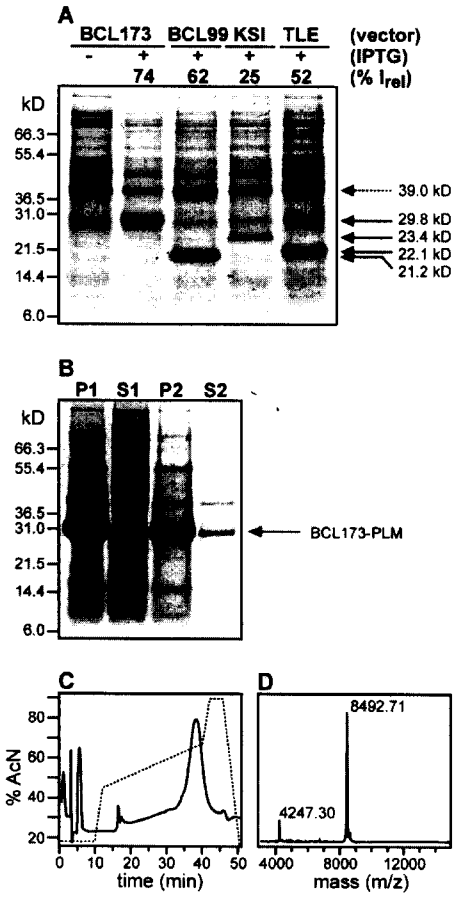

Figure 2. (*A*) Expression of PLM with four different fusion protein plasmid vectors: pBCL173, pBCL99, pKSI, and pTLE. The gel shows total lysates from cells, transformed with each plasmid, and harvested before (–) or after (+) induction with IPTG. Fusion protein overexpression is marked by the appearance of a distinct band (solid arrows) at the molecular weight of the corresponding fusion protein: BCL173-PLM (29.8 kDa), BCL99-PLM (21.2 kDa), KSI-PLM (23.4 kDa), and TLE-PLM (22.1 kDa). The intensity of each band is reported as ($\%I_{rel}$) the percentage relative to the intensity of the band at 39 kDa (dashed arrow). (*B*) Isolation of BCL173-PLM inclusion bodies (29.8 kDa) after cell lysis. The gel shows the pellet (P1) and supernatant (S1) obtained after centrifugation of the total cell lysate, and the pellet (P2) and supernatatnt (S2) obtained after resuspending the inclusion bodies pellet (P1) in buffer A and centrifuging again to separate it from the soluble fraction (S2). (*C*) Reverse-phase HPLC trace for the purification of PLM after CNBr cleavage and ion-exchange chromatography. PLM elutes at 65% acetonitrile. (*D*) MALDI-TOF mass spectrum of purified ^{15}N-labeled PLM at 8.5 kDa. The peak at 4.3 kDa is from the doubly charged protein.

the basic PLM (pI = 9.3) and its acidic fusion partner BCL173 (pI = 4.9) or BCL99 (pI = 5.7). This procedure is also useful for the other FXYD family members. PLM was further purified by reverse-phase HPLC (Fig. 2C), and its mass and purity were confirmed by mass spectrometry (Fig. 2D). The HPLC trace demonstrates that PLM elutes as a single well-resolved peak, in ~65% acetonitrile, as observed previously for purification from the TLE fusion partner (Crowell et al. 2003). The major peak in the MALDI-TOF mass spectrum matches the calculated mass of uniformly ^{15}N-labeled PLM (8.490 kDa), while the small peak at half mass arises from the doubly charged species. The spectrum shows no evidence of degradation or chemical modifications, and the absence of other intensity demonstrates that this procedure yields very pure protein. The typical yields of PLM obtained with the pBCL173 plasmid are in the range of 10 mg of purified PLM per liter of culture in M9 minimal medium.

We have also purified PLM by reverse-phase HPLC directly after CNBr cleavage, bypassing the ion-exchange step, and this method also yields pure protein but is more taxing on the HPLC column. Alternatively, Ni-affinity chromatography could be used to separate PLM from the BCL99 fusion partner, which retains its N-terminal His tag after cleavage, but not to separate it from BCL173, which has a cleavable Met residue, not mutated to Leu, after the His tag.

The two-dimensional ^{1}H/^{15}N HSQC spectrum of purified uniformly ^{15}N-labeled PLM, in SDS micelles, is shown in Figure 3. The spectrum is identical to that previously obtained from PLM prepared using the TLE expression system (Crowell et al. 2003), and the presence of one well-defined resonance for each amide site in the protein is indicative of a high-quality micelle sample. The resonances are well dispersed and clearly resolved, demonstrating that PLM is folded and adopts a unique conformation in micelles. The limited chemical shift dispersion reflects the helical structure of this protein, also observed by circular dichroism (Crowell et al. 2003). Helical secondary structures have also been determined by NMR for Mat-8 and CHIF, for which we have completed the resonance assignments and measured several structural parameters (Franzin et al. 2005).

Previously, we had assigned several resonances in the HSQC spectrum of PLM, including those from the six Gly residues labeled in Figure 3, using uniformly and selectively ^{15}N-labeled protein produced with the TLE system, and

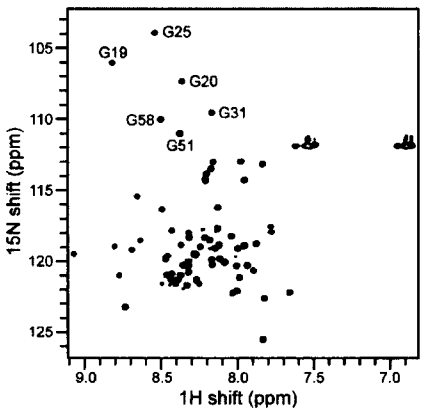

Figure 3. Solution NMR ^{1}H/^{15}N HSQC spectrum of uniformly ^{15}N-labeled PLM in SDS micelles.

HSQC–NOESY data. However, the low yields attainable with the TLE system precluded us from preparing sufficient quantities of isotopically labeled protein for complete resonance assignment and structure determination, and prompted us to explore alternative expression strategies. The ability to produce large quantities of isotopically labeled PLM with BCL, makes it feasible to perform multidimensional, triple-resonance experiments for resonance assignment and structure determination of this protein in lipid micelles. The high-level production of PLM also enables structure determination in lipid bilayers, using solid-state NMR spectroscopy, which will be important for understanding the mechanism with which this integral membrane protein binds and regulates the Na,K-ATPase.

The solid-state NMR spectra of membrane proteins, associated with planar lipid bilayers oriented perpendicular to the magnetic field, trace out characteristic patterns that reflect the protein structure and orientation within the membrane, and thus provide very useful structural restraints. Helical structures give ^{15}N chemical shift/^{1}H-^{15}N dipolar coupling correlation PISEMA spectra, where the resonances from amide sites in the protein track helical wheel projections (Schiffer and Edmunson 1967) that contain information on helix tilt and helix rotation within the membrane (Marassi and Opella 2000; Wang et al. 2000; Marassi 2001). Typically, *trans*-membrane helices have spectra with ^{15}N chemical shifts between 150 and 200 ppm, and ^{1}H-^{15}N dipolar couplings between 2 and 10 kHz, while helices that bind parallel to the membrane surface have spectra with shifts between 70 and 100 ppm and couplings between 0 and 5 kHz.

The solid-state NMR spectra of PLM in lipid bilayers, shown in Figure 4, demonstrate that it can be reconstituted in membranes, in its *trans*-membrane orientation. The ^{15}N chemical shift spectrum of PLM in unoriented lipid bilayer vesicles is a powder pattern (Fig. 4B, solid line) that spans the full range of the amide ^{15}N chemical shift interaction (Fig. 4B, dotted line) and provides no resolution of individual amide sites. The additional intensity at the isotropic resonance frequencies (100–130 ppm) is from amino acid sites that are mobile on the time scale of the ^{15}N chemical shift interaction. The peak at 35 ppm is from the amino groups at the N terminus and side chains of the protein.

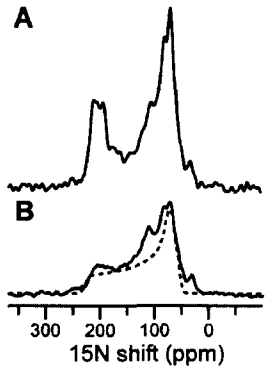

Figure 4. Solid-state NMR ^{15}N chemical shift spectra of uniformly ^{15}N-labeled PLM in DOPC/DOPG lipid bilayers. (*A*) Spectrum in oriented planar bilayers. (*B*) Spectrum in unoriented bilayer vesicles (solid line), and powder pattern calculated for a rigid ^{15}N amide site (dotted line).

The spectrum of PLM in oriented planar lipid bilayers is very different (Fig. 4A), with some of the amide resonances centered at a frequency (80 ppm) associated with NH bonds in helices parallel to the membrane surface, and a distinct set of resonances observed in a relatively narrow band of frequencies (200 ppm) typically associated with NH bonds in *trans*-membrane helices. This is consistent with a conformation where the *trans*-membrane helix of PLM crosses the bilayer with a small tilt angle, similar to CHIF, whose *trans*-membrane helix crosses the membrane with a tilt of 15° (±2.5°) (Franzin et al. 2005). Thus, purified PLM can be refolded in micelles and in lipid bilayers, where it adopts a unique *trans*-membrane conformation.

Conclusions

Producing milligram amounts of protein for structural studies often involves screening for protein expression levels in a variety of expression vectors, since no single system is equally well suited for all target proteins. The BCL fusion protein plasmid vector proved to be very useful for the high-level production of integral membrane proteins of the FXYD family, and particularly for PLM, a family member that had previously been difficult to produce in *E. coli*. The FXYD proteins, PLM, Mat-8, and CHIF, could not be expressed at substantial levels using pET plasmids without an auxiliary fusion protein partner, and while the TLE system has been used successfully for the production of membrane peptides and proteins ranging in length from ~20 to 200 amino acids (Opella et al. 2001) and is useful for the production of Mat-8 and CHIF (Crowell et al. 2003), the yields of purified PLM obtained with TLE are at least 10 times lower than those obtained with BCL. The KSI system, which is designed for the expression of either tandem repeats of 10–25 residues peptides, separated by Met residues for CNBr cleavage, or of individual 25–75 residues polypeptides, works very well for the production of some shorter *trans*-membrane peptides (Opella and Marassi 2004) but does not yield high expression of PLM, whose length of 72 residues is close to the limit for optimal expression with KSI. The GB-1 (B1 immunoglobulin binding domain of streptococcal protein G) fusion protein system was recently developed for the high-level expression of peptides with 10–25 amino acids of varying degrees of hydrophobicity (Lindhout et al. 2003) and offers another attractive expression alternative, although we did not test its usefulness for the production of PLM or other integral membrane proteins.

The ability to produce PLM and other FXYD family proteins, isotopically labeled and in large amounts, facilitates their structural study by NMR in lipid environments, and their functional characterization as regulators of the Na,K-ATPase. Given the efficiency of BCL as a fusion protein tag for the high-level production of PLM, we anticipate that it may also be useful for the production of other single-spanning membrane proteins with similar size and topology, and of shorter hydrophobic peptides, that can be substituted for the hydrophobic C terminus of Bcl-XL.

Materials and methods

Preparation of the plasmid vectors and inserts

We prepared two fusion protein plasmids, pBCL173 and pBCL99, which differ in the amino acid sequence of the Bcl-XL fusion partner (Fig. 1). For both pBCL173 and pBCL99, we deleted amino acids 213–233, spanning the hydrophobic C terminus of human Bcl-XL (accession: Z23115); we mutated two Met residues, M159 and M170, to Leu; and we introduced an AflII/XhoI cloning site at the C terminus of the construct. In addition, for pBCL173, we deleted residues 44–84, spanning the long flexible loop of human Bcl-XL, while for pBCL99 we deleted residues 1–116 spanning the loop as well as helices 1–4 of the protein (Muchmore et al. 1996). These mutant genes, BCL173 and BCL99, were each inserted in the EcoRI and XhoI cloning sites of a pET-21d(+) (Novagen) plasmid vector that had been previously modified to encode an N-terminal $(His)_6$ tag. The wild-type Bcl-XL gene in the modified pET-21d(+) plasmid was a gift from John Reed (The Burnham Institute).

The FXYD genes had been previously constructed by PCR, with synthetic, overlapping, single-stranded oligonucleotides, optimized for *E. coli* codons (Crowell et al. 2003). There are no Met residues in the amino acid sequence of PLM (accession: NP_005022), but those in the Mat-8 (accession: NP_068710; Met31 and Met36) and CHIF (accession: NP_071783; Met22 and Met35) sequences were mutated to Leu.

For cloning into the pBCL vectors, we introduced AflII and XhoI restriction sites at the 5′ (AflII) and 3′ (XhoI) ends of each FXYD gene, as well as a Met codon at the start of the sequences to allow CNBr cleavage. The plasmids and inserts were each digested with AflII and XhoI, purified by agarose gel electrophoresis, and ligated together. The cloning and production of Mat-8, CHIF, and PLM, using the TLE vector were described previously (Crowell et al. 2003). For cloning in the KSI vector, we introduced AlwNI and XhoI restriction sites at the ends of the FXYD genes, digested them with the enzymes, and ligated them with the similarly digested pET-31b(+) plasmid (Novagen). For each of the four systems, the resulting plasmid was transformed in DH5α, and positive clones were selected by PCR screening and DNA sequencing. For protein expression, the plasmid obtained from positive DH5α colonies was transformed in *E. coli* C41(DE3) (www.overexpress.com; Miroux and Walker 1996).

Protein expression

For protein expression, 5–10 μL of transformed C41(DE3) cells, from a frozen glycerol stock, were used to inoculate 10 mL of LB media and grown for 5 h at 37°C with vigorous shaking; then 1 mL of this starter culture was added to 100 mL of minimal M9 media and grown overnight. All media contained 100 μg/mL of ampicillin. In the morning, 1 L of fresh M9 media was inoculated with the overnight culture, and the cells were grown to a cell density of OD_{600} = 0.7. Protein expression was induced by the addition of 1 mM IPTG for 4 h at 37°C. The cells were subsequently harvested by centrifugation and stored overnight at −20°C. For uniformly ^{15}N-labeled proteins, $(^{15}NH_4)_2SO_4$ (Cambridge Isotope Laboratories) was supplied to the M9 salts as the sole nitrogen source. SDS-PAGE was performed with the Tris-Tricine system (Schagger and von Jagow 1987), and gels were stained with Coomassie Blue G250. The band intensities were quantified by using SigmaScan Pro5.0 (SPSS).

Protein purification

Frozen cells from 1 L of culture were lysed by French press in 30 mL of buffer A (50 mM Tris HCl at pH 8.0, 15% glycerol). The soluble fraction (Fig. 2B, lane S1) was removed by centrifugation (48,000*g*, 4°C, 30 min), and the pellet (Fig. 2B, lane P1) was washed twice by resuspension in 30 mL of buffer A, followed by centrifugation (48,000*g*, 4°C, 30 min) to remove the soluble fraction (Fig. 2B, lane S2). The resulting pellet (Fig. 2B, lane P2) was dissolved in 30 mL of 6 M GdnHCl and again centrifuged (48,000*g*, 4°C, 2 h) to remove any insoluble materials. The 6 M GdnHCl protein solution was adjusted to 0.1 N HCl (pH 0.2), a 100-fold molar excess of solid CNBr was added, and the mixture was allowed to react overnight in the dark at room temperature. In the morning, the reaction mixture was dialyzed against water until the pH reached ~ 5.0 (6 h with several changes of 4 L of water, in a dialysis membrane with molecular weight cutoff of 1 kDa), lyophilized to powder, and dissolved in buffer B (20 mM Tris HCl at pH 7.0, 8 M urea). PLM was purified by ion exchange chromatography with a NaCl gradient (FF-S column, Amersham Biosciences), followed by exchange in buffer C (20 mM Tris HCl at pH 7.0, 4 mM SDS), and preparative reverse-phase HPLC (Delta-Pak C4 column, Waters), with a gradient of acetonitrile in water and 0.1% trifluoroacetic acid. Purified protein was stored as lyophilized powder at −20°C. Alternatively, the lyophilized cleavage mixture was dissolved directly in buffer C, and PLM was purified with reverse-phase HPLC.

Mass spectrometry

The molecular weight of PLM was verified by MALDI-TOF mass spectrometry. Approximately 0.2 mg of lyophilized protein were dissolved in 10 μL of solution 1 (75% acetonitrile, 25% water, 0.1% TFA), and 1 μL of this protein solution was mixed with 1 L of solution II (15 mg/mL sinnapinic acid, 300 μL acetonitrile, 200 μL methanol, 500 μL Milli-Q ultra purified water). The resulting solution was spotted onto a seed layer spot on the MALDI target. The seed layer was prepared from matrix solution (6 mg sinnapinic acid, 600 μL methanol, 390 μL acetone, 10 μL of 0.1% aqueous TFA). The MALDI-TOF mass spectrum was collected in linear mode on a Voyager DE-PRO mass spectrometer (Applied Biosystems). Typically, 250–500 laser pulses were averaged for each spectrum.

Solution NMR spectroscopy

Samples were prepared by dissolving 4 mg of ^{15}N-labeled protein in 300 μL of NMR buffer (500 mM SDS, 10 mM DTT, 13% D_2O, 20 mM sodium citrate at pH 5.0). Solution NMR experiments were

performed on a Bruker AVANCE 600 spectrometer with a 600/54 Magnex magnet, equipped with a triple-resonance 5-mm probe with three-axis field gradients. The two-dimensional $^{1}H/^{15}N$ HSQC (Mori et al. 1995) spectrum was obtained at 40°C. The ^{15}N and ^{1}H chemical shifts were referenced to 0 ppm for liquid ammonia and tetramethylsilane, respectively. The NMR data were processed using NMR Pipe (Delaglio et al. 1995) and rendered in SPARKY (Goddard and Kneller 2004) on a Dell Precision 330 MT Linux workstation.

Solid-state NMR spectroscopy

The lipids, 1,2-dioleoyl-*sn*-glycero-3-phosphocholine (DOPC) and 1,2-dioleoyl-*sn*-glycero-3-(phospho-rac-[1-glycerol]) (DOPG) were from Avanti. Samples of PLM in lipid bilayers were prepared by adding 100 mg of the lipids (DOPC/DOPG in 8:2 molar ratio) dissolved in 1 mL of chloroform to 6 mg of ^{15}N-labeled protein. After 5 min of bath sonication and the addition of two to five drops of trifluoroethanol, to obtain an optically clear solution, the lipid and protein mixture was distributed over the surface of 15 glass slides (11 × 11, #00, Marienfeld). After allowing the organic solvents to evaporate under vacuum overnight, the slides were stacked and equilibrated for 24 h at 40°C and 93% relative humidity, to form oriented planar lipid bilayers. The samples were wrapped in parafilm and then sealed in thin polyethylene film prior to insertion in the NMR probe. Lipid bilayer vesicles with membrane-inserted PLM were prepared by crushing the glass slides supporting the protein-reconstituted lipid bilayers in additional water, and resealing this sample in a plastic bag.

Solid-state NMR experiments were performed on a Bruker AVANCE 500 spectrometer with a 500/89 AS Magnex magnet. The home-built $^{1}H/^{15}N$ double-resonance probe had a square radiofrequency coil (11 × 11 × 3 mm) wrapped directly around the samples. The one-dimensional ^{15}N chemical shift spectra were obtained with single contact CPMOIST (Pines et al. 1973; Levitt et al. 1986), with a cross polarization contact time of 1 msec, a ^{1}H 90° pulse width of 5 μsec, and continuous ^{1}H decoupling of 63 kHz. The ^{15}N chemical shifts were referenced to 0 ppm for liquid ammonia. The data were processed using NMR Pipe (Delaglio et al. 1995) and rendered in Sparky (Goddard and Kneller 2004) on a Dell Precision 330 MT Linux workstation.

Acknowledgments

We thank John Reed for his gift of the wild-type Bcl-XL gene. We thank Xiao-Min Gong for helpful discussions, Jinghua Yu for her assistance with NMR experiments, Andrey Bobkov for his assistance with the SDS-PAGE image analysis, and Dario Miranda for performing MALDI-TOF mass spectrometry. This research was supported by grants from the National Institutes of Health (R01 CA082864), the Department of the Army Breast Cancer Research Program (DAMD17-02-1-0313), and the California Breast Cancer Research Program (8WB0110). The NMR studies utilized the Burnham Institute NMR Facility, supported by a grant from the National Institutes of Health (P30 CA030199).

References

Adams, J.M. and Cory, S. 1998. The Bcl-2 protein family: Arbiters of cell survival. *Science* **281:** 1322–1326.

Bannwarth, M. and Schulz, G.E. 2003. The expression of outer membrane proteins for crystallization. *Biochim. Biophys. Acta* **1610:** 37–45.

Booth, P.J. 2003. The trials and tribulations of membrane protein folding in vitro. *Biochim. Biophys. Acta* **1610:** 51–56.

Crambert, G. and Geering, K. 2003. FXYD proteins: New tissue-specific regulators of the ubiquitous Na,K-ATPase. *Sci. STKE* **2003:** RE1.

Crowell, K.J., Franzin, C.M., Koltay, A., Lee, S., Lucchese, A.M., Snyder, B.C., and Marassi, F.M. 2003. Expression and characterization of the FXYD ion transport regulators for NMR structural studies in lipid micelles and lipid bilayers. *Biochim. Biophys. Acta* **1645:** 15–21.

Dawson, P.E., Muir, T.W., Clark-Lewis, I., and Kent, S.B. 1994. Synthesis of proteins by native chemical ligation. *Science* **266:** 776–779.

Delaglio, F., Grzesiek, S., Vuister, G.W., Zhu, G., Pfeifer, J., and Bax, A. 1995. NMRPipe: a multidimensional spectral processing system based on UNIX pipes. *J. Biomol. NMR* **6:** 277–293.

Franzin, C.M., Yu, J., and Marassi, F.M. 2005. Solid-state NMR of the FXYD family membrane proteins in lipid bilayers. In *NMR Spectroscopy of biological solids* (ed. A. Ramamoorthy). Marcel Dekker, New York, NY (in press).

Goddard, T.D. and Kneller, D.G. 2004. *SPARKY 3*. University of California, San Francisco.

Jones, D.H., Ball, E.H., Sharpe, S., Barber, K.R., and Grant, C.W. 2000. Expression and membrane assembly of a transmembrane region from Neu. *Biochemistry* **39:** 1870–1878.

Kiefer, H. 2003. In vitro folding of α-helical membrane proteins. *Biochim. Biophys. Acta* **1610:** 57–62.

Klammt, C., Lohr, F., Schafer, B., Haase, W., Dotsch, V., Ruterjans, H., Glaubitz, C., and Bernhard, F. 2004. High level cell-free expression and specific labeling of integral membrane proteins. *Eur. J. Biochem.* **271:** 568–580.

Kleid, D.G., Yansura, D., Small, B., Dowbenko, D., Moore, D.M., Grubman, M.J., McKercher, P.D., Morgan, D.O., Robertson, B.H., and Bachrach, H.L. 1981. Cloned viral protein vaccine for foot-and-mouth disease: responses in cattle and swine. *Science* **214:** 1125–1129.

Kochendoerfer, G.G. 2001. Chemical protein synthesis methods in drug discovery. *Curr. Opin. Drug Discov. Devel.* **4:** 205–214.

Kochendoerfer, G.G., Salom, D., Lear, J.D., Wilk-Orescan, R., Kent, S.B., and DeGrado, W.F. 1999. Total chemical synthesis of the integral membrane protein influenza A virus M2: Role of its C-terminal domain in tetramer assembly. *Biochemistry* **38:** 11905–11913.

Kochendoerfer, G.G., Jones, D.H., Lee, S., Oblatt-Montal, M., Opella, S.J., and Montal, M. 2004. Functional characterization and NMR spectroscopy on full-length Vpu from HIV-1 prepared by total chemical synthesis. *J. Am. Chem. Soc.* **126:** 2439–2446.

Kuliopulos, A., Nelson, N.P., Yamada, M., Walsh, C.T., Furie, B., Furie, B.C., and Roth, D.A. 1994. Localization of the affinity peptide-substrate inactivator site on recombinant vitamin K-dependent carboxylase. *J. Biol. Chem.* **269:** 21364–21370.

Levitt, M.H., Suter, D., and Ernst, R.R. 1986. Spin dynamics and thermodynamics in solid-state NMR cross-polarization. *J. Chem. Phys.* **84:** 4243–4255.

Lindhout, D.A., Thiessen, A., Schieve, D., and Sykes, B.D. 2003. High-yield expression of isotopically labeled peptides for use in NMR studies. *Protein Sci.* **12:** 1786–1791.

Majerle, A., Kidric, J., and Jerala, R. 2000. Production of stable isotope enriched antimicrobial peptides in *Escherichia coli*: An application to the production of a ^{15}N-enriched fragment of lactoferrin. *J. Biomol. NMR* **18:** 145–151.

Marassi, F.M. 2001. A simple approach to membrane protein secondary structure and topology based on NMR spectroscopy. *Biophys. J.* **80:** 994–1003.

Marassi, F.M. and Opella, S.J. 2000. A solid-state NMR index of helical membrane protein structure and topology. *J. Magn. Reson.* **144:** 150–155.

Miozzari, G.F. and Yanofsky, C. 1978. Translation of the leader region of the *Escherichia coli* tryptophan operon. *J. Bacteriol.* **133:** 1457–1466.

Miroux, B. and Walker, J.E. 1996. Over-production of proteins in *Escherichia coli*: Mutant hosts that allow synthesis of some membrane proteins and globular proteins at high levels. *J. Mol. Biol.* **260:** 289–298.

Mori, S., Abeygunawardana, C., Johnson, M.O., and Vanzijl, P.C.M. 1995. Improved sensitivity of HSQC spectra of exchanging protons at short interscan delays using a new fast HSQC (FHSQC) detection scheme that avoids water saturation. *J. Magn. Reson. B* **108:** 94–98.

Muchmore, S.W., Sattler, M., Liang, H., Meadows, R.P., Harlan, J.E., Yoon, H.S., Nettesheim, D., Chang, B.S., Thompson, C.B., Wong, S.L., et al. 1996. X-ray and NMR structure of human Bcl-xL, an inhibitor of programmed cell death. *Nature* **381:** 335–341.

Opella, S.J., and Marassi, F.M. 2004. Structure determination of membrane proteins by NMR spectroscopy. *Chem. Rev.* **104:** 3587–3606.

Opella, S.J., Ma, C., and Marassi, F.M. 2001. Nuclear magnetic resonance of

membrane-associated peptides and proteins. *Methods Enzymol.* **339:** 285–313.

Pines, A., Gibby, M.G., and Waugh, J.S. 1973. Proton-enhanced NMR of dilute spins in solids. *J. Chem. Phys.* **59:** 569–590.

Reed, J.C. 1998. Bcl-2 family proteins. *Oncogene* **17:** 3225–3236.

Rogl, H., Kosemund, K., Kuhlbrandt, W., and Collinson, I. 1998. Refolding of *Escherichia coli* produced membrane protein inclusion bodies immobilised by nickel chelating chromatography. *FEBS Lett.* **432:** 21–26.

Schagger, H. and von Jagow, G. 1987. Tricine-sodium dodecyl sulfate–polyacrylamide gel electrophoresis for the separation of proteins in the range from 1 to 100 kDa. *Anal. Biochem.* **166:** 368–379.

Schiffer, M. and Edmunson, A.B. 1967. Use of helical wheels to represent the structures of proteins and to identify segments with helical potential. *Biophys. J.* **7:** 121–135.

Sharon, M., Gorlach, M., Levy, R., Hayek, Y., and Anglister, J. 2002. Expression, purification, and isotope labeling of a gp120 V3 peptide and production of a Fab from a HIV-1 neutralizing antibody for NMR studies. *Protein Expr. Purif.* **24:** 374–383.

Smith, V.R. and Walker, J.E. 2003. Purification and folding of recombinant bovine oxoglutarate/malate carrier by immobilized metal-ion affinity chromatography. *Protein Exp. Purif.* **29:** 209–216.

Staley, J.P. and Kim, P.S. 1994. Formation of a native-like subdomain in a partially folded intermediate of bovine pancreatic trypsin inhibitor. *Protein Sci.* **3:** 1822–1832.

Studier, F.W., Rosenberg, A.H., Dunn, J.J., and Dubendorff, J.W. 1990. Use of T7 RNA polymerase to direct expression of cloned genes. *Methods Enzymol.* **185:** 60–89.

Sweadner, K.J. and Rael, E. 2000. The FXYD gene family of small ion transport regulators or channels: cDNA sequence, protein signature sequence, and expression. *Genomics* **68:** 41–56.

Wang, J., Denny, J., Tian, C., Kim, S., Mo, Y., Kovacs, F., Song, Z., Nishimura, K., Gan, Z., Fu, R., et al. 2000. Imaging membrane protein helical wheels. *J. Magn. Reson.* **144:** 162–167.

Wiener, M.C. 2004. A pedestrian guide to membrane protein crystallization. *Methods* **34:** 364–372.

In Lipid Protein Interactions, Biophysics Monographs, Gonzalez Ros JM, ed. (Berlin, Springer).
IN PRESS

NMR of Membrane Proteins in Lipid Environments: the Bcl-2 family of apoptosis regulators.

Xiao-min Gong, Jungyuen Choi, and Francesca M. Marassi

The Burnham Institute, 10901 North Torrey Pines Road, La Jolla, CA 92037 USA.

Address correspondence to:

Francesca M. Marassi
The Burnham Institute
10901 North Torrey Pines Road
La Jolla, CA 92037 USA

Email: fmarassi@burnham.org
Phone: 858-713-6282
Fax: 858-713-6268

(1) Introduction.

Many fundamental cellular functions are regulated by proteins that are integral to membranes, or that associate peripherally with their surfaces. Understanding the structures of these molecules is a major goal of structural biology, however, despite their importance, only a few structures of membrane proteins have been deposited in the Protein Data bank, compared to the thousands of coordinates deposited for globular proteins (www.rcsb.org/pdb/). This deficit reflects the lipophilic character of membrane proteins, which makes them difficult to over-express and purify, complicates crystallization for X-ray analysis, and results in highly overlapped and broadened solution NMR spectral lines. NMR spectroscopy offers two complementary approaches to membrane protein structure determination: solution NMR with samples of membrane proteins dissolved in lipid micelles, and solid-state NMR with samples of proteins incorporated in lipid bilayers, a method that is particularly attractive because it enables structures to be determined in an environment that closely mimics the biological membrane.

High-quality solution NMR spectra can be obtained for some large, helical, membrane proteins in micelles, but it is very difficult to measure and assign a sufficient number of long-range NOEs for structure determination (Klein-Seetharaman et al. 2002, Oxenoid et al. 2004). This limitation can be overcome by preparing weakly aligned micelle samples for the measurement of residual dipolar couplings (RDCs) and residual chemical shift anisotropies (RCSAs) (Bax et al. 2001, Prestegard and Kishore 2001), as demonstrated for the structure of the bacterial mercury detoxification membrane protein MerF (Howell et al. 2005).

High-resolution solid-state NMR spectra can be obtained for membrane proteins that are expressed, isotopically labeled, and reconstituted in uniaxially oriented planar lipid bilayers. The spectra have characteristic resonance patterns that directly reflect protein structure and topology, and this direct relationship between spectrum and structure provides the basis for methods that enable the simultaneous sequential assignment of resonances and the measurement of orientation restraints for protein structure determination (Marassi and Opella 2000, Wang et al. 2000, Marassi 2001). Recent developments in sample preparation, recombinant bacterial expression systems for the preparation of isotopically labeled membrane proteins, pulse sequences for high-resolution spectroscopy, and structural indices that guide the structure assembly process, have greatly extended the capabilities of the technique. The structures of a variety of membrane peptides and proteins have been examined using this approach, and several atomic-resolution structures have been determined and deposited in the PDB (Ketchem et al. 1993, Opella et al. 1999, Valentine et al. 2001, Wang et al. 2001, Marassi and Opella 2003, Park et al. 2003).

In this chapter, the methods are illustrated with examples from the Bcl-2 family proteins, which regulate a major mechanism for commitment to programmed cell death (apoptosis), and play critical roles in tissue development, differentiation, and homeostasis.

(2) The Bcl-2 family proteins and programmed cell death.

Programmed cell death is initiated when death signals activate the caspases, a family of otherwise dormant cysteine proteases. External stress stimuli trigger the ligation of cell surface death receptors, thereby activating the upstream initiator caspases, which in turn process and activate the downstream cell death executioner caspases (Denault and Salvesen 2002). In addition, caspases can be activated when stress or developmental cues within the cell induce the release of cytotoxic proteins from mitochondria. This intrinsic mitochondrial pathway for cell death is regulated by the relative ratios of the pro- and anti-apoptotic members of the Bcl-2 protein family.

Several Bcl-2 family members have been identified in humans, including both anti-apoptotic (cytoprotective) and pro-apoptotic (death-promoting) proteins (Green and Reed 1998, Kroemer and Reed 2000, Cory and Adams 2002, Danial and Korsmeyer 2004). The relative ratios of the pro- and anti-apoptotic proteins determine the ultimate sensitivity and resistance of cells to diverse death-inducing stimuli, including chemotherapeutic drugs, radiation, growth factor deprivation, loss of cell attachment to

extracellular matrix, hypoxia, infection, and lysis by cytolytic T cells. Imbalances in their relative expression levels and activities are associated with major human diseases, characterized by either insufficient (cancer, autoimmunity) or excessive (AIDS, Alzheimer's disease) cell death.

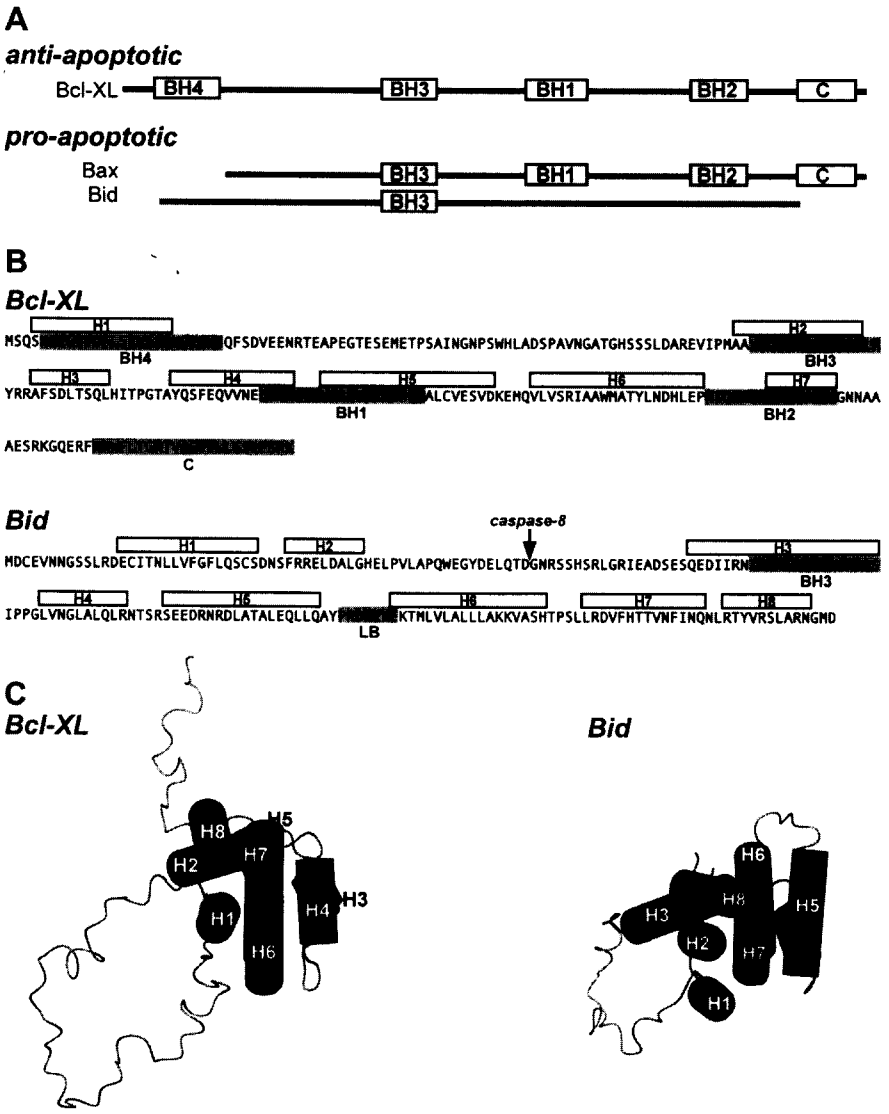

Figure 1. Domain organization (A) and amino acid sequences (B) of human Bcl-XL and Bid. The helices (H1 to H8) are those identified in the solution NMR structures of Bcl-XL (Muchmore et al. 1996, Aritomi et al. 1997) and Bid (Chou et al. 1999, McDonnell et al. 1999) shown in (C). The central core helices are H5 and H6 in Bcl-XL and H6 and H7 in Bid. The C-terminal hydrophobic segment of Bcl-XL is denoted as C. the putative lipid binding motif of Bid is denoted as LB. The sequence of tBid starts at Gly61, and the arrow marks the caspase-8 cleavage site at Asp60.

The Bcl-2 proteins span approximately 200 amino acids, and share sequence homology in four evolutionarily conserved domains (BH1 - BH4), of which the BH3 domain is highly conserved and essential for both cell killing and oligomerization among Bcl-2 family members (Figure 1). The anti-apoptotic family members have all four domains, while all of the pro-apoptotic members lack BH4, and some others only have BH3. These BH3-only proteins are activated by upstream death signals, which trigger their transcriptional induction or post-translational modification, providing a key link between the extrinsic death receptor and intrinsic mitochondrial pathways to cell death. Most family members also have a hydrophobic C-terminus (C) which is sufficiently long to span the membrane, and is essential for membrane targeting.

The apoptosis regulatory activities of the Bcl-2 family proteins are exerted through binding with other Bcl-2 family members, binding with other non-homologous proteins, and through the modulation of ion-conducting pores that are thought to influence cell fate by regulating mitochondrial physiology. Their functions are also regulated by subcellular location, as the proteins cycle between soluble and membrane-bound forms. For example, some family members, like anti-apoptotic Bcl-XL, localize to mitochondrial, endoplasmic reticulum, or nuclear membranes, while others, like pro-apoptotic Bid, are found in the cytosol, but are stimulated by death signals to target the mitochondrial outer membrane, where they participate in cytochrome-c release and apoptosis.

The structures of Bcl-XL and Bid, in solution, are very similar. They consist of seven (Bcl-XL) or eight (Bid) β-helices arranged with two central somewhat more hydrophobic helices which form the core of the molecule (Figure 1). In Bcl-XL, the third helix spans the BH3 domain, and is connected to the first helix by a long flexible loop, while helices 5 and 6 form the central hydrophobic hairpin (Muchmore et al. 1996, Aritomi et al. 1997). The structure was determined for a truncated form of the protein lacking the hydrophobic C-terminus. In Bid, the third helix contains the BH3 domain and is connected to the first two helices by a long flexible loop, which includes Asp60, the caspase-8 cleavage site. The hydrophobic hairpin is formed by helices 6 and 7 (Chou et al. 1999, McDonnell et al. 1999). Despite the lack of sequence homology, the structures of Bcl-XL and Bid are strikingly similar to each other, and those of other pro- and anti-apoptotic Bcl-2 family proteins (Suzuki et al. 2000, Petros et al. 2001, Huang et al. 2002, Denisov et al. 2003, Hinds et al. 2003, Huang et al. 2003, Day et al. 2004, Day et al. 2005). Interestingly, they are also similar to the structure of the pore-forming domains of bacterial toxins, and, like the toxins and other Bcl-2 family members, they also forms ion-conducting pores in lipid bilayers (Cramer et al. 1995, Schendel et al. 1998, Schendel et al. 1999).

The structural basis for Bcl-2 pore formation is not known, since the structures that have been determined are for the soluble forms of the proteins, and pore formation by the Bcl-2 family proteins has not been established in-vivo. Nevertheless, by analogy to the bacterial toxins, the Bcl-2 pores are thought to form by a rearrangement of their compactly-folded helices upon contact with the mitochondrial membrane. One model proposes membrane insertion of the core helical hairpin with the other helices folding up to rest on the membrane surface, while an alternative model envisions the helices rearranging to bind the membrane surface without insertion. A third possible mechanism for the regulation of mitochondrial physiology by the Bcl-2 proteins is through their interaction with other mitochondrial channels.

(3) Protein expression and purification.

NMR structural studies require milligram quantities of isotopically labeled proteins, and the most versatile and widely used method for obtaining recombinant proteins is by expression in *E. coli*, since this enables a wide variety of isotopic labeling schemes to be incorporated in the NMR experimental strategy. Smaller peptides can be prepared by solid phase peptide synthesis, however this is impractical for larger proteins and for the preparation of uniformly labeled samples, where efficient expression systems are essential. The ability to produce milligram quantities of pure FXYD proteins also facilitates functional studies that, together with structure determination, can provide important structure-activity correlations.

Some polypeptides, however, are toxic to the bacterial hosts that express them. For example, some membrane proteins and peptides, including some of bacterial origin, congest the cell membranes when they are over-expressed, and act as toxic, anti-bacterial agents, regardless of their actual biological functions. For these difficult polypeptides, solid-phase synthesis is not a practical alternative, because it is typically limited to sequences shorter than 50 amino acids, and while this size limit can be extended through the use of chemical ligation methods (Dawson et al. 1994, Kochendoerfer 2001) that can also be applied to membrane proteins (Kochendoerfer et al. 1999, Kochendoerfer et al. 2004), NMR studies still require bacterial expression of the polypeptide precursors for the practical introduction of various isotopic labels.

Several *E. coli* cell strains and expression strategies have been developed to address this problem (Miroux and Walker 1996, Rogl et al. 1998, Jones et al. 2000, Majerle et al. 2000, Opella et al. 2001, Sharon et al. 2002, Bannwarth and Schulz 2003, Booth 2003, Kiefer 2003, Lindhout et al. 2003, Smith and Walker 2003, Wiener 2004), and more recently, cell-free expression has been used to obtain milligram quantities of isotopically labeled membrane proteins (Klammt et al. 2004). Many strategies rely on the use of fusion protein tags to improve expression and facilitate purification, and many involve protein expression in inclusion bodies, to keep the hydrophobic polypeptide away from the bacterial membranes, and thus increase the level of expression. The formation of inclusion bodies also limits proteolytic degradation, and simplifies protein purification, which can be further assisted by the incorporation of an engineered His tag for metal affinity chromatography.

The TLE (a portion of the Trp βLE 1413 polypeptide) (Miozzari and Yanofsky 1978, Kleid et al. 1981, Staley and Kim 1994), and KSI (ketosteroid isomerase) (Kuliopulos et al. 1994) fusion partners promote the accumulation of expressed proteins as inclusion bodies, and have been used to express several membrane peptides and proteins ranging in size from 20 to 200 amino acids (Opella et al. 2001, Opella and Marassi 2004).

Recently, we developed a fusion protein expression vector, pBCL, that directs the expression of a target polypeptide fused to the C-terminus of a mutant form of the Bcl-2 family protein Bcl-XL, where the hydrophobic C-terminus has been deleted, and Methionine residues have been mutated to Leucine, to facilitate CNBr cleavage after a single Methionine inserted at the beginning of the target polypeptide sequence (Thai et al. 2005). As shown in Figure 2, this fusion partner yields the high-level expression of membrane proteins belonging to the FXYD family of Na,K-ATPase regulators, including some that had resisted expression with TLE and KSI.

The pTLE and pBCL vectors may be generally useful for the high-level expression of other membrane-associated proteins that are difficult to express because of their toxic properties. The use of chemical cleavage eliminates the difficulties, poor specificity and enzyme inactivation, often encountered with protease treatment of insoluble proteins. However, in cases where Met mutation is not feasible, protein cleavage from the fusion partner can be obtained enzymatically, by engineering specific protease cleavage sites for the commonly used enzymes thrombin, Fxa, enterokinase, and tobacco etch virus (TEV) protease. Thrombin and TEV retain activity in the presence of detergents, including low mM concentrations of SDS.

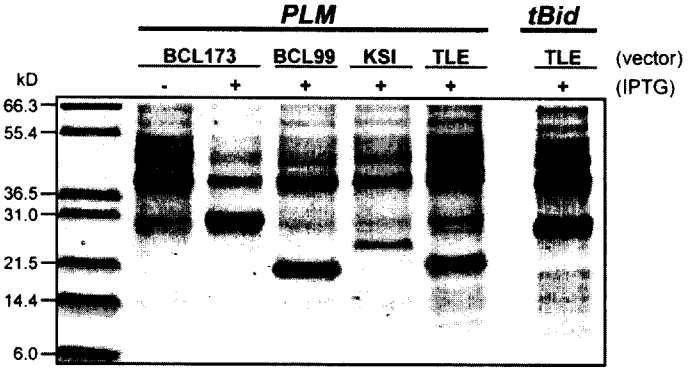

Figure 2. Expression of the membrane protein phospholemman (PLM) and of tBid with four different fusion protein plasmid vectors: pBCL173, pBCL99, pKSI, and pTLE. The gel shows total lysates from cells, transformed with each plasmid, and harvested before (-) or after (+) induction with IPTG. Fusion protein over-expression is marked by the appearance of a distinct band (solid arrows) at the molecular weight of the corresponding fusion protein: BCL173-PLM (29.8 kD), BCL99-PLM (21.2 kD), KSI-PLM (23.4 kD), TLE-PLM (22.1 kD), and TLE-tBid (30.0 kD) (Gong et al. 2004, Thai et al. 2005).

The pro-apoptotic Bcl-2 family protein, Bid, is activated upon cleavage by caspase-8, to release the 15 kD C-terminal fragment tBid, which translocates from the cytosol to the outer mitochondrial membrane inducing massive cytochrome-c release and cell death (Scorrano and Korsmeyer 2003). Full-length Bid can be expressed at high levels, in *E. coli*, as a soluble protein, however tBid is toxic for bacterial cells. To produce milligram quantities of ^{15}N-labeled tBid for NMR studies we used the TLE fusion protein vector (Figure 2). tBid was separated from the fusion partner by means of CNBr cleavage at the engineered N-terminal Met residue, and this method yields approximately 10 mg of purified ^{15}N-labeled tBid from 1 L of culture. To avoid cleavage within the tBid segment, the four Met residues in the tBid amino acid sequence,

were mutated to Leu, and therefore, it was important to demonstrate that the recombinant protein retained its biological activity. Recombinant tBid, isolated from inclusion bodies, was fully active in its ability to induce cytochrome-c and SMAC release from isolated mitochondria, and retained its capacity to bind anti-apoptotic Bcl-X_L through its BH3 domain despite the M97L mutation in its sequence (Gong et al. 2004).

(4) NMR in micelles.

Solution NMR methods rely on rapid molecular reorientation for line narrowing, and can be successfully applied to membrane proteins in micelles (Henry and Sykes 1994, Williams et al. 1996, Almeida and Opella 1997, Gesell et al. 1997, MacKenzie et al. 1997, Arora et al. 2001, Fernandez et al. 2001, Hwang et al. 2002, Ma et al. 2002, Mascioni et al. 2002, Oxenoid et al. 2002, Sorgen et al. 2002, Crowell et al. 2003, Krueger-Koplin et al. 2004, Howell et al. 2005). The size limitation is substantially more severe than for globular proteins, because the many lipid molecules associated with each polypeptide slow its overall reorientation rate. Micelles afford rapid and effectively isotropic reorientation of the protein, and their amphipathic nature simulates that of membranes, offering a realistic alternative to organic solvents for studying membrane proteins. Moreover, for the proteins examined by both solution and solid-state NMR, similar structural features have been found in micelle and bilayer samples (Lee et al. 2003, Mesleh et al. 2003).

The first step in solution NMR studies of proteins is the preparation of folded, homogeneous, and well-behaved samples, and several lipids are available for membrane protein solubilization (Krueger-Koplin et al. 2004). For membrane-bound proteins, small micelles containing approximately sixty lipids and one protein provide a generally effective model membrane environment, without the damaging effects of organic solvents. The primary goal in micelle preparation is to reduce the effective rotational correlation time of the protein so that resonances will have the narrowest possible line widths. Careful handling of the protein throughout the purification is essential, since subtle changes in the protocol can have a significant impact on the quality of the resulting spectra. It is essential to optimize the protein concentration, lipid nature and concentration, counter ions, pH and temperature, in order to obtain well-resolved NMR spectra, with narrow ^{1}H and ^{15}N resonance line widths.

Although high-quality solution NMR spectra can be obtained even for some large helical membrane proteins in micelles (Krueger-Koplin et al. 2004, Oxenoid et al. 2004, Howell et al. 2005), there are only very few cases where it has been possible to measure and assign sufficient long-range NOEs for structure determination. This limitation can be overcome by preparing weakly aligned micelle samples for the measurement of RDCs (Bax et al. 2001, Prestegard and Kishore 2001) from the backbone amide sites, and the analysis of these orientation restraints in terms of *Dipolar Waves* (Mesleh et al. 2002, Lee et al. 2003, Mesleh et al. 2003, Mesleh and Opella 2003). Stressed polyacrylamide gels provide an ideal orientable medium for membrane proteins in micelles, because they do not suffer from the drawbacks of bicelles, which bind tightly to membrane proteins, or phage particles, which are destroyed by micelles (Sass et al. 2000, Tycko et al. 2000, Chou et al. 2001, Meier et al. 2002, Howell et al. 2005). Another useful approach to compensate for insufficient NOEs involves the combination of site-directed spin labeling and NMR (Battiste and Wagner 2000), where distances derived from paramagnetic broadening of NMR resonances is used to determine global fold. In addition, spin label probes and metal ions can be incorporated within the micelles in order to probe protein insertion (Papavoine et al. 1994, Van Den Hooven et al. 1996, Jarvet et al. 1997, Damberg et al. 2001, Sorgen et al. 2002, Kutateladze et al. 2004).

(4.1) Determining the structures of proteins in micelles.

The measurements of as many homonuclear $^{1}H/^{1}H$ NOEs as possible among the assigned resonances provide the short-range and long-range distance restraints required for structure determination (Clore and Gronenborn 1989, Wuthrich 1989, Ferentz and Wagner 2000). These are supplemented by other structural restraints, such as spin-spin coupling constants, chemical shift correlations, deuterium exchange data, and

RDCs in order to assign resonances and to characterize the secondary structure of the protein. The HSQC (heteronuclear single quantum coherence) spectra of samples in D_2O solutions identify the most stable helical residues, and can provide useful information on the topology of membrane proteins in micelles (Czerski et al. 2000). In addition, hydrogen-deuterium fractionation experiments extend the range of exchange rates that can be monitored to identify more subtle structural features (Veglia et al. 2002).

The two-dimensional HSQC spectra also serve as the basis for the measurement of the ^{1}H and ^{15}N relaxation parameters of protein backbone amide site, which are useful for describing protein dynamics. The heteronuclear ^{1}H-^{15}N NOEs of the backbone amide sites provide remarkably direct and sensitive information on local protein dynamics (Gust et al. 1975, Boguski et al. 1987, Bogusky et al. 1988). They can be measured with and without ^{1}H irradiation to saturate the ^{1}H magnetization (Farrow et al. 1994).

RDCs are extremely useful both for structure refinement, and for the de novo determination of protein folds (Tolman et al. 1995, Clore and Gronenborn 1998, Delaglio et al. 2000, Fowler et al. 2000, Hus et al. 2000, Mueller et al. 2000). During refinement, these measurements supplement an already large number of chemical shifts, approximate distance measurements, and dihedral angle restraints. Among the principal advantages of anisotropic spectral parameters in solution NMR spectroscopy is that they can report on the global orientations of separate domains of a protein and of individual bonds relative to a reference frame, which reflects the preferred alignment of the molecule in the magnetic field. This does not preclude their utility in characterizing the local backbone structure of a protein molecule.

The RDCs and RCSAs measured in solution NMR experiments provide direct angular restraints with respect to a molecule-fixed reference frame (Bax et al. 2001, Prestegard and Kishore 2001, Lee et al. 2003). They are analogous to the non-averaged dipolar couplings and chemical shift anisotropies measured in solid-state NMR experiments (Marassi and Opella 2000, Wang et al. 2000, Marassi 2001). These orientation restraints are the principal mechanism for overcoming the limitations resulting from having few reliable long-range NOEs available as distance restraints, often encountered with samples of membrane-bound proteins in micelles.

Dipolar Waves are very effective at identifying the helical residues in membrane-bound proteins and the relative orientations of the helical segments, and also serve as indices of the helix regularity in proteins (Mesleh et al. 2002). The magnitudes of the RDCs are plotted as a function of residue number and fit to a sine wave with a period of 3.6 residues (Mesleh et al. 2002, Mesleh et al. 2003, Mesleh and Opella 2003). The quality of fit is monitored by a scoring function in a four-residue sliding window and the phase of the fit. *Dipolar Waves* from solution NMR data give relative orientations of helices in a common molecular frame. On the other hand *Dipolar Waves* from solid-state NMR data give absolute measurements of helix orientations because the polypeptides are immobile and the samples have a known alignment in the magnetic field.

(4.2) tBid in micelles.

The cleavage of Bid by caspase-8 results in a C-terminal product, tBid, which targets mitochondria and induces apoptosis with strikingly enhanced activity. To characterize the conformation of tBid in lipid environments, we obtained its CD (circular dichroism) and solution NMR $^{1}H/^{15}N$ HSQC spectra in the absence or in the presence of lipid micelles (Figure 3) (Gong et al. 2004). The HSQC spectra of proteins are the starting point for additional multi-dimensional NMR experiments that lead to structure determination. In these spectra, each ^{15}N-labeled protein site gives rise to a single peak, characterized by ^{1}H and ^{15}N chemical shift frequencies that reflect the local environment. In addition, the peak line widths and line shapes, and their dispersion in the ^{1}H and ^{15}N frequency dimensions, are sensitive indicators of protein conformational stability and aggregation state.

In the absence of lipids, the CD spectrum of tBid displays minima at 202 nm and 222 nm, characteristic of predominantly helical proteins (Figure 3A, solid line). However, while tBid retains its helical conformation even when it is separated from the 60-residue N-terminal segment, many of the resonances in its HSQC

spectrum cannot be detected (Figure 3B), suggesting that the protein aggregates in solution, adopts multiple conformations, or undergoes dynamic conformational exchange on the NMR timescales. This is consistent with the dramatic changes in the physical properties of the protein that result from caspase-8 cleavage.

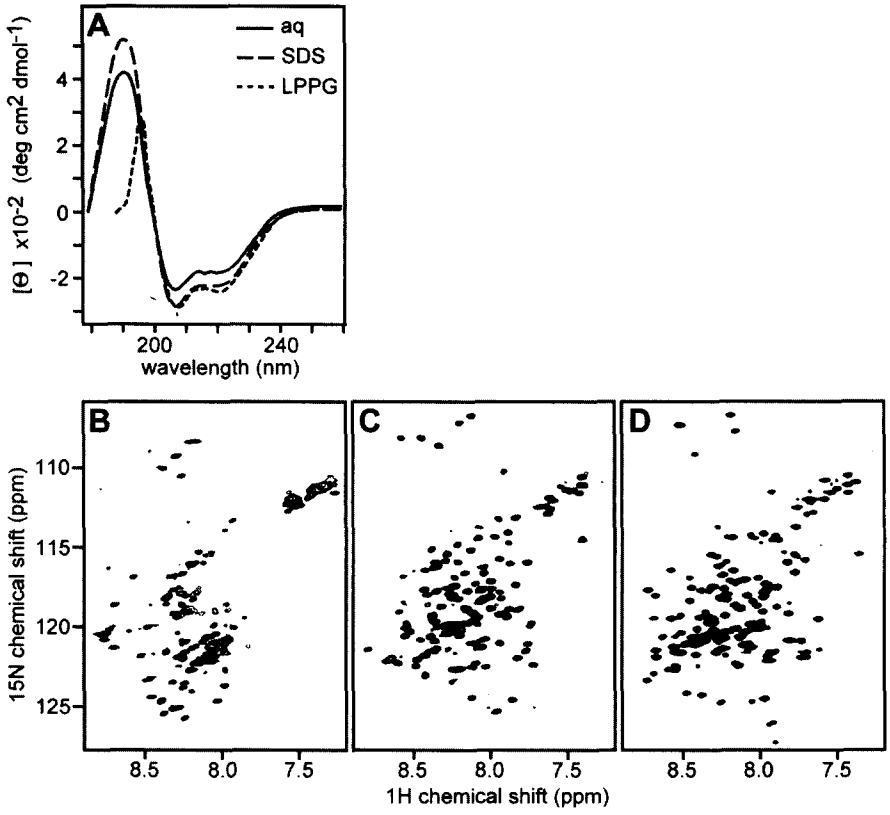

Figure 3. tBid adopt well-defined helical fold in lipid micelles. The CD spectra in (A) were obtained at 25°C for tBid in aqueous solution (solid line), SDS micelles (broken line), or LPPG micelles (dotted line). The $^{1}H/^{15}N$ HSQC NMR spectra in (B, C, D) were obtained at 40°C for uniformly ^{15}N-labeled tBid in (A) aqueous solution, (B) SDS micelles, or (C) LPPG micelles. Aqueous samples were in 20 mM sodium phosphate, pH 5; SDS micelle samples were in 20 mM sodium phosphate, pH 7, 500 mM SDS; and LPPG micelle samples were in 20 mM sodium phosphate, pH 7, 100 mM LPPG.

When tBid is dissolved in lipid micelles its HSQC spectrum changes dramatically, and single, well-defined $^{1}H/^{15}N$ resonances are observed for each ^{15}N-labeled NH site, indicating that it adopts a unique conformation in this environment (Figures 3C, 3D). Several lipids are available for protein solubilization, and we tested both SDS and LPPG for their ability to yield high-quality HSQC spectra of tBid for structure determination. Both gave excellent spectra where most of the 130 amide resonances of tBid could be resolved; for example the resonances from the five Gly amide sites are resolved in SDS (Figure 3C), and four out of five are resolved in LPPG (Figure 3D). Both SDS and LPPG are negatively charged but they differ in the lengths of their hydrocarbon chains (C12 for SDS; C16 for LPPG), and their polar headgroups (sulfate for SDS; phosphatidylglycerol for LPPG), thus the differences in ^{1}H and ^{15}N chemical shifts between the two HSQC spectra most likely reflect the different lipid environments. The spectrum in LPPG has exceptionally well-dispersed resonances with homogeneous intensities and line-widths. LPPG was recently identified as a superior lipid for NMR studies of several membrane proteins (Krueger-Koplin et al. 2004), and is particularly interesting for this study because it is a close analog of cardiolipin and monolysocardiolipin, the major components of mitochondrial membranes that binds tBid. The limited chemical shift dispersion in the two spectra is typical of helical proteins in micelles, and this is confirmed by the corresponding CD spectra, which are dominated by minima at 202 nm and 222 nm, and thus show that tBid retains a predominantly helical fold in both SDS and LPPG (Figure 3A, broken and dashed lines).

(5) NMR in bilayer membranes.

When the lipid bilayers are oriented with their surface perpendicular to the magnetic field, the solid-state NMR spectra of the membrane-associated proteins trace out maps of their structure and orientation within the membrane, and thus provide very useful structural information prior to complete structure determination (Marassi and Opella 2000, Wang et al. 2000, Marassi 2001). For example, helices give characteristic solid-state NMR spectra where the resonances from amide sites in the protein trace-out helical wheels that contain information regarding helix tilt and rotation within the membrane. Typically, trans-membrane helices have PISEMA spectra with ^{15}N chemical shifts between 150 and 200 ppm, and ^{1}H-^{15}N dipolar couplings between 2 and 10 kHz, while helices that bind parallel to the membrane surface have spectra with shifts between 70 and 100 ppm and couplings between 0 and 5 kHz. We refer to these as the trans-membrane and in-plane regions of the PISEMA spectrum, respectively.

Glass-supported oriented phospholipid bilayers containing membrane proteins accomplish the principal requirements of immobilizing and orienting the protein for solid-state NMR structure determination. The planar lipid bilayers are supported on glass slides, and are oriented in the NMR probe so that the bilayer normal is parallel to the field of the magnet, as shown in Figure 4A. The choice of lipid can be used to control the lateral spacing between neighboring phospholipid molecules as well as the vertical spacing between bilayers. The use of phospholipids with unsaturated chains leads to more expanded and fluid bilayers, and the addition of negatively charged lipids increases inter-bilayer repulsions leading to larger interstitial water layers between bilayer leaflets.

Samples of membrane proteins in lipid bilayers oriented on glass slides can be prepared by deposition from organic solvents followed by evaporation and lipid hydration, or by fusion of reconstituted unilamellar lipid vesicles with the glass surface (Marassi 2002). The choice of solvents in the first method, and of detergents in the second, is critical for obtaining highly oriented lipid bilayer preparations. In all cases the thinnest available glass slides are utilized to obtain the best filling factor in the coil of the probe. With carefully prepared samples it is possible to obtain ^{15}N resonance line widths of less than 3 ppm (Marassi et al. 1997). Notably, these line widths are less than those typically observed in single crystals of peptides, demonstrating that the proteins in the bilayers are very highly oriented, with mosaic spreads of less than about 2°.

(5.1) Bcl-XL and tBid in bilayers.

To examine the conformations of Bcl-XL and tBid associated with membranes, we obtained one-dimensional ^{15}N chemical shift and two-dimensional $^{1}H/^{15}N$ PISEMA solid-state NMR spectra of the ^{15}N-labeled proteins reconstituted in lipid bilayers (Franzin et al. 2004, Gong et al. 2004). In these samples, the lipid composition of 60% DOPC and 40% DOPG was chosen to mimic the highly negative charge of mitochondrial membranes. This lipid composition is identical to that of the liposomes used for the measurement of the ion channel activities of Bcl-XL, Bid, and tBid (Minn et al. 1997, Schendel et al. 1999), which were prepared in the same way as the oriented lipid bilayers used in the NMR study.

The samples of Bcl-XL and tBid in bilayers were prepared by spreading lipid vesicles, reconstituted with ^{15}N-labeled protein, on the surface of the glass slides, allowing bulk water to evaporate, and incubating the sample in a water-saturated atmosphere (Franzin et al. 2004, Gong et al. 2004). Each sample was wrapped in parafilm and then sealed in thin polyethylene film prior to insertion in the NMR probe. The degree of phospholipid bilayer alignment can be assessed with solid-state ^{31}P NMR spectroscopy of the lipid phosphate headgroup. The ^{31}P NMR spectra obtained for lipid bilayers with Bcl-XL are characteristic of a liquid-crystalline bilayer arrangement, in both oriented (Figure 4B) and unoriented samples (Figure 4C). The spectrum from the oriented sample has a single peak near 30 ppm, as expected for highly oriented bilayers.

Membrane-associated Bcl-XL.

The spectra in Figure 4 were obtained from samples of uniformly ^{15}N-labeled Bcl-xL in oriented and unoriented lipid bilayers (Franzin et al. 2004). The spectrum obtained from oriented Bcl-xL (Figure 4D) is separated into discernable resonances with distinct intensities near 80 and 170 ppm. These spectral features reflect a structural model where the helices of Bcl-XL associate with the membrane surface with limited transmembrane helix insertion.

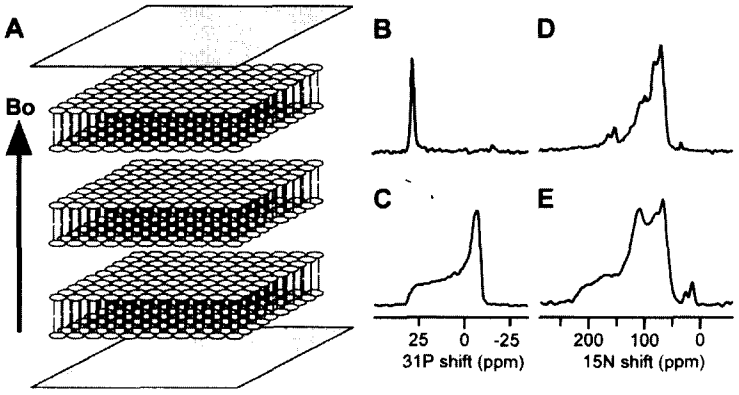

Figure 4. Effect of sample orientation on the solid-state NMR spectra of isotopically labeled proteins. (A) The glass-supported phospholipid bilayer samples are oriented in the NMR probe so that the bilayer normal is parallel to the direction of the magnetic field (Bo). (B) Oriented phospholipid bilayers give single-line one-dimensional ^{31}P chemical shift NMR spectra, while (C) spherical lipid bilayer vesicles give powder patterns. (D) The one-dimensional ^{15}N chemical shift NMR spectrum of uniformly ^{15}N labeled Bcl-XL in oriented lipid bilayers displays multiple resonances, compared to (E) the powder pattern that is obtained for the same protein in unoriented lipid bilayer vesicles. The ^{15}N chemical shifts are referenced to 0 ppm for liquid ammonia.

The spectrum from unoriented bilayers (Figure 4E) provides no resolution among resonances, but it provides an indication of protein dynamics, because of the pronounced effects of motional averaging on such spectra.

Most of the backbone sites are structured and immobile on the timescale of the ^{15}N chemical shift interaction (10 kHz), contributing to the characteristic amide powder pattern between 220 and 60 ppm. Some of the Bcl-XL backbone sites, probably near the termini and loop regions, are mobile, and give rise to the resonance band centered near 120 ppm. Therefore, while certain resonances near 120 ppm, in the spectrum of oriented Bcl-XL, may reflect specific orientations of their corresponding sites, some others arise from mobile backbone sites. The intensity near 35 ppm, also present in the spectrum from the oriented sample, is from the protein amino groups, which have a considerably narrower ^{15}N chemical shift anisotropy. Taken together, the ^{15}N and ^{31}P spectra provide evidence that Bcl-xL, an anti-apoptotic Bcl-2 family protein, associates predominantly with the membrane surface, without disruption of the membrane integrity.

Membrane-associated tBid.

The ^{15}N chemical shift spectrum of tBid in spherical lipid bilayer vesicles is a powder pattern (Figure 5A, solid line) that spans the full range (60-220 ppm) of the amide ^{15}N chemical shift interaction (Figure 5A, dashed line). The absence of additional intensity at the isotropic resonance frequencies (100-130 ppm) demonstrates that the majority of amino acid sites are immobile on the time scale of the ^{15}N chemical shift interaction, although it is possible that some mobile unstructured residues could not be observed by cross-polarization. The peak at 35 ppm is from the amino groups at the N-terminus and sidechains of the protein. The spectrum of tBid in planar oriented lipid bilayers is very different (Figure 5C). All of the amide resonances are centered at a frequency associated with NH bonds in helices parallel to the membrane surface (80 ppm), while no intensity is observed at frequencies associated with NH bonds in trans-membrane helices (200 ppm). The NMR data show no evidence of conformational exchange on the millisecond to second time scales of the channel opening and closing events, thus eliminating the possibility of transient insertion of tBid in the membrane. Thus tBid binds strongly to the membrane surface and adopts a unique conformation and orientation in the presence of phospholipids (Gong et al. 2004).

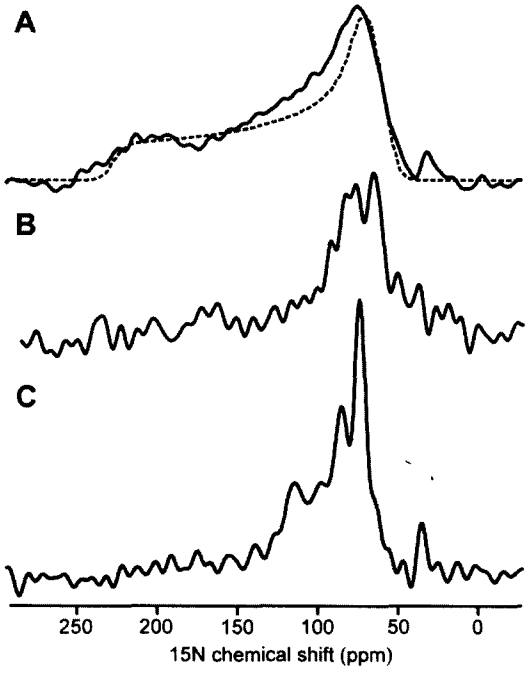

Figure 5. One-dimensional ^{15}N chemical shift spectra of tBid in lipid bilayers. (A) uniformly ^{15}N-labeleld tBid in unoriented lipid bilayer vesicles (solid line), and powder pattern calculated for a rigid ^{15}N amide site (dotted line). (B) One-dimensional ^{15}N spectrum of selectively ^{15}N-Lys-labeled tBid in oriented lipid bilayers. (C) One-dimensional ^{15}N spectrum of uniformly ^{15}N-labeled tBid in oriented lipid bilayers.

Amide hydrogen exchange rates are useful for identifying residues that are involved in hydrogen bonding, and that are exposed to water. Typically, the amide hydrogens in trans-membrane helices have very slow exchange rates due to their strong hydrogen bonds in the low dielectric of the lipid bilayer environment, and their ^{15}N chemical shift NMR signals persist for days after exposure to D_2O (Franzin et al. 2004). Trans-membrane helices that are in contact with water because they participate in channel pore formation, and other water-exposed helical regions proteins, have faster exchange rates, and their NMR signals disappear on the order of hours (Tian et al. 2003). To examine the amide hydrogen exchange rates for membrane-bound tBid, we obtained solid-state NMR spectra after exposing the oriented lipid bilayer sample to D_2O for 2 hours, 5 hours, and finally for 7 hours. The majority of resonances in the ^{15}N chemical shift spectrum of tBid disappeared within 8 hours, indicating that the amide hydrogens exchange and hence, are in contact with the bilayer interstitial water.

The tBid amino acid sequence has four Lys residues (Lys144, Lys146, Lys157, and Lys158) all located in or near helix-6, one of the two helices thought to insert in the membrane and form the tBid ion-conducting pore. The spectrum of ^{15}N-Lys labeled tBid in bilayers is notable because its amide resonances all have chemical shifts near 80 ppm, in the in-plane region of the spectrum, and this cannot be reconciled with membrane insertion (Figure 5B). Since tBid maintains a helical fold in lipid micelles and it is reasonable to assume that the helix boundaries are not changed from those of full-length Bid, the solid-state NMR data demonstrate that helix-6 does not insert through the membrane but associates parallel to its surface. This is also supported by a recent EPR study (Oh et al. 2004).

(5.2) Determining the structures of proteins in bilayers.

When membrane proteins are incorporated in planar lipid bilayers that are oriented in the field of the NMR magnet, the frequencies measured in their multi-dimensional solid-state NMR spectra contain orientation-dependent information that can be used for structure determination (Marassi 2002). The PISEMA (polarization inversion with spin exchange at the magic angle) experiment gives high-resolution, two-dimensional, ^{1}H-^{15}N dipolar coupling / ^{15}N chemical shift correlation spectra of oriented membrane proteins where the individual resonances contain orientation restraints for structure determination (Wu et al. 1994). PISEMA spectra of membrane proteins in oriented lipid bilayers also provide sensitive indices of protein secondary structure and topology because they exhibit characteristic wheel-like patterns of resonances, called *Pisa Wheels*, that reflect helical wheel projections (Schiffer and Edmunson 1967) of

residues in both β-helices and β-sheets (Marassi and Opella 2000, Wang et al. 2000, Marassi 2001). When a *Pisa Wheel* is observed, no assignments are needed to determine the tilt of a helix, and a single resonance assignment is sufficient to determine the helix rotation in the membrane. This information is extremely useful for determining the supramolecular architectures of membrane proteins and their assemblies.

The shape and position of the *Pisa Wheel* in the spectrum depends on the protein secondary structure and its orientation relative to the lipid bilayer surface, as well as the amide N-H bond length and the magnitudes and orientations of the principal elements of the amide ^{15}N chemical shift tensor. This direct relationship between spectrum and structure makes it possible to calculate solid-state NMR spectra for specific structural models of proteins, and provides the basis for a method of backbone structure determination from a limited set of uniformly and selectively ^{15}N-labeled samples (Marassi and Opella 2002, Marassi and Opella 2003).

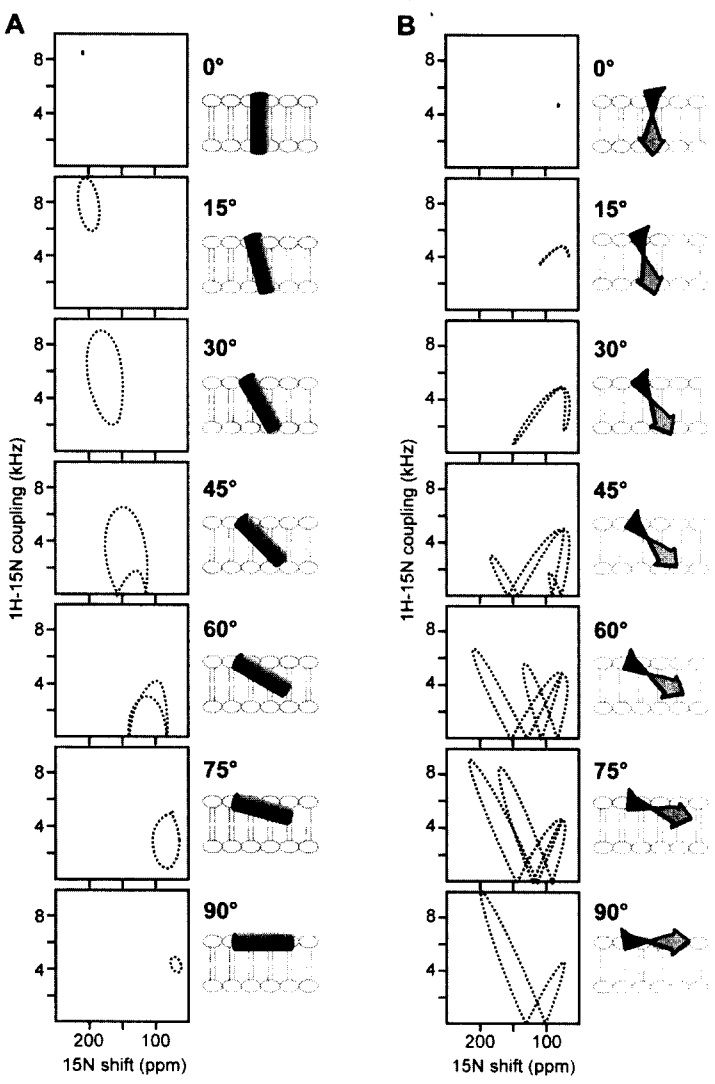

Figure 6. Helices and strands in oriented planar lipid bilayers give characteristic solid-state NMR spectra called *Pisa Wheels*. The ^{1}H-^{15}N dipolar coupling /^{15}N chemical shift PISEMA spectra were calculated for (A) an ideal β-helix with uniform dihedral angles (phi/psi = -65°/-40°), and (B) an ideal β-strand with uniform dihedral angles (phi/psi = -135°/140°), at different tilts relative to the magnetic field direction and the membrane normal. The ^{15}N chemical shifts are referenced to 0 ppm for liquid ammonia. Spectra were calculated as described (Marassi 2001).

The *Pisa Wheels* calculated for single helices or strands, oriented at varying degrees in a lipid bilayer are shown in Figure 6. When the helix or strand cross the membrane with their long axes exactly parallel to the lipid bilayer normal and to the magnetic field direction (0°), all of the amide sites in each structure have an identical orientation relative to the direction of the applied magnetic field, and therefore all of the resonances overlap with the same dipolar coupling and chemical shift frequencies. Tilting the helix or strand away from the membrane normal introduces variations in the orientations of the amide NH bond vectors in the magnetic field, and leads to dispersion of the ^{1}H-^{15}N dipolar coupling and ^{15}N chemical shift

frequencies, manifest in the appearance of *Pisa Wheel* resonance patterns in the spectra. Since helices and strands yield clearly different resonance patterns, with circular wheels for helices and twisted wheels for strands, these spectra represent signatures of secondary structure (Marassi 2001). The spectra also demonstrate that it is possible to determine the tilt of a helix or strand in lipid bilayers without resonance assignments. *Pisa wheels* have been observed in the PISEMA spectra of many uniformly ^{15}N labeled β-helical membrane proteins (Opella et al. 1999, Marassi et al. 2000, Wang et al. 2001, Marassi and Opella 2003, Park et al. 2003, Zeri et al. 2003).

(5.3) Conformation of tBid in lipid bilayers.

The two-dimensional $^{1}H/^{15}N$ PISEMA spectrum of tBid in bilayers is shown in Figure 7 (Gong et al. 2004). Each amide site in the protein contributes one correlation peak, characterized by ^{1}H-^{15}N dipolar coupling and ^{15}N chemical shift frequencies that reflect NH bond orientation relative to the membrane. For tBid, the circular wheel-like pattern of resonances in the spectral region bounded by 0 - 5 kHz and 70 - 90 ppm, provides definitive evidence that tBid associates with the membrane as surface-bound helices without trans-membrane insertion. The substantial peak overlap reflects a similar orientation of the tBid helices parallel to the membrane, and spectral resolution in this region requires three-dimensional correlation spectroscopy and selective isotopic labeling (Marassi et al. 2000).

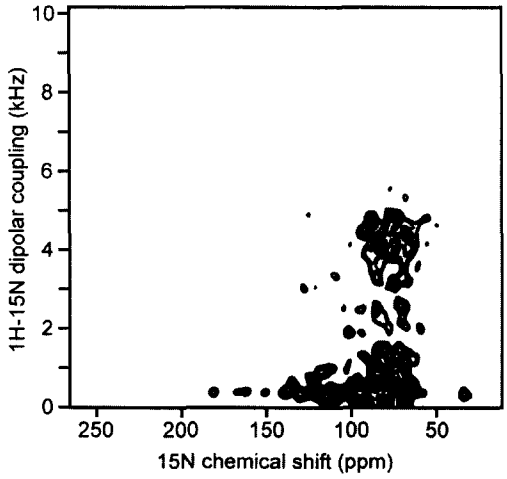

Figure 7. Two-dimensional $^{1}H/^{15}N$ PISEMA spectrum of uniformly ^{15}N-labeled tBid in oriented lipid bilayers

As shown in Figure 6, the NMR frequencies directly reflect the angles between individual bonds and the direction of the applied magnetic field, and, therefore, it is possible to calculate solid-state NMR spectra for specific models of proteins in oriented samples. A comparison of the calculated and experimental spectra then provides useful structural information prior to complete structure determination, which requires sequential assignment of the resonances. The spectra calculated for several orientations of an ideal 18-residue helix, with 3.6 residues per turn and identical backbone dihedral angles for all residues (phi, psi = -57°, -47°), are shown in Figure 8. This analysis demonstrates that trans-membrane helices with orientations between 90° and 45°, have wheel-like spectra in a completely unpopulated region of the tBid spectrum. Based on a comparison of the calculated spectra with the PISEMA spectrum of tBid in lipid bilayers we place the helices of tBid nearly parallel to the lipid bilayer plane (0° orientation), with a tilt of no more than 20° from the membrane surface.

Solution and solid-state NMR studies demonstrate that tBid adopts a unique helical fold in lipid environments, and that it binds the membrane without insertion of its helices. Solid-state NMR studies of the anti-apoptotic Bcl-2 family member, Bcl-X_L, also indicate that membrane insertion of the Bcl-X_L helices is only partial (Franzin et al. 2004), and solution NMR studies show that Bcl-X_L adopts an extended helical conformation in lipid micelles (Losonczi et al. 2000). Both tBid and Bcl-X_L form ion-conductive pores that are thought to play a role in apoptosis through their regulation of mitochondrial physiology, and

it is important to note that, since the samples in both the solid-state NMR and ion channel activity studies of Bcl-XL and tBid were identical in their lipid composition and the manner of sample preparation, the membrane surface association of Bcl-XL and tBid, observed by solid-state NMR, represents the channel-active conformation of the proteins.

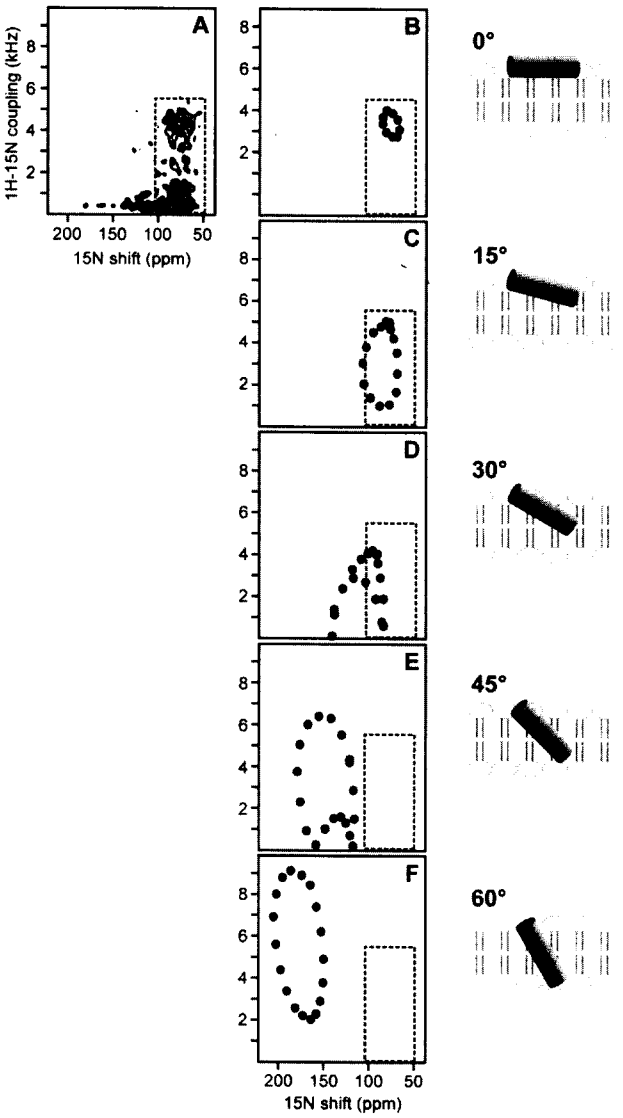

Figure 8. Two-dimensional solid-state NMR $^{1}H/^{15}N$ PISEMA spectrum of uniformly ^{15}N-labeleld tBid in oriented lipid bilayers. The experimental spectrum (black) is compared with the spectra (red) calculated for an 18-residue β-helix, with uniform backbone dihedral angles (phi = -57°; psi = -47°), and different helix tilts (0° to 75°) relative to the membrane, depicted in the cartoon above the spectra. The 0° orientation is for a helix parallel to the membrane surface.

A model for the mode of membrane association by tBid is shown in Figure 9. Cleavage by caspase-8 in the flexible loop of the soluble Bid structure (Figure 9A), generates the C-terminal product tBid (Figure 9B), which undergoes a conformational change and binds the surface of mitochondrial membranes (Figure 9C). It is possible that the structure of tBid, destabilized by dissociation from the N-terminal fragment after caspase-8 cleavage, undergoes a conformational change, whereby it opens about the flexible loops that connect its helical segments, to an extended helical conformation which binds to the membrane surface. This would be similar to the mechanism proposed for the lipoprotein apolipophorin-III, which adopts a marginally stable helix bundle topology that allows for concerted opening of the bundle about hinged loops (Wang et al. 2002). It is notable that the Bid amino acid sequence (P_{141}RDMEKE$_{147}$) at the beginning of helix-6, is similar to the conserved sequence (P_{95}DVEKE$_{100}$) that forms a short lipid recognition helix in apolipophorin-III. In Bid, this sequence forms a short loop that is perpendicular to the axis of helix-6 and solvent-exposed, while in apolipophorin-III it forms a short helix that is perpendicular to the helix bundle and at one solvent-exposed end of the molecule. This short motif is conserved in the Bid sequences from

various species, suggesting that it plays a role in the protein biological function, and may constitute a lipid recognition domain for Bid similar to that of apolipophorin-III.

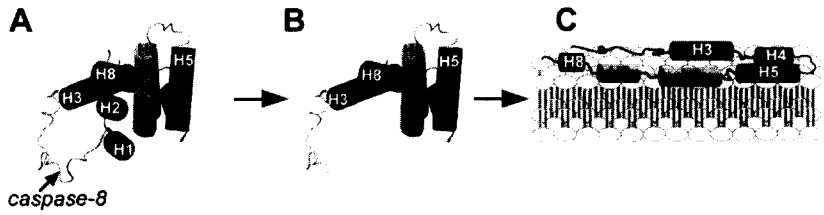

Figure 9. Model for the association of tBid with the membrane surface. (A) Cleavage by caspase-8 in the flexible loop of the soluble Bid structure (Chou et al. 1999, McDonnell et al. 1999), generates the C-terminal product tBid (B), which undergoes a conformational change and binds the surface of mitochondrial membranes (C).

Pore formation by the Bcl-2 family proteins has been thought to involve translocation of the central core helices through the membrane, and the helices of both Bid and Bcl-X_L are sufficiently long to span the lipid bilayer. However, their amphipathic character is also compatible with membrane surface association, in a manner that is reminiscent of the antimicrobial polypeptides where binding of the polypeptide helices to the bacterial membrane surface is thought to transiently destabilize the membrane and change its morphology, inducing leakage of the cell contents, disruption of the electrical potential, and ultimately cell death (Boman 1995, Marassi et al. 1999, Marassi et al. 2000). It is notable that bacterial and mitochondrial membranes have very similar structures and surface charge, and that tBid is both capable of altering bilayer curvature, and of remodeling the mitochondrial membrane, which would be sufficient to cause the release of mitochondrial cytotoxic molecules. Thus, the BH3-independent mechanism of pore-formation and mitochondrial cytochrome-c release by tBid, may be similar to that of the antimicrobial polypeptides. In addition, the membrane surface association of tBid may serve to display the BH3 domain on the mitochondrial membrane surface, making it accessible for binding by other Bcl-2 family members. Although tBid does not insert in DOPC/DOPG lipid bilayers, it is possible that trans-membrane insertion may be driven by the presence of natural mitochondrial lipids, such as cardiolipin and monolysocardiolipin. It is also possible that the interactions with other Bcl-2 family proteins such as Bak and Bax, or with other non-homologous proteins such as the mitochondrial voltage dependent anion channel, may promote insertion of the tBid helices through the mitochondrial membrane.

Acknowledgements

We thank David Cowburn, Stephen Fesik, and Gerhard Wagner, for sharing their solution NMR assignments for Bid and Bcl-XL. This research is supported by grants from the National Institutes of Health (R01GM065374), and the Department of the Army Breast Cancer Research Program (DAMD17-02-1-0313). The NMR studies utilized the Burnham Institute NMR Facility and the Biomedical Technology Resources for Solid-State NMR of Proteins at the University of California San Diego, supported by grants from the National Institutes of Health (P30CA30199; P41EB002031).

References

Almeida FC, and Opella SJ (1997) fd coat protein structure in membrane environments: structural dynamics of the loop between the hydrophobic trans-membrane helix and the amphipathic in-plane helix. J Mol Biol 270:481-495.

Aritomi M, Kunishima N, Inohara N, Ishibashi Y, Ohta S, and Morikawa K (1997) Crystal structure of rat Bcl-xL. Implications for the function of the Bcl-2 protein family. J Biol Chem 272:27886-27892.

Arora A, Abildgaard F, Bushweller JH, and Tamm LK (2001) Structure of outer membrane protein A transmembrane domain by NMR spectroscopy. Nat Struct Biol 8:334-338.

Bannwarth M, and Schulz GE (2003) The expression of outer membrane proteins for crystallization. Biochimica et Biophysica Acta (BBA) - Biomembranes 1610:37-45.

Battiste JL, and Wagner G (2000) Utilization of site-directed spin labeling and high-resolution heteronuclear nuclear magnetic resonance for global fold determination of large proteins with limited nuclear overhauser effect data. Biochemistry 39:5355-5365.

Bax A, Kontaxis G, and Tjandra N (2001) Dipolar couplings in macromolecular structure determination. Methods Enzymol 339:127-174.

Boguski MJ, Schiksnis RA, Leo GC, and Opella SJ (1987) Protein Backbone Dynamics by Solid-state and Solution 15N NMR Spectroscopy. J Magn Reson 72:186-190.

Bogusky MJ, Leo GC, and Opella SJ (1988) Comparison of the dynamics of the membrane-bound form of fd coat protein in micelles and in bilayers by solution and solid-state nitrogen-15 nuclear magnetic resonance spectroscopy. Proteins 4:123-130.

Boman HG (1995) Peptide antibiotics and their role in innate immunity. Annu Rev Immunol 13:61-92.

Booth PJ (2003) The trials and tribulations of membrane protein folding in vitro. Biochimica et Biophysica Acta (BBA) - Biomembranes 1610:51-56.

Chou JJ, Gaemers S, Howder B, Louis JM, and Bax A (2001) A simple apparatus for generating stretched polyacrylamide gels, yielding uniform alignment of proteins and detergent micelles. J Biomol NMR 21:377-382.

Chou JJ, Li H, Salvesen GS, Yuan J, and Wagner G (1999) Solution structure of BID, an intracellular amplifier of apoptotic signaling. Cell 96:615-624.

Clore GM, and Gronenborn AM (1989) Determination of three-dimensional structures of proteins and nucleic acids in solution by nuclear magnetic resonance spectroscopy. Crit Rev Biochem Mol Biol 24:479-564.

Clore GM, and Gronenborn AM (1998) New methods of structure refinement for macromolecular structure determination by NMR. Proc Natl Acad Sci U S A 95.

Cory S, and Adams JM (2002) The Bcl2 family: regulators of the cellular life-or-death switch. Nat Rev Cancer 2:647-656.

Cramer WA, Heymann JB, Schendel SL, Deriy BN, Cohen FS, Elkins PA, and Stauffacher CV (1995) Structure-function of the channel-forming colicins. Annu Rev Biophys Biomol Struct 24:611-641.

Crowell KJ, Franzin CM, Koltay A, Lee S, Lucchese AM, Snyder BC, and Marassi FM (2003) Expression and characterization of the FXYD ion transport regulators for NMR structural studies in lipid micelles and lipid bilayers. Biochim Biophys Acta 1645:15-21.

Czerski L, Vinogradova O, and Sanders CR (2000) NMR-Based amide hydrogen-deuterium exchange measurements for complex membrane proteins: development and critical evaluation. J Magn Reson 142:111-119.

Damberg P, Jarvet J, and Graslund A (2001) Micellar systems as solvents in peptide and protein structure determination. Methods Enzymol 339:271-285.

Danial NN, and Korsmeyer SJ (2004) Cell death: critical control points. Cell 116:205-219.

Dawson PE, Muir TW, Clark-Lewis I, and Kent SB (1994) Synthesis of proteins by native chemical ligation. Science 266:776-779.

Day CL, Chen L, Richardson SJ, Harrison PJ, Huang DC, and Hinds MG (2004) Solution structure of pro-survival Mcl-1 and characterization of its binding by pro-apoptotic BH3-only ligands. J Biol Chem.

Day CL, Chen L, Richardson SJ, Harrison PJ, Huang DC, and Hinds MG (2005) Solution structure of prosurvival Mcl-1 and characterization of its binding by proapoptotic BH3-only ligands. J Biol Chem 280:4738-4744.

Delaglio F, Kontaxis G, and Bax A (2000) Protein Structure Determination Using Molecular Fragment Replacement and NMR Dipolar Couplings. J Am Chem Soc 122:2142-2143.

Denault JB, and Salvesen GS (2002) Caspases: keys in the ignition of cell death. Chem Rev 102:4489-4500.

Denisov AY, Madiraju MS, Chen G, Khadir A, Beauparlant P, Attardo G, Shore GC, and Gehring K (2003) Solution structure of human BCL-w: modulation of ligand binding by the C-terminal helix. J Biol Chem.

Farrow NA, Zhang O, Forman-Kay JD, and Kay LE (1994) A heteronuclear correlation experiment for simultaneous determination of 15N longitudinal decay and chemical exchange rates of systems in slow equilibrium. J Biomol NMR 4:727-734.

Ferentz AE, and Wagner G (2000) NMR spectroscopy: a multifaceted approach to macromolecular structure. Q Rev Biophys 33:29-65.

Fernandez C, Adeishvili K, and Wuthrich K (2001) Transverse relaxation-optimized NMR spectroscopy with the outer membrane protein OmpX in dihexanoyl phosphatidylcholine micelles. Proc Natl Acad Sci U S A 98:2358-2363.

Fowler CA, Tian F, Al-Hashimi HM, and Prestegard JH (2000) Rapid determination of protein folds using residual dipolar couplings. J Mol Biol 304:447-460.

Franzin CM, Choi J, Zhai D, Reed JC, and Marassi FM (2004) Structural studies of apoptosis and ion transport regulatory proteins in membranes. Magn Reson Chem 42:172-179.

Gesell J, Zasloff M, and Opella SJ (1997) Two-dimensional 1H NMR experiments show that the 23-residue magainin antibiotic peptide is an alpha-helix in dodecylphosphocholine micelles, sodium dodecylsulfate micelles, and trifluoroethanol/water solution. J Biomol NMR 9:127-135.

Gong XM, Choi J, Franzin CM, Zhai D, Reed JC, and Marassi FM (2004) Conformation of Membrane-associated Proapoptotic tBid. J Biol Chem 279:28954-28960.

Green DR, and Reed JC (1998) Mitochondria and apoptosis. Science 281:1309-1312.

Gust D, Moon RB, and Roberts JD (1975) Applications of natural-abundance nitrogen-15 nuclear magnetic resonance to large biochemically important molecules. Proc Natl Acad Sci U S A 72:4696-4700.

Henry GD, and Sykes BD (1994) Methods to study membrane protein structure in solution. Methods Enzymol 239:515-535.

Hinds MG, Lackmann M, Skea GL, Harrison PJ, Huang DC, and Day CL (2003) The structure of Bcl-w reveals a role for the C-terminal residues in modulating biological activity. Embo J 22:1497-1507.

Howell SC, Mesleh MF, and Opella SJ (2005) NMR Structure Determination of a Membrane protein with two Transmembrane helices in Micelles: MerF of the Bacterial Mercury Detoxification System. Biochemistry in press.

Huang Q, Petros AM, Virgin HW, Fesik SW, and Olejniczak ET (2002) Solution structure of a Bcl-2 homolog from Kaposi sarcoma virus. Proc Natl Acad Sci U S A 99:3428-3433.

Huang Q, Petros AM, Virgin HW, Fesik SW, and Olejniczak ET (2003) Solution structure of the BHRF1 protein from Epstein-Barr virus, a homolog of human Bcl-2. J Mol Biol 332:1123-1130.

Hus JC, Marion D, and Blackledge MJ (2000) De novo Determination of Protein Structure by NMR using Orientational and Long-range Order Restraints. J Mol Biol 298:927-936.

Hwang PM, Choy WY, Lo EI, Chen L, Forman-Kay JD, Raetz CR, Prive GG, Bishop RE, and Kay LE (2002) Solution structure and dynamics of the outer membrane enzyme PagP by NMR. Proc Natl Acad Sci U S A 99:13560-13565.

Jarvet J, Zdunek J, Damberg P, and Graslund A (1997) Three-dimensional structure and position of porcine motilin in sodium dodecyl sulfate micelles determined by 1H NMR. Biochemistry 36:8153-8163.

Jones DH, Ball EH, Sharpe S, Barber KR, and Grant CW (2000) Expression and membrane assembly of a transmembrane region from Neu. Biochemistry 39:1870-1878.

Ketchem RR, Hu W, and Cross TA (1993) High-resolution conformation of gramicidin A in a lipid bilayer by solid-state NMR. Science 261:1457-1460.

Kiefer H (2003) In vitro folding of alpha-helical membrane proteins. Biochimica et Biophysica Acta (BBA) - Biomembranes 1610:57-62.

Klammt C, Lohr F, Schafer B, Haase W, Dotsch V, Ruterjans H, Glaubitz C, and Bernhard F (2004) High level cell-free expression and specific labeling of integral membrane proteins. Eur J Biochem 271:568-580.

Kleid DG, Yansura D, Small B, Dowbenko D, Moore DM, Grubman MJ, McKercher PD, Morgan DO, Robertson BH, and Bachrach HL (1981) Cloned viral protein vaccine for foot-and-mouth disease: responses in cattle and swine. Science 214:1125-1129.

Klein-Seetharaman J, Reeves PJ, Loewen MC, Getmanova EV, Chung J, Schwalbe H, Wright PE, and Khorana HG (2002) Solution NMR spectroscopy of [alpha -15N]lysine-labeled rhodopsin: The single peak observed in both conventional and TROSY-type HSQC spectra is ascribed to Lys-339 in the carboxyl-terminal peptide sequence. Proceedings of the National Academy of Sciences of the United States of America 99:3452-3457.

Kochendoerfer GG (2001) Chemical protein synthesis methods in drug discovery. Curr Opin Drug Discov Devel 4:205-214.

Kochendoerfer GG, Jones DH, Lee S, Oblatt-Montal M, Opella SJ, and Montal M (2004) Functional characterization and NMR spectroscopy on full-length Vpu from HIV-1 prepared by total chemical synthesis. J Am Chem Soc 126:2439-2446.

Kochendoerfer GG, Salom D, Lear JD, Wilk-Orescan R, Kent SB, and DeGrado WF (1999) Total chemical synthesis of the integral membrane protein influenza A virus M2: role of its C-terminal domain in tetramer assembly. Biochemistry 38:11905-11913.

Kroemer G, and Reed JC (2000) Mitochondrial control of cell death. Nat Med 6:513-519.

Krueger-Koplin RD, Sorgen PL, Krueger-Koplin ST, Rivera-Torres IO, Cahill SM, Hicks DB, Grinius L, Krulwich TA, and Girvin ME (2004) An evaluation of detergents for NMR structural studies of membrane proteins. J Biomol NMR 28:43-57.

Kuliopulos A, Nelson NP, Yamada M, Walsh CT, Furie B, Furie BC, and Roth DA (1994) Localization of the affinity peptide-substrate inactivator site on recombinant vitamin K-dependent carboxylase. J Biol Chem 269:21364-21370.

Kutateladze TG, Capelluto DG, Ferguson CG, Cheever ML, Kutateladze AG, Prestwich GD, and Overduin M (2004) Multivalent mechanism of membrane insertion by the FYVE domain. J Biol Chem 279:3050-3057.

Lee S, Mesleh MF, and Opella SJ (2003) Structure and dynamics of a membrane protein in micelles from three solution NMR experiments. J Biomol NMR 26:327-334.

Lindhout DA, Thiessen A, Schieve D, and Sykes BD (2003) High-yield expression of isotopically labeled peptides for use in NMR studies. Protein Sci 12:1786-1791.

Losonczi JA, Olejniczak ET, Betz SF, Harlan JE, Mack J, and Fesik SW (2000) NMR studies of the anti-apoptotic protein Bcl-xL in micelles. Biochemistry 39:11024-11033.

Ma C, Marassi FM, Jones DH, Straus SK, Bour S, Strebel K, Schubert U, Oblatt-Montal M, Montal M, and Opella SJ (2002) Expression, purification, and activities of full-length and truncated versions of the integral membrane protein Vpu from HIV-1. Protein Sci 11:546-557.

MacKenzie KR, Prestegard JH, and Engelman DM (1997) A transmembrane helix dimer: structure and implications. Science 276:131-133.

Majerle A, Kidric J, and Jerala R (2000) Production of stable isotope enriched antimicrobial peptides in Escherichia coli: an application to the production of a 15N-enriched fragment of lactoferrin. J Biomol NMR 18:145-151.

Marassi FM (2001) A simple approach to membrane protein secondary structure and topology based on NMR spectroscopy. Biophys J 80:994-1003.

Marassi FM (2002) NMR of peptides and proteins in membranes. Concepts Magn Resonance 14:212-224.

Marassi FM, Ma C, Gesell JJ, and Opella SJ (2000) Three-dimensional solid-state NMR spectroscopy is essential for resolution of resonances from in-plane residues in uniformly (15)N-labeled helical membrane proteins in oriented lipid bilayers. J Magn Reson 144:156-161.

Marassi FM, and Opella SJ (2000) A solid-state NMR index of helical membrane protein structure and topology. J Magn Reson 144:150-155.

Marassi FM, and Opella SJ (2002) Using pisa pies to resolve ambiguities in angular constraints from PISEMA spectra of aligned proteins. J Biomol NMR 23:239-242.

Marassi FM, and Opella SJ (2003) Simultaneous assignment and structure determination of a membrane protein from NMR orientational restraints. Protein Sci 12:403-411.

Marassi FM, Opella SJ, Juvvadi P, and Merrifield RB (1999) Orientation of cecropin A helices in phospholipid bilayers determined by solid-state NMR spectroscopy. Biophys J 77:3152-3155.

Marassi FM, Ramamoorthy A, and Opella SJ (1997) Complete resolution of the solid-state NMR spectrum of a uniformly 15N-labeled membrane protein in phospholipid bilayers. Proc Natl Acad Sci U S A 94:8551-8556.

Mascioni A, Karim C, Barany G, Thomas DD, and Veglia G (2002) Structure and orientation of sarcolipin in lipid environments. Biochemistry 41:475-482.

McDonnell JM, Fushman D, Milliman CL, Korsmeyer SJ, and Cowburn D (1999) Solution structure of the proapoptotic molecule BID: a structural basis for apoptotic agonists and antagonists. Cell 96:625-634.

Meier S, Haussinger D, and Grzesiek S (2002) Charged acrylamide copolymer gels as media for weak alignment. J Biomol NMR 24:351-356.

Mesleh MF, Lee S, Veglia G, Thiriot DS, Marassi FM, and Opella SJ (2003) Dipolar waves map the structure and topology of helices in membrane proteins. J Am Chem Soc 125:8928-8935.

Mesleh MF, and Opella SJ (2003) Dipolar Waves as NMR maps of helices in proteins. J Magn Reson 163:288-299.

Mesleh MF, Veglia G, DeSilva TM, Marassi FM, and Opella SJ (2002) Dipolar waves as NMR maps of protein structure. J Am Chem Soc 124:4206-4207.

Minn AJ, Velez P, Schendel SL, Liang H, Muchmore SW, Fesik SW, Fill M, and Thompson CB (1997) Bcl-x(L) forms an ion channel in synthetic lipid membranes. Nature 385:353-357.

Miozzari GF, and Yanofsky C (1978) Translation of the leader region of the Escherichia coli tryptophan operon. J Bacteriol 133:1457-1466.

Miroux B, and Walker JE (1996) Over-production of proteins in Escherichia coli: mutant hosts that allow synthesis of some membrane proteins and globular proteins at high levels. J Mol Biol 260:289-298.

Muchmore SW, Sattler M, Liang H, Meadows RP, Harlan JE, Yoon HS, Nettesheim D, Chang BS, Thompson CB, Wong SL, Ng SL, and Fesik SW (1996) X-ray and NMR structure of human Bcl-xL, an inhibitor of programmed cell death. Nature 381:335-341.

Mueller GA, Choy WY, Yang D, Forman-Kay JD, Venters RA, and Kay LE (2000) Global Folds of Proteins with Low Densities of NOEs Using Residual Dipolar Couplings: Application to the 370-Residue Maltodextrin-binding Protein. J Mol Biol 300:197-212.

Oh KJ, Barbuto S, Meyer N, Kim RS, Collier RJ, and Korsmeyer SJ (2004) Conformational changes in BID, a pro-apoptotic BCL-2 family member, upon membrane-binding: A site-directed spin labeling study. J Biol Chem.

Opella SJ, Ma C, and Marassi FM (2001) Nuclear magnetic resonance of membrane-associated peptides and proteins. Methods Enzymol 339:285-313.

Opella SJ, and Marassi FM (2004) Structure determination of membrane proteins by NMR spectroscopy. Chem Rev 104:3587-3606.

Opella SJ, Marassi FM, Gesell JJ, Valente AP, Kim Y, Oblatt-Montal M, and Montal M (1999) Structures of the M2 channel-lining segments from nicotinic acetylcholine and NMDA receptors by NMR spectroscopy. Nat Struct Biol 6:374-379.

Oxenoid K, Kim HJ, Jacob J, Sonnichsen FD, and Sanders CR (2004) NMR assignments for a helical 40 kDa membrane protein. J Am Chem Soc 126:5048-5049.

Oxenoid K, Sonnichsen FD, and Sanders CR (2002) Topology and secondary structure of the N-terminal domain of diacylglycerol kinase. Biochemistry 41:12876-12882.

Papavoine CH, Konings RN, Hilbers CW, and van de Ven FJ (1994) Location of M13 coat protein in sodium dodecyl sulfate micelles as determined by NMR. Biochemistry 33:12990-12997.

Park SH, Mrse AA, Nevzorov AA, Mesleh MF, Oblatt-Montal M, Montal M, and Opella SJ (2003) Three-dimensional structure of the channel-forming trans-membrane domain of virus protein "u" (Vpu) from HIV-1. J Mol Biol 333:409-424.

Petros AM, Medek A, Nettesheim DG, Kim DH, Yoon HS, Swift K, Matayoshi ED, Oltersdorf T, and Fesik SW (2001) Solution structure of the antiapoptotic protein bcl-2. Proc Natl Acad Sci U S A 98:3012-3017.

Prestegard JH, and Kishore AI (2001) Partial alignment of biomolecules: an aid to NMR characterization. Curr Opin Chem Biol 5:584-590.

Rogl H, Kosemund K, Kuhlbrandt W, and Collinson I (1998) Refolding of Escherichia coli produced membrane protein inclusion bodies immobilised by nickel chelating chromatography. FEBS Lett 432:21-26.

Sass HJ, Musco G, Stahl SJ, Wingfield PT, and Grzesiek S (2000) Solution NMR of proteins within polyacrylamide gels: diffusional properties and residual alignment by mechanical stress or embedding of oriented purple membranes. J Biomol NMR 18:303-309.

Schendel SL, Azimov R, Pawlowski K, Godzik A, Kagan BL, and Reed JC (1999) Ion channel activity of the BH3 only Bcl-2 family member, BID. J Biol Chem 274:21932-21936.

Schendel SL, Montal M, and Reed JC (1998) Bcl-2 family proteins as ion-channels. Cell Death Differ 5:372-380.

Schiffer M, and Edmunson AB (1967) Use of helical wheels to represent the structures of proteins and to identify segments with helical potential. Biophys J 7:121-135.

Scorrano L, and Korsmeyer SJ (2003) Mechanisms of cytochrome c release by proapoptotic BCL-2 family members. Biochem Biophys Res Commun 304:437-444.

Sharon M, Gorlach M, Levy R, Hayek Y, and Anglister J (2002) Expression, purification, and isotope labeling of a gp120 V3 peptide and production of a Fab from a HIV-1 neutralizing antibody for NMR studies. Protein Expr Purif 24:374-383.

Smith VR, and Walker JE (2003) Purification and folding of recombinant bovine oxoglutarate/malate carrier by immobilized metal-ion affinity chromatography. Protein Expression and Purification 29:209-216.

Sorgen PL, Cahill SM, Krueger-Koplin RD, Krueger-Koplin ST, Schenck CC, and Girvin ME (2002) Structure of the Rhodobacter sphaeroides light-harvesting 1 beta subunit in detergent micelles. Biochemistry 41:31-41.

Staley JP, and Kim PS (1994) Formation of a native-like subdomain in a partially folded intermediate of bovine pancreatic trypsin inhibitor. Protein Sci 3:1822-1832.

Suzuki M, Youle RJ, and Tjandra N (2000) Structure of Bax: coregulation of dimer formation and intracellular localization. Cell 103:645-654.

Thai K, Choi J, Franzin CM, and Marassi FM (2005) Bcl-XL as a fusion protein for the high-level expression of membrane-associated proteins. Protein Sci 14:948-955.

Tian C, Gao PF, Pinto LH, Lamb RA, and Cross TA (2003) Initial structural and dynamic characterization of the M2 protein transmembrane and amphipathic helices in lipid bilayers. Protein Sci 12:2597-2605.

Tolman JR, Flanagan JM, Kennedy MA, and Prestegard JH (1995) Nuclear magnetic dipole interactions in field-oriented proteins: information for structure determination in solution. Proc Natl Acad Sci U S A 92:9279-9283.

Tycko R, Blanco FJ, and Ishii Y (2000) Alignment of Biopolymers in Strained Gels: A New Way To Create Detectable Dipole-Dipole Couplings in High-Resolution Biomolecular NMR. J Am Chem Soc 122:9340-9341.

Valentine KG, Liu SF, Marassi FM, Veglia G, Opella SJ, Ding FX, Wang SH, Arshava B, Becker JM, and Naider F (2001) Structure and topology of a peptide segment of the 6th transmembrane domain of the Saccharomyces cerevisae alpha-factor receptor in phospholipid bilayers. Biopolymers 59:243-256.

Van Den Hooven HW, Doeland CC, Van De Kamp M, Konings RN, Hilbers CW, and Van De Ven FJ (1996) Three-dimensional structure of the lantibiotic nisin in the presence of membrane-mimetic micelles of dodecylphosphocholine and of sodium dodecylsulphate. Eur J Biochem 235:382-393.

Veglia G, Zeri AC, Ma C, and Opella SJ (2002) Deuterium/hydrogen exchange factors measured by solution nuclear magnetic resonance spectroscopy as indicators of the structure and topology of membrane proteins. Biophys J 82:2176-2183.

Wang J, Denny J, Tian C, Kim S, Mo Y, Kovacs F, Song Z, Nishimura K, Gan Z, Fu R, Quine JR, and Cross TA (2000) Imaging membrane protein helical wheels. J Magn Reson 144:162-167.

Wang J, Kim S, Kovacs F, and Cross TA (2001) Structure of the transmembrane region of the M2 protein H(+) channel. Protein Sci 10:2241-2250.

Wang J, Sykes BD, and Ryan RO (2002) Structural basis for the conformational adaptability of apolipophorin III, a helix-bundle exchangeable apolipoprotein. Proc Natl Acad Sci U S A 99:1188-1193.

Wiener MC (2004) A pedestrian guide to membrane protein crystallization. Methods 34:364-372.

Williams KA, Farrow NA, Deber CM, and Kay LE (1996) Structure and dynamics of bacteriophage IKe major coat protein in MPG micelles by solution NMR. Biochemistry 35:5145-5157.

Wu CH, Ramamoorthy A, and Opella SJ (1994) High-resolution heteronuclear dipolar solid-state NMR spectroscopy. J Magn Reson A 109:270-272.

Wuthrich K (1989) Determination of three-dimensional protein structures in solution by nuclear magnetic resonance: an overview. Methods Enzymol 177:125-131.

Zeri AC, Mesleh MF, Nevzorov AA, and Opella SJ (2003) Structure of the coat protein in fd filamentous bacteriophage particles determined by solid-state NMR spectroscopy. Proc Natl Acad Sci U S A 100:6458-6463.